| 1. Report No.<br>FHWA/TX-93+1239-4F | 2. Government Accession No. | 3. Recipient's Catalog No. |
|---|---|---|
| 4. Title and Subtitle<br><br>BRACING OF STEEL BEAMS IN BRIDGES | | 5. Report Date<br>October 1992 |
| | | 6. Performing Organization Code |
| 7. Author(s)<br>Joseph Yura, Brett Phillips, Swarna Raju, and Stuart Webb | | 8. Performing Organization Report No.<br>Research Report 1239-4F |
| 9. Performing Organization Name and Address<br>Center for Transportation Research<br>The University of Texas at Austin<br>3208 Red River, Suite 200<br>Austin, Texas    78705-2650 | | 10. Work Unit No. (TRAIS) |
| | | 11. Contract or Grant No.<br>Research Study 3-5-90/1-1239 |
| 12. Sponsoring Agency Name and Address<br>Texas Department of Transportation<br>Transportation Planning Division, Research Section<br>P. O. Box 5051<br>Austin, Texas    78763-5051 | | 13. Type of Report and Period Covered<br>Final |
| | | 14. Sponsoring Agency Code |

15. Supplementary Notes

Study conducted in cooperation with the U.S. Department of Transportation, Federal Highway Administration
Research Study Title: "Bracing Effects of Bridge Decks"

16. Abstract

The report summarizes the research conducted to evaluate the lateral bracing effect of bridge decks. Design requirements for bracing steel beams to control lateral-torsional buckling are developed. Braces are classified as torsional braces (diaphragms, cross frames) or lateral braces (top chord laterals, bridge decks). Analytical studies were conducted which investigated the effect of brace type, size, location, and number of braces on the lateral buckling of beams subject to different loading conditions. Results of tests conducted on twin beams compared favorably with the analytical solution. Both the tests and the theoretical solution showed the cross section distortion had a significant effect on torsional braces. The tests with no bracing or full bracing compared favorably with the new AASHTO lateral buckling formulas.

From the tests and the theory, simple formulas for brace force and brace stiffness are presented which are suitable for design and specifications. For lateral bracing, the brace force is 0.8 percent of the beam force, which includes some provision for beam out-of-straightness. For torsional bracing, the design formulas can be used to determine web stiffener requirements to control cross section distortion. Five design examples illustrate the use of the bracing formulas.

| 17. Key Words<br><br>bracing, lateral torsional buckling, steel beams, wooden decks, web stiffeners, experiments, load rating, load distribution, friction, brace design | 18. Distribution Statement<br><br>No restrictions. This document is available to the public through the National Technical Information Service, Springfield, Virginia 22161. | | |
|---|---|---|---|
| 19. Security Classif. (of this report)<br>Unclassified | 20. Security Classif. (of this page)<br>Unclassified | 21. No. of Pages<br>96 | 22. Price |

Form DOT F 1700.7 (8-72)          Reproduction of completed page authorized

# BRACING OF STEEL BEAMS IN BRIDGES

by

## Joseph Yura, Brett Phillips, Swarna Raju and Stuart Webb

Research Report Number 1239-4F

Research Project 3-5-90/1-1239
"BRACING EFFECTS OF BRIDGE DECKS"

Conducted for

Texas Department of Transportation

In Cooperation with the
U.S. Department of Transportation
Federal Highway Administration

by

CENTER FOR TRANSPORTATION RESEARCH
BUREAU OF ENGINEERING RESEARCH
THE UNIVERSITY OF TEXAS AT AUSTIN

OCTOBER 1992

NOT INTENDED FOR CONSTRUCTION,
BIDDING, OR PERMIT PURPOSES

Joseph A. Yura, P.E. (Texas No. 29859)

*Research Supervisor*

The contents of this report reflect the views of the authors, who are responsible for the facts and accuracy of the data presented herein. The contents do not necessarily reflect the official views or policies of the Federal Highway Administration or the Texas Department of Transportation. This report does not constitute a standard, specification, or regulation.

There was no invention or discovery conceived or first actually reduced to practice in the course of or under this contract, including any art, method, process, machine, manufacture, design or composition of matter, or any new and useful improvement thereof, or any variety of plant which is or may be patentable under the patent laws of the United States of America or any foreign country.

# PREFACE

The report summarizes the research conducted to evaluate the lateral bracing effect of bridge decks. The research concentrated on timber decks that are common in off system bridges in Texas. The purpose of the research was to establish the design requirements for lateral bracing and to determine if typical decks provide this bracing. Specifically, *is a wheel load location a brace point* is the question addressed.

The work reported herein is the final report of Research Study 3-5-90/1-1239, *"Bracing Effects of Bridge Decks."* Three other reports give additional details:

1239-1 "Bracing Requirements for Elastic Steel Beams"

1239-2 "An Ultimate Load Test to Study the Bracing Effects of Bridge Decks"

1239-3 "Evaluation of Bridge Decks as Lateral Bracing for Supporting Steel Stringers"

# SUMMARY

Design requirements for bracing steel beams to control lateral-torsional buckling are developed. Braces are classified as torsional braces (diaphragms, cross frames) or lateral braces (top chord laterals, bridge decks). Analytical studies were conducted which investigated the effect of brace type, size, location, and number of braces on the lateral buckling of beams subject to different loading conditions.

Seventy-six buckling tests were conducted on twin beams. The results compared very favorably with the analytical solution. Both the tests and the theoretical solution showed that cross section distortion had a significant effect on torsional braces. The tests with no bracing or full bracing compared very favorably with the new AASHTO lateral buckling formulas.

From the tests and the theory, simple formulas for brace force and brace stiffness are presented which are suitable for design and specifications. For lateral bracing the brace force is 0.8% of the beam force which includes some provision for beam out-of-straightness. The design formulas can be used for braces at a discrete number of locations along the span or continuous bracing. For torsional bracing the design formulas can be used to determine web stiffener requirements to control cross-section distortion. Five design examples illustrate the use of the bracing formulas.

A full-size test on a five-girder short span bridge showed that timber decks that are not positively attached to the steel stringers can provide lateral bracing at the wheel load location through friction. Common timber decks have enough lateral bracing stiffness to permit the stringers to reach yielding without buckling, but a stiffness check on the deck is recommended. Short span bridges with concrete decks can be considered laterally supported at the wheel load location near midspan. The bracing effect of bridge decks coupled with the improved AASHTO lateral buckling formula can significantly increase the load rating of steel bridges that are controlled by lateral buckling.

# IMPLEMENTATION

The Texas Bridge Rating Manual needs to be updated immediately to use the new AASHTO 1990 lateral buckling formula. The new formulation gives more realistic capacities compared to older versions of the AASHTO Specification.

For short span bridges with no positive connection between the deck and the steel stringers, the wheel load can be considered a brace point if the deck is concrete. If the deck is wooden, it probably has enough stiffness to permit the wheel load to act as a brace point but a design check is recommended, as given in Appendix A.

The simple design formulation summarized in Appendix A are recommended for use in all steel bridges. Since the current AASHTO Bridge Sepcification does not contain any design provisions for lateral bracing, it is suggested that the design formulas in Appendix A be included in the AASHTO Specification.

## TABLE OF CONTENTS

# LIST OF FIGURES

# LIST OF TABLES

# METRIC (SI*) CONVERSION FACTORS

## APPROXIMATE CONVERSIONS TO SI UNITS

| Symbol | When You Know | Multiply by | To Find | Symbol |
|---|---|---|---|---|
| | | **LENGTH** | | |
| in | inches | 2.54 | centimeters | cm |
| ft | feet | 0.3048 | meters | m |
| yd | yards | 0.914 | meters | m |
| mi | miles | 1.61 | kilometers | km |
| | | **AREA** | | |
| in² | square inches | 645.2 | millimeters squared | mm² |
| ft² | square feet | 0.0929 | meters squared | m² |
| yd² | square yards | 0.836 | meters squared | m² |
| mi² | square miles | 2.59 | kilometers squared | km² |
| ac | acres | 0.395 | hectares | ha |
| | | **MASS (weight)** | | |
| oz | ounces | 28.35 | grams | g |
| lb | pounds | 0.454 | kilograms | kg |
| T | short tons (2,000 lb) | 0.907 | megagrams | Mg |
| | | **VOLUME** | | |
| fl oz | fluid ounces | 29.57 | milliliters | mL |
| gal | gallons | 3.785 | liters | L |
| ft³ | cubic feet | 0.0328 | meters cubed | m³ |
| yd³ | cubic yards | 0.0765 | meters cubed | m³ |

NOTE: Volumes greater than 1,000 L shall be shown in m³.

| | | **TEMPERATURE (exact)** | | |
|---|---|---|---|---|
| °F | Fahrenheit temperature | 5/9 (after subtracting 32) | Celsius temperature | °C |

## APPROXIMATE CONVERSIONS FROM SI UNITS

| Symbol | When You Know | Multiply by | To Find | Symbol |
|---|---|---|---|---|
| | | **LENGTH** | | |
| mm | millimeters | 0.039 | inches | in |
| m | meters | 3.28 | feet | ft |
| m | meters | 1.09 | yards | yd |
| km | kilometers | 0.621 | miles | mi |
| | | **AREA** | | |
| mm² | millimeters squared | 0.0016 | square inches | in² |
| m² | meters squared | 10.764 | square feet | ft² |
| m² | meters squared | 1.20 | square yards | yd² |
| km² | kilometers squared | 0.39 | square miles | mi² |
| ha | hectares (10,000 m²) | 2.53 | acres | ac |
| | | **MASS (weight)** | | |
| g | grams | 0.0353 | ounces | oz |
| kg | kilograms | 2.205 | pounds | lb |
| Mg | megagrams (1,000 kg) | 1.103 | short tons | T |
| | | **VOLUME** | | |
| mL | milliliters | 0.034 | fluid ounces | fl oz |
| L | liters | 0.264 | gallons | gal |
| m³ | meters cubed | 35.315 | cubic feet | ft³ |
| m³ | meters cubed | 1.308 | cubic yards | yd³ |
| | | **TEMPERATURE (exact)** | | |
| °C | Celsius temperature | 9/5 (then add 32) | Fahrenheit temperature | °F |

°F  -40   0   32   98.6   212
°C  -40  -20  0  20  37  40  60  80  100
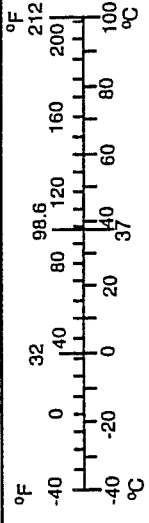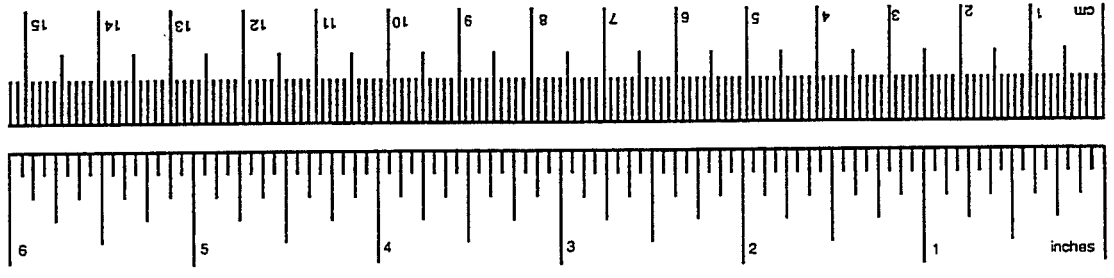
These factors conform to the requirement of FHWA Order 5190.1A.

* SI is the symbol for the International System of Measurements

# CHAPTER 1
# INTRODUCTION

## 1.1    Problem Statement

There are many older rural off-system short span steel bridges in Texas which must be periodically rated for capacity and overall condition. Typical construction consists of a timber or concrete deck supported by steel stringers. Depending upon the details of construction, the capacity of a stringer may be limited by lateral torsional buckling considerations to a value less than the yield strength of the material. Bracing is frequently provided to increase the buckling strength. This can take the form of cross frames between the stringers at discrete points located intermittently along the span or by continuous bracing provided by composite action between the stringer and deck. A common problem with short span off-system bridges is that no intermediate bracing between stringers or positive connection of the deck to the stringers has been provided, thus apparently rendering the compression flange unsupported over the full span. An engineer charged with the responsibility of evaluating the capacity of such a bridge system faces a difficult task. An assumption that the steel stringers are laterally unbraced over the full span often results in a calculated capacity which is much lower than the loads these bridges actually support. The apparent observed strength has led to the contention that the stringers are braced at the location of the truck wheels. The deck, though not positively attached, increases the lateral buckling strength of the steel stringers by providing some degree of lateral and/or torsional restraint. An understanding of the bracing characteristics provided by the deck to the supporting stringers is necessary for an engineer to properly evaluate the capacity of the overall bridge system.

## 1.2    Objectives and Scope

The purpose of the research project was to determine the bracing requirements to increase the lateral buckling capacity of beams and to determine the bracing contribution of typical bridge decks. The concept of the truck wheel location as a brace point was to be investigated. While the research was directed principally toward short span steel bridges, the bracing principles and design recommendations herein are applicable to steel beams in general. Also, the stability bracing requirements and recommendations presented herein should not be confused with the lateral bracing requirements for lateral forces such as wind in Section 10.21 of the 1992 AASHTO Bridge Specification. There are no beam stability bracing requirements in AASHTO at the present time.

The research was divided into three main phases: theoretical studies, beam experiments and full-size bridge test. The theoretical studies were conducted on beams with a variety of loading conditions and bracing arrangements which form the basis of the design recommendations. These bracing studies and design recommendations are presented in Chapter 2. Experimental studies were conducted on twin 24-ft. long W12 X 14 steel beams with concentrated loads at midspan to check the validity of the theoretical studies. Beams with different levels of initial out-of-straightness and brace sizes were tested. Different types of bracing and stiffener details at the brace points were also considered. Chapter Three contains the results of the seventy-six twin-beam experiments and comparisons with the theoretical studies. A full-size, five-girder steel bridge with a wooden deck was tested to failure using a standard truck axle to study the bracing effect of an actual unattached deck. The bridge test results are presented in Chapter Four. Recommendations for bracing design and an evaluation of some typical short span bridges are given in Chapter Five. In the remaining sections of this chapter, a general review of the lateral-torsional buckling

phenomenon and the lateral buckling provisions in the AASHTO Bridge Specification are given along with a general discussion of the types of stability bracing.

## 1.3    Beam Buckling Strength

The flexural capacity of beams with large unbraced lengths is often limited by a mode of failure known as a lateral torsional buckling which generally involves both an out-of-plane displacement and a twist of the beam cross section as shown in Figure 1.1. Timoshenko (1961) presented the following equation for the elastic critical buckling moment of a doubly-symmetric beam under uniform moment.



θ Angle of Twist

Center of Rotation

Section A-A
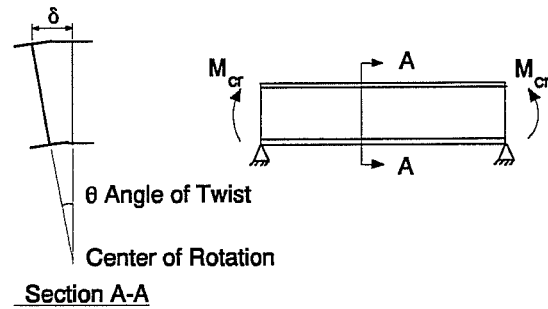
Figure 1.1    Geometry of buckled beam.

$$M_{cr} = \frac{\pi}{L_b} \sqrt{EI_y GJ + \frac{\pi^2 E^2 I_y^2 h^2}{4L_b^2}} \qquad (1.1)$$

where $L_b$ = unbraced length, E = modulus of elasticity, $I_y$ = weak axis moment of inertia, G = shear modulus, J = St. Venant's torsional constant, and h = distance between flange centroids. Equation 1.1, which was derived by Timoshenko in 1913, is applicable to beams where the twist at the ends of the unbraced length is prevented. The first term under the radical denotes St. Venant torsional resistance of the cross section while the second term is related to the warping torsional resistance. The unbraced length used in this equation should be the distance between points of full lateral support (no twist).

When a beam load causes a non-uniform moment diagram, the lateral buckling capacity may be significantly greater than that given by Eq. (1.1). For a non-uniform moment diagram a modifying factor, $C_b$, may be applied to account for portions of a beam which are subjected to a lower moment due to a moment gradient along the span. The 1990 AASHTO Bridge Specification $C_b$ factor for moment gradient between brace points is

$$C_b = 1.75 + 1.05 \left[ \frac{M_1}{M_2} \right] + 0.3 \left[ \frac{M_1}{M_2} \right]^2 \le 2.3 \qquad (1.2)$$

where $M_1$ is the smaller and $M_2$ is the larger end moment in the unbraced segment of the beam. However, this equation is only applicable to cases with a linear moment gradient between brace points. The 1990 AASHTO conservatively suggests $C_b = 1.0$ when the maximum moment occurs between brace points, but AASHTO does permit the use of more exact $C_b$ factors for such cases as given in the SSRC Guide (Galambos, 1988). For a simply supported unbraced beam with a concentrated load at midspan, $C_b = 1.35$ which represents a 35% increase in allowable buckling moment over the $C_b = 1.0$ approximation.

The critical buckling moment is affected by the location of the load point with respect to the centroid of the cross section. In general, buckling strength is significantly reduced when load is applied above the centroid, due

to an increase in twist caused by the eccentricity; buckling strength is significantly increased when load is applied below the centroid, due to a reduction in twist caused by the restoring action of the eccentric load. When the first term under the radical of Eq. (1.1) dominates, load position will have only a small effect on the critical buckling moment. If the second term under the radical dominates, load position will have a significant effect on the buckling moment. If the load point is also a full brace point, load position will have no effect since the load does not twist during buckling. The top flange loading effect can be handled exactly by factors given in the SSRC Guide (Galambos, 1988) or approximately by neglecting the warping term in Eq. (1.1). The solutions presented so far have assumed that the cross section does not distort; that is, the two flanges and the web rotate through the same angle of twist at buckling. This assumptions is accurate (error < 5%) for the loading and support conditions in Figure 1.1 if the beam has an unstiffened web slenderness ratio less than 200 which covers most cases. For braced beams and other loading conditions, cross section distortion may have a significant effect on buckling strength as shown later in this report.

The load position effect discussed above assumes that the load remains vertical during buckling and passes through the plane of the web. In the laboratory, a top flange loading condition is achieved by loading through a knife edge at the middle of the flange. In bridges the load is applied to the stringers through secondary members or the bridge deck itself. Loading through the deck provides beneficial "tipping" effect illustrated in Figure 1.2. As the beam tries to buckle, the contact point shifts from mid-flange to the flange tip resulting in a restoring torque which increases the buckling capacity. This tipping effect phenomenon has been studied theoretically by Flint (1951a) and Fischer (1970) assuming no cross section distortion. Under this condition, they found that no twist could occur at the load point, so this position would be a brace point. Buckling could only occur between supports. Unfortunately, cross section distortion severely limits the beneficial effects of tipping. Linder (1982, in German) has developed a solution for the tipping effect which considers the flange-web distortion. The test data indicates that a cross member merely resting (not positively attached) on the top flange can significantly increase the lateral buckling capacity. The tipping solution is sensitive to the initial shape of the cross section and location of the load point on the flange. Because of these difficulties, it is recommended that the tipping effect be considered in design only when cross section distortion is prevented by stiffeners. In this case, the load point can be considered a brace point. Unfortunately, in a bridge structure subjected to moving concentrated loads, stiffening the web at the load point is impractical.

For an ideal, perfectly straight beam, there are no out-of-plane deformations until the moment reaches the critical value given by Eq. (1.1), modified by $C_b$ and load height effects if applicable. At buckling the ideal beam suddenly moves laterally and twists. Real beams have some initial out-of-straightness which alters the ideal behavior. Figure 1.3 shows the theoretical behavior from the finite element program ABAQUS for twin beams loaded at the top flange at midspan. The W12 X 14 sections were not stiffened or braced at midspan but they were linked together. The top flange of both beams was initially deflected in the same direction 0.16-in. out-of-plane. The solution labeled BASP represents the idealized buckling behavior at P



Restoring Torque
(a)

Cross Section Distortion
(b)
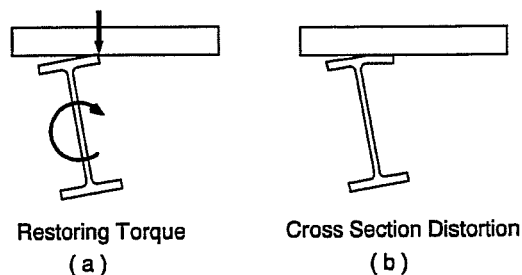
Figure 1.2    Tipping effect.

4
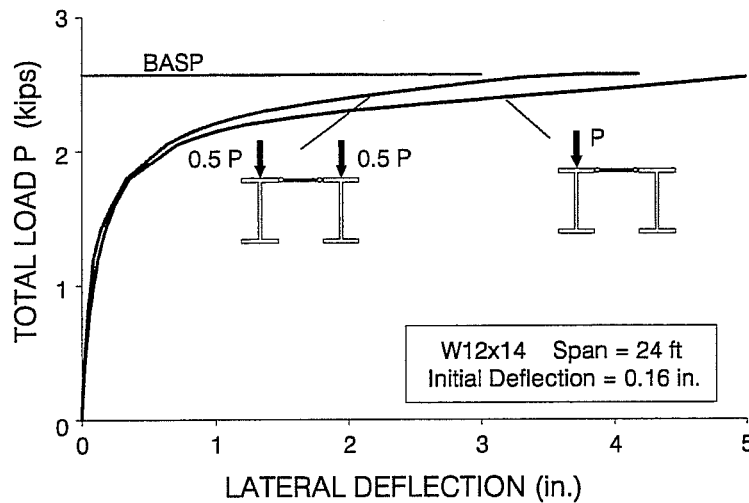


Figure 1.3    Twin girders with initial lateral displacement.

= 2.6 kips. When the two beams were loaded equally they deflected laterally 0.5 in. at approximately 80% of the buckling load. Lateral deflections increased rapidly to 3.0 in. as the load reached the buckling load. When only one of the beams was loaded, the system still carried the same total load. The beam with no load was able to partially "brace" the loaded beam until the load reached twice the individual beam buckling capacity Thus, in systems in which the beams are linked together at the load point, through friction or actual attachments, lateral buckling at the load point will not occur until the total system load reaches the sum of the individual beam buckling capacities (2 x 1.3 kips in this example). The load distribution among the individual stringers or girders is only important for checking yielding or buckling considering the load point as a brace point. That is, the other adjacent girders may have sufficient lateral buckling strength to fully brace on stringer at the load point. This beam behavior is analogous to the ΣP concept used for columns in unbraced building frames (Yura, 1971). One column cannot sway alone; all the columns in a story must sway The sum of the individual stringer strengths will be illustrated in the evaluation of the full-size five girder bridge test.

## 1.4    AASHTO Bridge Specification

Prior to 1989, the American Association of State Highway and Transportation Officials Bridge Specification, hereinafter referred to as AASHTO, recommended that beam buckling be treated as inelastic column buckling and that the following equation be utilized in Load Factor Design (LFD):

$$M_u = F_y \, S_x \left[ 1 - \frac{3F_y}{4 \, \pi^2 \, E} \left[ \frac{L_b}{b'} \right]^2 \right] \tag{1.3}$$

where $M_u$ = lateral torsional buckling moment; $F_y$ = yield stress of the material; $S_x$ = major axis section modulus; $L_b$ = unbraced length; $b'$ = flange width/2. In Allowable Stress Design (ASD), the allowable moment at service

load was based on Eq. (1.3) with a factor of safety of 1.82 which limits the maximum allowable moment to 0.55 $F_y S_x$.

In the 1990 Interim AASHTO, a more accurate and less conservative equation was adopted for the determination of beam buckling strength, based on the Timoshenko formula, Eq. (1.1).

$$M_r = 91 \times 10^6 \, C_b \, \frac{I_{yc}}{L_b} \sqrt{0.772 \, \frac{J}{I_{yc}} + 9.87 \left( \frac{d}{L_b} \right)^2} < M_y \qquad (1.4)$$

where $I_{yc}$ = weak axis moment of inertia of compression flange, J = torsional constant = $(2bt^3 + dw^3)/3$, d = depth of beam, t = flange thickness, w = web thickness, $M_y$ = yield moment and $M_r$ is the maximum strength in lb-in. units. $C_b$ is the modification factor for the moment diagram within the unbraced length discussed previously. Equation (1.4) is more general than Eq. (1.1) because it is applicable to unsymmetric girders. For cross sections with equal flanges, Eqs. (1.1) and (1.4) give almost identical results.

Figure 1.4 shows values of beam buckling strength given by the 1983 and 1990 AASHTO specifications for a S6 X 12.5 beam with $F_y$ = 42 ksi. As can be seen from the graph, the 1983 AASHTO buckling formula gives very conservative estimates of strength. In cases where the unbraced length is greater than 13 feet, the formula gives negative capacities. For example, for an unbraced length of 13 feet, the 1983 formula gives 0 k-ft whereas the 1990 formula with $C_b$ = 1.35 gives 20.74 k-ft ($M_y$ = 25.8 k-ft).

To counteract the unrealistic predictions given by the AASHTO Specifications prior to 1990, it has been common practice to assume that the truck wheel at midspan, which is the controlling loading condition for short span bridges, provides lateral support at that point. If this assumption is made in the previous example, the unbraced length would be assumed as 6.5 ft and the 1983 AASHTO formula would give a buckling moment $M_u$ = 19.6 k-ft, a very significant increase from the no-brace case. Now that AASHTO has adopted a less conservative buckling strength formula, it is even more important to establish the validity of the truck wheel as a brace point.

## 1.5    Beam Bracing

When a beam experiences lateral torsional buckling there is a relative lateral movement between the top and bottom flanges of the beam, as shown in Figure 1.1. An effective beam brace resists twist of the cross section. As a simply supported beam buckles, the lateral deflection of the tension flange is usually small when compared with that of the compression flange. Such a beam is considered to be braced at a point when lateral displacement of the compression flange is
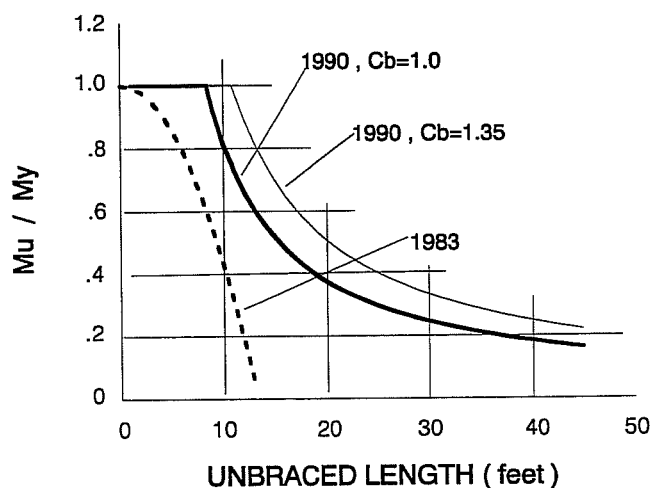


Figure 1.4    Comparison of AASHTO beam buckling strengths.

6

prevented since twist of the cross section is also restricted. In the case of twin beams with a diaphragm or cross frame between the members, lateral displacement of the system is permitted at the cross frame. This location, while able to displace laterally, is still considered a brace point because twist is prevented.

In general, bracing may be divided into two main categories, lateral and torsional bracing, as illustrated in Figure 1.5. Lateral bracing restrains lateral displacement of the top flange as its name implies. The effectiveness of a lateral brace is directly related to the degree that twist of the cross section is restrained. For the uniform moment case illustrated in Figure 1.1, the center of twist is located at a point near or outside of the tension flange. A lateral brace is most efficient in restricting twist when it is located at the top flange. Lateral bracing applied at the bottom flange of a simply supported beam is almost totally ineffective. A torsional brace can be differentiated from a lateral brace in that twist of the cross section is restrained directly, as in the case of cross frames or diaphragms located between adjacent stringers. Braces can be continuous along

## LATERAL BRACING



Beam "b" has lower load so it can laterally brace the top flange of girder "a".

buckled shape if framing is weak

buckled shape if framing is strong

Girder    Top Flange Framing

PLAN VIEW

Metal Deck Forms

## TORSIONAL BRACING



Diaphragms

Cross Frames

Through Girders

floor beam

PLAN VIEW

Decking

A        A

BUCKLED SHAPE

SECT A - A

Figure 1.5    Types of bracing.

the beam span as with metal deck forms or located at discrete points as with cross frames. Some systems such as concrete decks can act both as lateral and torsional braces.

In the case of a wood or concrete deck resting on steel stringers, there can be restraint from different sources. The friction that may be mobilized at the deck-beam interface acts as a lateral brace, since it restrains lateral movement of the top flange as shown in Figure 1.6a if the deck has lateral stiffness. As the beam tries to twist during buckling, the deck planks provide torsional restraint in two ways. For the plank supporting the wheel loads there are contact forces $P_0$ on the beam as shown in Figure 1.6a. There can be a restraining moment $M = 6EI\theta/S$ provided by the deck even when there is no positive attachment between the deck and steel stringer. In such cases M will produce contact force $P_1$ given by the relationship $P_1 a = 6EI\theta/S$ which is valid if $P_1 < P_0$. When the angle $\theta$ gets sufficiently large so $P_1 = P_0$, one side of the flange will separate from the wood plank and the restraint provided by the wood deck (6EI/S) goes to zero. However, at this stage the force on the other flange tip is $2P_0$ which provides a beneficial restoring torque for lateral stability called "tipping effect." In reality, the bracing may
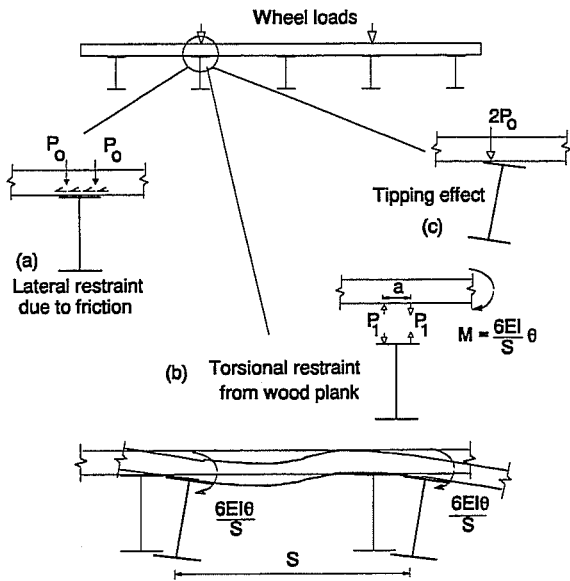
Figure 1.6       Bracing restraint of a deck.

be a combination of lateral, torsional and tipping restraint.

Some of the factors that affect the effectiveness of a brace are shown in Figure 1.7. A lateral brace should be attached where it best resists the twist. For a cantilever beam in (a), the best location is the top tension flange, not the compression flange. Top flange loading reduces the effectiveness of a top flange brace because such loading causes the center of twist to shift toward the top flange as shown in (b). Larger lateral braces are required for top flange loading. If a brace is located above the top flange, by cross members, the compression flange can still deflect laterally if cross section distortion is not prevented by stiffeners. In the following chapter the effect of loading conditions, load location and cross section distortion on beams with bracing will be discussed.
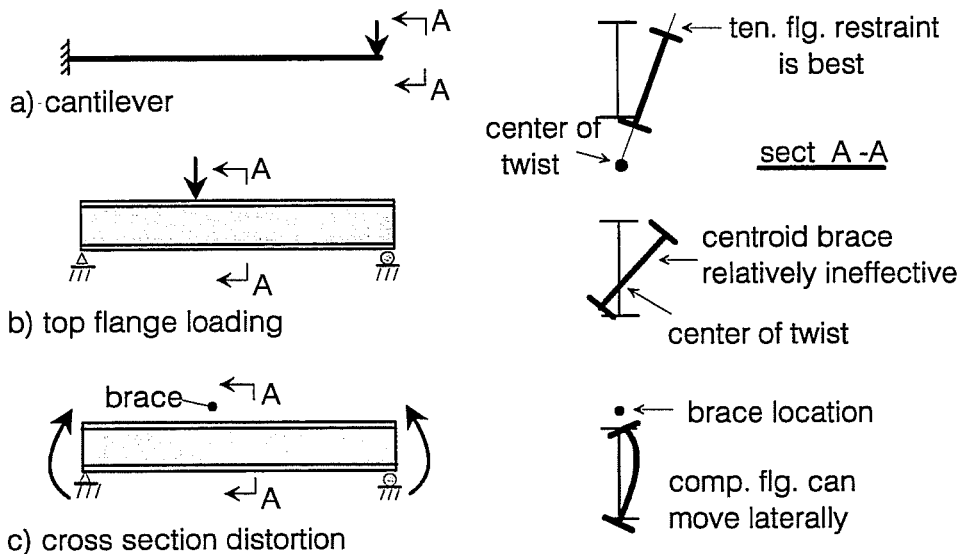


Figure 1.7      Factors that affect brace effectiveness.

# CHAPTER 2
# STRENGTH OF BEAMS WITH BRACING

## 2.1  Background

Trahair and Nethercot (1982) provide a summary of the various theoretical studies that have been conducted on beams with continuous and discrete braces. The general solutions provided are in many instances complicated for design purposes or are in graphical form which are difficult to incorporate into design codes. Most of the solutions did not consider the possibility of cross section distortion which may be important. Winter (1958) established that bracing must possess both stiffness and strength, and that initial out-of-straightness of the member has a significant effect on brace requirements. Most published solutions and recommendations for bracing consider only stiffness, not strength. Some of the important previous research on beam bracing is discussed in an earlier report (Yura and Phillips, 1992).

In order to develop a general design approach for beam bracing, beams with various bracing arrangements, sizes, details and types were analyzed using the finite element computer program, BASP. BASP, an acronym for Buckling Analysis of Stiffened Plates, was developed at The University of Texas by Akay (1977) and extended for use on a personal computer by Choo (1987). The BASP program will handle many types of restraints including lateral and torsional braces at any node point along the span. It is limited, however, to elastic modeling of initially straight beams with loads acting only in the plane of the web. Due to these limitations, the effects of initial imperfections were not studied using this program. However, BASP does account for web distortion and was used extensively in the development of basic design equations for straight beams. These results were extended to beams with initial out-of straightness using an adaptation of Winter's approach.

In the following sections BASP results for beams with lateral bracing, torsional bracing and combinations of lateral and torsional bracing are presented. These results are used to study the effects of various brace and load conditions and to develop the bracing recommendations later in this report.

## 2.2  Lateral Bracing of Beams

### 2.2.1  Behavior.
The uniform moment condition is the basic case for lateral buckling of beams. If a lateral brace is placed at the midspan of such a beam, the effect of different brace size (stiffness) is illustrated by the BASP solutions for a W16X26 section 20 ft long in Figure 2.1. For a brace attached to the top (compression) flange, the beam buckling capacity initially increases almost linearly as the brace stiffness increases. If the brace stiffness is less than 1.6 k/in., the beam buckles in a shape resembling a half sine curve. Even though there is lateral movement at the brace point, the load increase
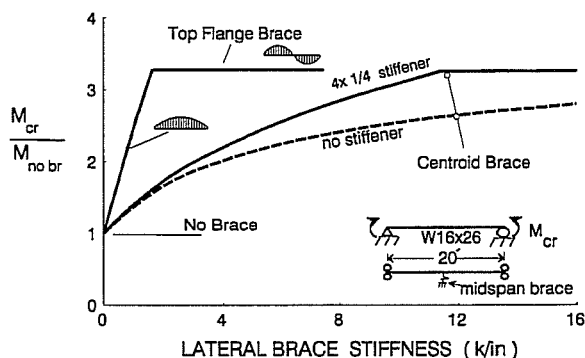


Figure 2.1  Effect of lateral brace location.
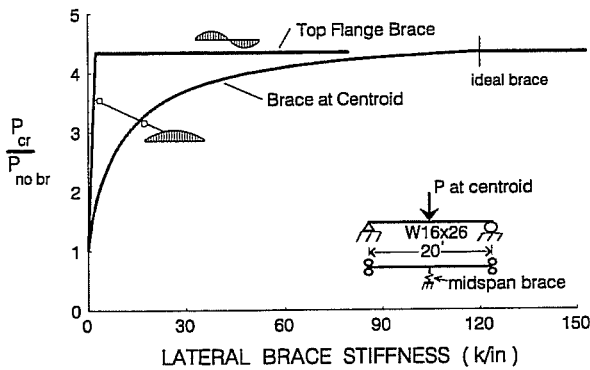
Figure 2.2  Midspan loading - effect of brace location.
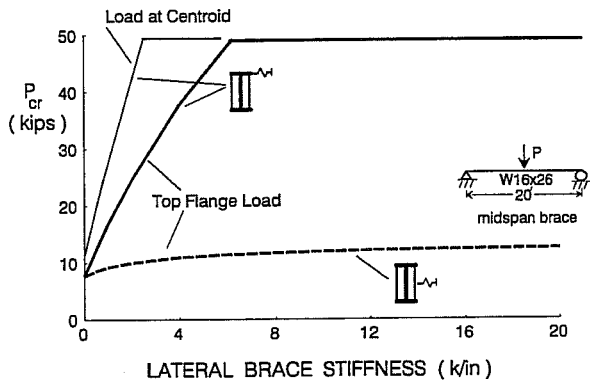


Figure 2.3  Effect of load position.

can be more than three times the unbraced case. The brace stiffness required to force the beam to buckle between lateral supports is called ideal brace stiffness, 1.6 k/in. in this example. Any brace stiffness greater than this value does not increase the beam buckling capacity and the buckled shape is a full sine curve. When the brace is attached at the top flange, there is no cross section distortion. No stiffener is required at the brace point.

A lateral brace placed at the centroid of the cross section requires an ideal stiffness of 11.4 k/in. if a 4 X 1/4 stiffener is attached at midspan and 53.7 k/in. (off scale) if no stiffener is used. Substantially more bracing is required for the no stiffener case because of web distortion at the brace point. The centroid bracing system is less efficient than the top flange brace because the centroid brace point is closer to the center of twist located above the bottom flange.

For the case of a beam with a concentrated load at midspan, shown in Figure 2.2, the moment varies along the length the ideal centroid brace (110 k/in.) is 44 times larger than the ideal top flange brace (2.5 k/in.). For both brace locations cross section distortion had a minor effect (<3%). The maximum beam moment at midspan when the beam buckles between the braces is 1.82 times greater than the uniform moment case which is close to the $C_b$ factor = 1.75 recommended by AASHTO. This higher buckling moment is the main reason why the ideal top flange brace requirement is 1.56 times greater (2.49 vs. 1.6 k/in.) than the uniform moment case.

Figure 2.3 shows the effect of load position on the buckling strength of laterally braced beams. If the load is at the top flange, the effectiveness of a top flange brace is greatly reduced. For example, for a brace stiffness of 2.5 k/in., the beam would buckle between the ends and the midspan brace at a load close to 50 kips. If the load is at the top flange, the beam will buckle at a load of 28 kips. For top flange loading, the ideal top flange brace would have to be increased to 6.2 k/in. to force buckling between the braces. The load position effect must be considered in the brace design requirements. This effect is even more important if the lateral brace is attached at the centroid. The results shown in Figure 2.3 indicate that a centroid brace is almost totally ineffective for top flange loading. This is not due to cross section distortion since a stiffener was used at the brace point. The top flange loading causes the center of twist at buckling to shift to a position close to mid-depth for most practical unbraced lengths, as shown in Figure 1.5. Since there is virtually no lateral displacement near the centroid for top flange loading, a lateral brace at the centroid will not brace the beam. Because of cross-section distortion and top flange loading effects, lateral braces at the centroid are not recommended. Lateral braces must be placed near the top flange of simply supported
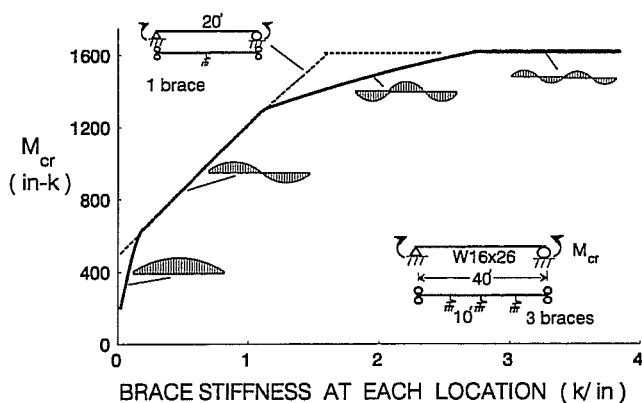
Figure 2.4  Multiple lateral braces.

Table 2.1          Ideal Brace Stiffness Requirements

| Number of Evenly Spaced Braces | Ideal Brace Stiffness |
|---|---|
| 1 | $2\,P_e / \ell$ |
| 2 | $3\,P_e / \ell$ |
| 3 | $3.41\,P_e / \ell$ |
| 4 | $3.63\,P_e / \ell$ |
| Many | $4.0\,P_e / \ell$ |

and overhanging spans.  Design recommendations will be developed only for the top flange lateral bracing situation. Torsional bracing near the centroid or even the bottom flange can be effective as discussed later.

Up to this point only beams with a single midspan lateral brace have been discussed. The bracing effect of a beam with multiple braces is shown in Figure 2.4. The response of a beam with three equally spaced braces is shown by the solid line. When the lateral brace stiffness, $\beta_L$, is less than 0.14 k/in., the beam will buckle in a single wave. In this region a small increase in brace stiffness greatly increases the buckling load. For $0.14 < \beta_L < 1.14$, the buckled shape switches to two waves and the relative effectiveness of the lateral brace is reduced. For $1.4 < \beta_L < 2.75$, the bucked shape is three waves. The ideal brace stiffness is 2.75 k/in. at which the unbraced length can be considered 10 ft. For the 20 ft span with a single brace at midspan which is shown dashed which was discussed previously, a brace stiffness of only 1.6 k/in. was required to reduce the unbraced length to 10 ft. Thus the number of lateral braces along the span affects the brace requirements. A similar behavior has been derived for columns (Timoshenko and Gere, 1961) as shown in Table 2.1 where $P_e$ is the Eular column buckling load between braces and $\ell$ is the distance between column braces. Going from one brace to three braces requires an increase in ideal column brace stiffness of $3.41/2 = 1.71$, which is the same as that shown in Figure 2.4 for beams, $2.75/1.6 = 1.72$.

Continuous lateral bracing follows the behavior shown in Figure 2.4 except that there can be no ideal brace. As the brace stiffness increases, the buckling capacity will continue to increase until the beam yields, rather than buckles. Continuous bracing solutions are generally treated separately from discrete bracing solutions (Trahair and Nethercot, 1982).

In summary, moment gradient, brace location, load location, cross section distortion, brace stiffness and number of braces affect the buckling strength of braced beams. The effect of cross section distortion can be effectively eliminated by placing the brace near the top flange. Any amount of bracing improves the strength. The use of computer programs such as BASP can be used to determine the strength of braced beams.

***2.2.2   Approximate Buckling Strength.***   The use of computer programs such as BASP can be used to determine the strength of braced beams, but such sophistication is usually warranted only in failure investigation.

12

Yura (1990) has developed the following general equation for the strength of beams braced laterally by discrete or continuous bracing.

$$M_{cr} = \sqrt{\left(C_{bu}^2\, M_o^2 + \frac{C_{bb}^2\, P_y^2\, h^2\, A}{4}\right)\left(1 + A\right)} \;\leq\; M_s \text{ or } M_y \qquad (2.1)$$

where

$$A = \frac{L^2}{\pi} \sqrt{\frac{.67\overline{\beta}_L}{C_L\, EI_y}} \qquad (2.2)$$

$$C_L = 1 + \frac{1.2}{n} \quad \left(\text{top flange loading}\right) \qquad (2.3)$$
$$= 1.0 \quad \left(\text{centroid or moment loading}\right)$$

$$P_y = \frac{\pi^2\, EI_y}{L^2} \qquad (2.4)$$

where $M_o$ is given by Eq. (1.1), assuming the beam is unbraced, $M_s$ = buckling strength assuming the unbraced length is the bracing spacing, $M_y$ = yield moment, L = span length, $\overline{\beta}_L$ = equivalent continuous lateral brace stiffness in k/in./in., A = bracing factor, n = number of discrete braces. $C_{bu}$ and $C_{bb}$ are the two limiting $C_b$ factors corresponding to an unbraced beam (very weak braces) and an effectively braced beam (buckling between the braces). $C_L$ is a top flange loading modification factor; $C_L$ = 1.0 for centroid loading. When using Eq. (2.1), a finite number of discrete lateral braces along a beam should be converted to an effective continuous lateral brace as shown in Figure 2.5. In general, multiple braces can be represented by summing the stiffness of each brace and dividing by the beam length. This approach is accurate for two or more intermediate braces. A single discrete brace at midspan can be more accurately represented as a continuous brace by dividing the brace stiffness by 75 percent of the beam length.
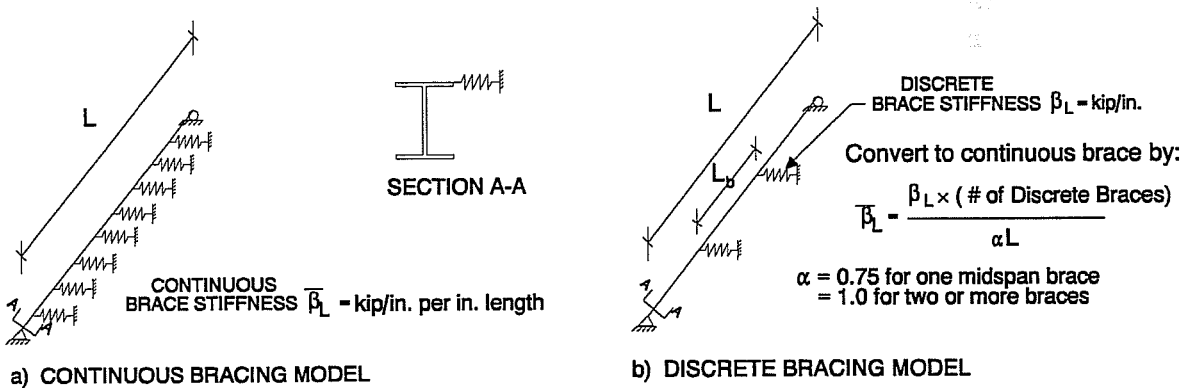


Figure 2.5  Continuous and discrete bracing.
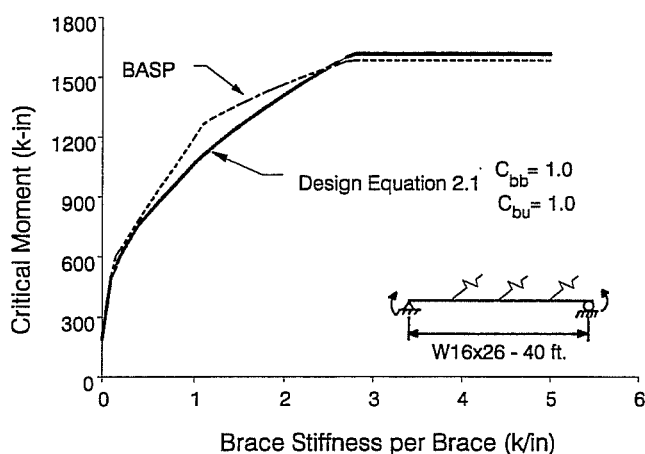
Figure 2.6    Lateral bracing with uniform moment
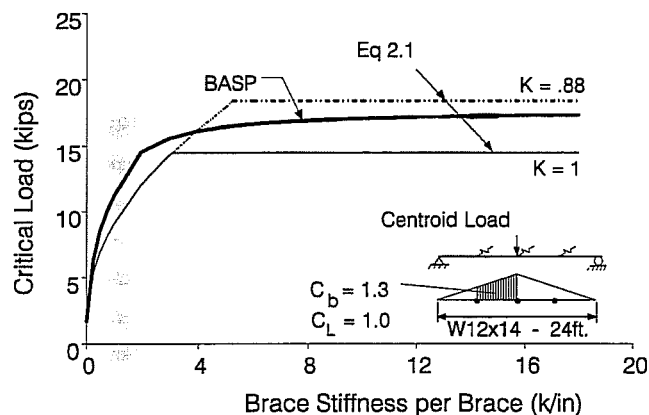


Figure 2.7    Three lateral braces with centroid midspan loading.

Equation (2.1) has no limit except yielding as the stiffness of continuous bracing is increased. When Eq. (2.1) is used with discrete braces, the critical moment must be limited to the value corresponding to buckling between the braces, $M_s$. Also $M_{cr}$ is not valid beyond the yield moment. Figure 2.6 shows a comparison of Eq. (2.1) and solutions given by the BASP program for W 16X26 beam under uniform moment with three equally spaced braces. Equation (2.1) shows good agreement with the theoretical solution. In this case, both $C_b$ factors are 1.0 and $C_L$ = 1.0 for moment loading.

In Figure 2.7, the approximate bracing Eq. (2.1) is compared to the exact theory for a simple span beam with three lateral braces on the top flange and a midspan concentrated load at the centroid. Buckling between all three braces has been reached as denoted by the K = 1 curve. The limiting moment, $M_s$, was calculated by Eq. (1.1) with the AASHTO $C_b$ factor of 1.3 corresponding to $M_1 / M_s = -0.5$.

In this example, $C_{bu} = 1.35$ from the SSRC Guide (Galambos, 1988), the $C_b$ factor for an unbraced beam with a concentrated load at midspan. AASHTO conservatively recommends 1.0 for this case. $C_{bb} = 1.3$ for the critical braced span. In this example the two $C_b$ values are similar. For centroid load, $C_L = 1.0$. The conservatism of the design equation at high load level is due to the method used to determine the buckling moment between brace points. Each unbraced length was treated independently and for equal brace spacing, the interior unbraced lengths are critical. The moment levels are much higher between the midspan brace and the 1/4-span brace and the interior section also has the lowest $C_b$ factor. The exterior spans are not critical so they provide additional lateral restraint to the interior spans. The out-of-plane restraint provided to the most critical portions of the beam can be accounted for through the use of an effective length factor, $KL_b$, as outlined in the SSRC Guide (Galambos, 1988). For the example shown, K = 0.88 was determined. The buckling solution given by Eq. (2.1) is unconservative at the high load levels associated with K < 1.0, therefore the use of effective length factors for lateral buckling of beams is not to K = 1.0; conversely, a large brace is required to force buckling between the braces when the load in each unbraced length is not uniform. In the example problem, a brace stiffness = 1000 k/in. was still not sufficient to reach a K = 0.88. The AASHTO Specification does not use effective length factors for beams.

The effect of top flange loading on the buckling capacity of laterally braced beams is illustrated in Figure 2.8. The $C_L$ factor in Eq. (2.1) varies with the number of braces since it was found that the difference in required

Figure 2.8    Three lateral braces with top flange loading.
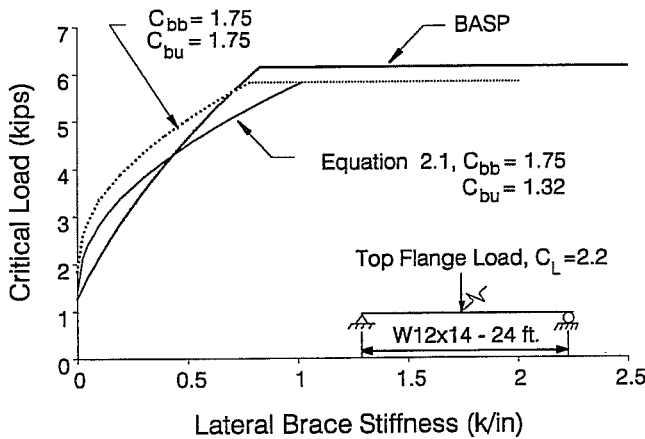


Figure 2.9    Midspan lateral brace and top flange loading.

stiffness of lateral braces due to load position decreased as the number of braces increased. For one brace $C_L$ = 2.2; for three braces, $C_L$ = 1.4. Figure 2.8 shows good correlation between the bracing equations and the exact solution. $M_o$ in Eq. (2.1) is the beam capacity assuming no bracing which should consider the effect of top flange loading. The SSRC Guide recommendations give load position effects. The top flange loading effect can also be approximated by neglecting the warping term in Eq. (1.1). This approach was used in all examples with top flange loading.

For the case of one lateral brace and top flange loading at midspan in Figure 2.9, the comparison between Eq. (2.1) and the exact theory is not as good as the previous cases. The buckling equation is conservative as the load approaches the limit of buckling between the braces. The equation indicates that a brace stiffness of about 1 k/in. is required to force the beam to buckle between braces (ideal brace). The theory indicates 0.8 k/in. would be sufficient. Since this amount of bracing is still extremely small, the difference has little practical significance. At low loads the bracing equation is unconservative. The difficulty of developing a simple expression that accurately predicts the buckling load for any brace stiffness is illustrated in this figure. At low load $C_b$ = 1.32; at $M_s$, $C_b$ = 1.75. The effect of top flange loading on bracing increases as the load increases. Once the beam buckles between the braces, top flange loading then has no effect. In addition, it is more approximate to convert a single brace into an equivalent continuous brace than the multiple brace examples given earlier. In Figure 2.9, $C_L$ = 2.2 and the equivalent continuous brace stiffness was obtained by dividing the single brace stiffness (k/in) by 0.75 times the span as discussed earlier. If $C_{bu}$ = $C_{bb}$ = 1.75 is used, as shown by dashed curves, the ideal stiffness is predicted accurately but the results are unconservative for less than ideal bracing.

## 2.3    Torsional Bracing of Beams

Examples of torsional bracing systems were shown in Figure 1.5. Twist can be prevented by attaching a deck to the top compression flange of a simply supported beam, through floor beams attached near the bottom tension flange of through girders or by diaphragms located near the centroid of the stringer, as shown in Figure 2.10. Twist can also be restrained by cross frames constructed from angles that prevent the relative movement of the top and
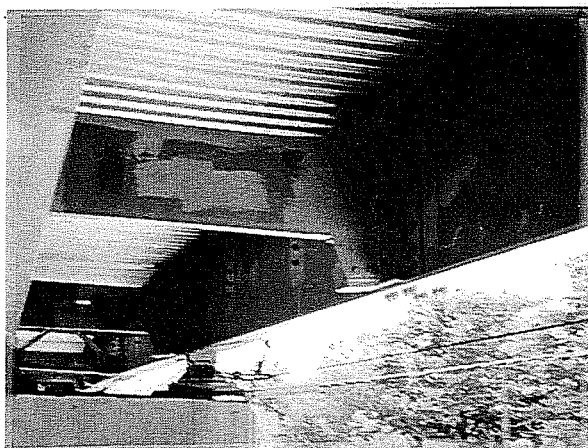
Figure 2.10    Diaphragm torsional bracing.



TORSIONAL BRACE STIFFNESS ( in-k/rad )
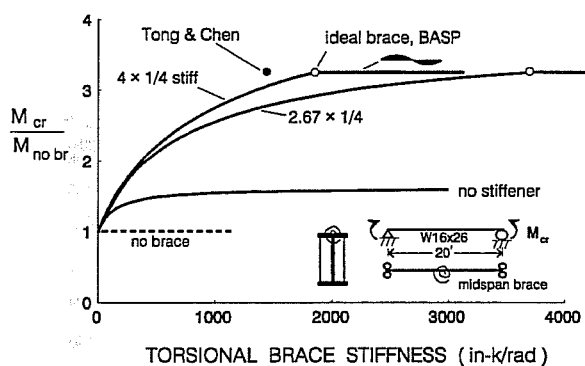
Figure 2.11    Torsional brace at midspan.

bottom flanges.  The effectiveness of torsional braces attached at different locations on the cross section will be presented.

***2.3.1    Behavior.***  The BASP solution for a simply supported beam with a top flange torsional brace attached at midspan is shown in Figure 2.11. The buckling strength - brace stiffness relationships shown in Figure 2.11 are non-linear and quite different from the top flange lateral bracing linear response given in Figure 2.1 for the same beam and loading. For top flange lateral bracing a stiffener has no effect. If no stiffener is used, the torsional brace can only increase the beam buckling capacity about fifty percent above the no brace case.  Local cross section distortion at the brace point reduces the effectiveness of the midspan brace.  Cross section distortion is illustrated in Figure 2.12 for an actual torsional bracing failure.  The W30 section on a 32-ft span was loaded and braced at midspan by the twin cross beams attached to the flange of the W30, as shown in Figure 2.12a.  The web stiffener which was a few inches short of the braced flange did not maintain the 90° angle between the flange and the web (b) and lateral buckling occurred. The torsional brace cross members prevented the W30 flange from rotating at the brace point but the local distortion shown in (c) permitted twisting of the cross section as a whole.

If a web stiffener attached to the compression flange is used with the torsional brace, then the buckling strength can be increased until buckling occurs between the braces at 3.3 times the no brace case.  The ideal or full bracing requires a stiffness of 1580 in-k/radian for a 4 X 1/4 stiffener and a 3700 in-k/radian for a 2.67 X 1/4 stiffener.  Tong and Chen (1988) have studied the buckling behavior of a simply supported beam under uniform moment.  Their solutions are applicable to doubly-symmetric or monosymmetric beams braced laterally or torsionally at the midspan.  A closed-form solution for the ideal torsional bracing stiffness for doubly-symmetric sections is given by the following equations:

$$\text{Ideal } \beta_T = \frac{2\pi \left( 8 + \alpha_c^2 \right) \sqrt{\left( 4 + \alpha_c^2 \right)}}{\alpha_c^2} \qquad (2.5)$$

16

where

$$\alpha_c^2 = \frac{4\,G\,J\,L^2}{\pi^2\,E\,I_y\,h^2} \qquad (2.6)$$

The Tong and Chen solutions do not consider web distortion which often has a significant effect on the bracing requirements. Their solutions should not be used unless substantial stiffeners are provided at the brace point. Equation (2.5) gives an ideal stiffness of 1450 in-k/radian shown by the solid dot in Figure 2.11. If this stiffness was provided, a 6 X 3/8 stiffener would be required to reach the maximum buckling load. If a 2.67 X 1/4 stiffener is attached, the buckling load is reduced by 14%; no stiffener and a brace stiffness = 1450 in-k/radian gives a 51% reduction.



TOTAL TORSIONAL BRACE STIFFNESS ( in-k/rad )
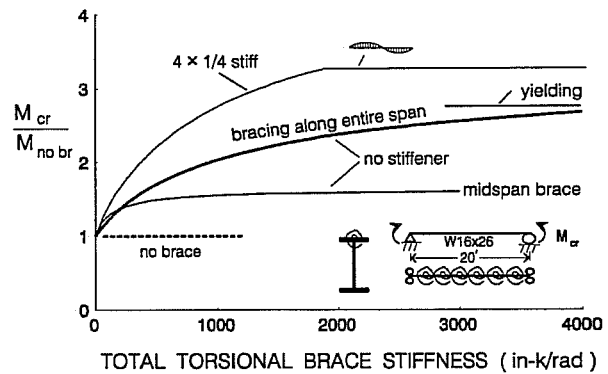
Figure 2.13   Continuous torsional bracing.



Figure 2.12   Torsional bracing failure.

If continuous bracing is placed on the top flange over the entire span with no stiffeners, there will be an increase in buckling strength as shown by the heavy line in Figure 2.13 compared to midspan brace case. The light lines are just a repetition of the single brace at midspan solutions presented in Figure 2.11. Even with continuous bracing, the 20-ft beam cannot reach load levels associated with a single brace at midspan with a stiffener to control distortion. The continuous bracing, however, does increase the buckling capacity sufficiently so that yielding, not buckling, controls the beam strength. The moment at first yield is shown in Figure 2.13. Figure 2.14 shows that torsional bracing on the tension flange (dashed line) is just as effective as compression flange bracing (solid line), even with no stiffener. If the beam has no stiffeners, splitting the bracing equally between the two flanges gives a greater capacity than placing all the bracing on just one flange. The dot-dash curve is the solution if web distortion is prevented by transverse stiffeners. The distortion does not have to be gross to affect strength, as shown in Figure 2.15, for a total torsional brace

stiffness of 3000 in-k/radian. If the W16 X 26 section has transverse stiffeners, the buckled cross section at midspan has no distortion as shown by the heavy solid lines and $M_{cr}$ = 1582 in-k. If no stiffeners are used, the buckling load drops to 1133 in-k, a 28% decrease, yet there is only slight distortion as shown by the dashed shape. The overall angle of twist for the braced beam is much smaller than the twist in the unbraced case (dot-dash curve). If the continuous torsional bracing is split 1500 in-k/radian to each flange, the capacity of the unstiffened beam would be 1416 in-k/radian and increase of 25% of the single flange braced case.
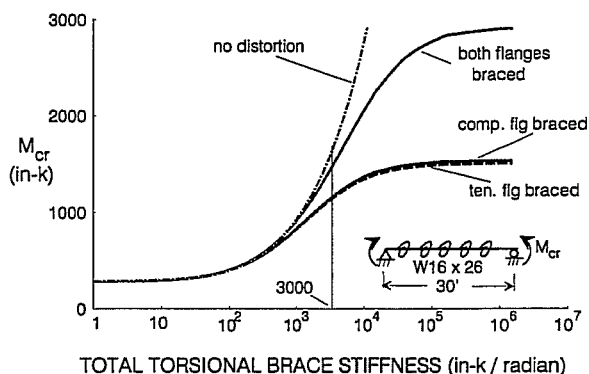


Figure 2.14    Effect of torsional brace location.

The effect of load position or torsionally braced beams is not very significant, as shown in Figure 2.16. The difference in load between the two curves for top flange and centroid loading for braced beams is almost equal to the difference in strength for the unbraced beams (zero brace stiffness). The ideal brace stiffness for top flange loading is 18% greater than for centroid loading. This behavior is different from that shown in Figure 2.3 for lateral bracing where the top flange loading ideal brace is 2.5 times that for centroid loading.
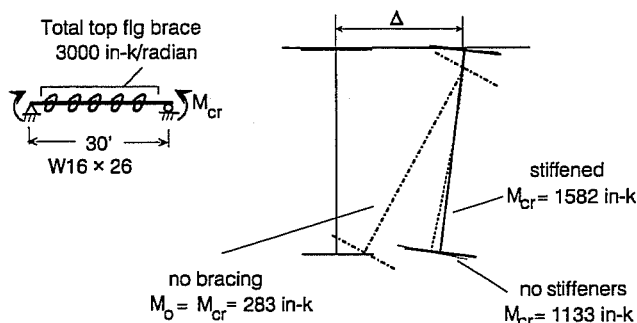


Figure 2.15    Effect of cross section distortion.

Figure 2.17 summarizes the behavior of a 40-ft span with three equal torsional braces spaced 10-ft apart. The beam was stiffened at each brace point to control the distortion. The response is non-linear and follows the pattern discussed earlier for a single brace. For brace stiffness less than 1400 in-k/radian, the stringer buckled into a single wave. Only in the stiffness range of 1400-1600 in-k/radian did multi-wave buckled shapes appear. The ideal brace stiffness at each location was slightly greater than 1600 in-k/radian. This behavior is very different from the multiple lateral bracing case for the same beam shown in Figure 2.4.



Figure 2.16    Effect of load position.

For multiple lateral bracing the beam buckled into two waves when the moment reached 600 in-k and then into three waves at $M_{cr}$ = 1280 in-k. For torsional bracing, the single wave controlled up to $M_{cr}$ = 1520 in-k. Since the maximum moment of 1600 corresponds to buckling between the braces, it can be assumed, for design purposes, that torsionally braced beams buckle in a single wave until the brace stiffness is sufficient to force buckling between the braces. The figure also shows that a single torsional brace at midspan of a 20-ft span (unbraced length = 10 ft) requires the same ideal brace stiffness as three braces spaced

18
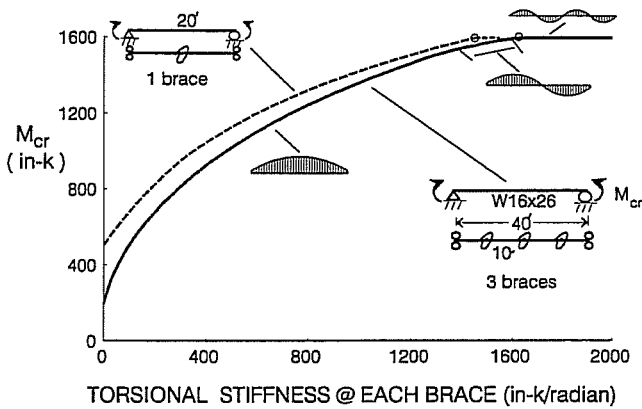


Figure 2.17 Multiple torsional braces.



TORSIONAL BRACE STIFFNESS (in-k/radian)
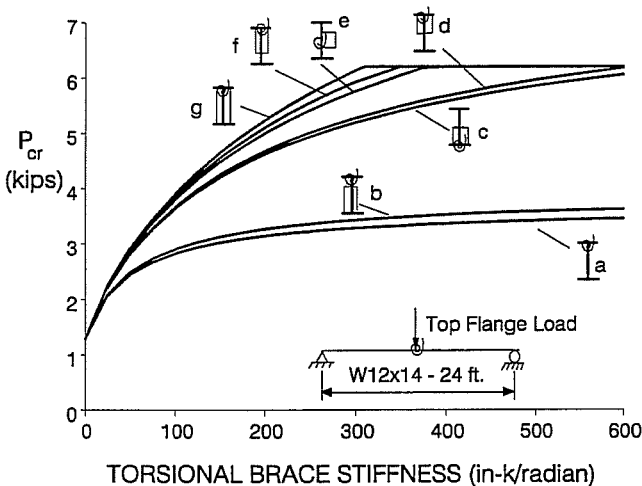
Figure 2.18 Torsional bracing details.

at 10 ft. In the lateral brace case the three brace system requires 1.7 times the ideal stiffness of the single brace system, as shown in Figure 2.4 and Table 2.1.

The effect of different brace arrangements and stiffener depths are shown in Figure 2.18 for a W12 X 14 section with a span of 24 ft with top flange loading and one midspan brace. Seven torsional bracing conditions were studied:

a)  compression flange brace - no stiffener

b)  compression flange brace - 3/4 depth stiffener attached to the tension flange

c)  tension flange brace - 1/2 depth stiffener attached to the tension flange

d)  compression flange brace - 1/2 depth stiffener attached to the compression flange

e)  centroid brace - 1/2 depth stiffener not attached to either flange

f)  compression flange brace - 3/4 depth stiffener attached to the compression flange

g)  compression flange brace - full depth stiffener attached to both flange.

The results are typical for a number of different spans and cross sections that were analyzed. If the stiffener is not attached to the flange that is braced (curve b), the behavior is very similar to the unstiffened case. Such a brace system is not capable of forcing the beam to buckle between the braces. If a half-depth stiffener is attached to the braced flange, the beam is able to reach the ideal brace condition but the required brace stiffness is almost twice that for a stiffener that is at least 3/4 depth. There is no difference in performance between compression flange torsional braces and tension flange torsional braces (curves c and d). A diaphragm placed at the centroid that is 1/2 the depth of the beam to be braced will be almost as effective as a braced flange with a full depth stiffener (compare curves e and g). In general, flange connected braces should extend at least 3/4 depth and should be attached to the braced flange. Connections for diaphragms should stiffen the web over at least 1/2 the depth for rolled beams. The detail shown in Figure 2.10 shows a full depth web connection. The stiffeners or connection angles do not have to be welded to the flanges when diaphragms are used..

## 2.3.2 Approximate Buckling Strength.

Taylor and Ojalvo (1973) give the following exact equation for the critical moment of a doubly symmetric beam under uniform moment with continuous torsional bracing
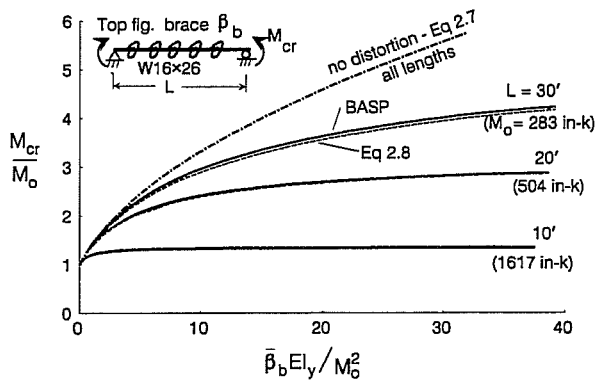
Figure 2.19    Approximate buckling formula.

$$M_{cr} = \sqrt{M_o^2 + \overline{\beta}_b E I_y} \qquad (2.7)$$

where $M_o$ is given by Eq. (1.1) and $\overline{\beta}_b$ = attached torsional brace stiffness (k-in/rad per in. length). Equation (2.7), which assumes no cross section distortion, is shown by the dot-dash line in Figure 2.19. The solid lines are BASP results for a W16 X 26 section with no stiffeners and spans of 10 ft, 20 ft, and 30 ft under uniform moment. Cross section distortion causes the poor correlation between Eq. (2.7) and the BASP results.    For discrete or continuous bracing, Milner and Rao (1978) and analytical studies using BASP showed that the effect of distortion could be handled by using an effective torsional brace stiffness, $\beta_T$ or $\overline{\beta}_b$, defined by

$$\frac{1}{\beta_T} = \frac{1}{\beta_b} + \frac{1}{\beta_{sec}} \qquad (2.8)$$

and

$$\beta_{sec} = 3.3 \, \frac{E}{h} \left[ \frac{\left( N + 1.5h \right) t_w^3}{12} + \frac{t_s b_s^3}{12} \right] \qquad (2.9)$$

where $\beta_b$ = attached discrete brace stiffness, $\beta_{sec}$ = cross section web stiffness, $t_w$ = thickness of web, h = depth of web, $t_s$ = thickness of stiffener, $b_s$ = width of stiffener, and N = contact length of the torsional brace as shown in Figure 2.20. The effective brace stiffness is less than or at best equal to the smaller of $\beta_b$ or $\beta_{sec}$. The possibility of a stiffener at the brace point is considered in Eq. (2.9) if it extends at least 3/4 depth and is attached to the brace. For continuous bracing use an effective net width of 1 in. instead of (N + 1.5h) in $\beta_{sec}$ and $\overline{\beta}_b$ in place of $\beta_b$ to get $\overline{\beta}_T$. The dashed lines in Figure 2.19 based on Eqs. (2.8) and (2.9) show good agreement with the theoretical solutions (BASP). For the 10 ft and 20 ft spans, BASP and Eq. (2.8) are almost identical. Other cases with discrete braces and different size stiffeners also show good agreement. Cross frames without web stiffeners should have a depth of at least 3/4 of the beam depth in which case distortion will have no effect and $\beta_T = \beta_b$.

Equation (2.7) can be used to represent multiple discrete torsional braces by summing the stiffness of each brace and dividing by the beam length. For a single brace at midspan the equivalent continuous brace stiffness can be found by dividing the brace stiffness of the single brace by 75 percent of the beam length. This is the same procedure that was suggested for lateral bracing in Figure 2.5. Figure 2.21 shows a comparison of Eq. (2.7) and solutions predicted by the BASP program for a beam under uniform moment with



Figure 2.20    Effective web width for distortion.

20
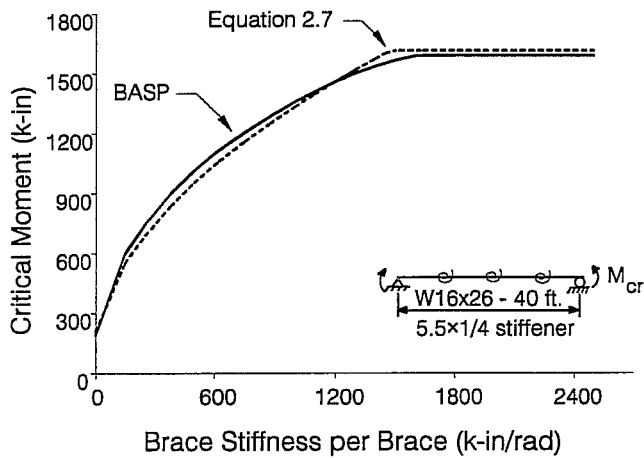


Figure 2.21    Buckling strength with three torsional braces.
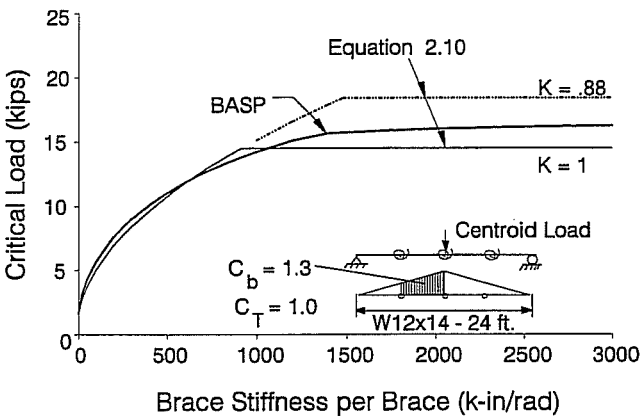


Figure 2.22    Three torsional braces - centroid loading.

three equally spaced braces (N = 0) and stiffeners at the brace points. The 5.5 X 1/4   stiffeners were large enough to make $\bar{\beta}_T \approx \bar{\beta}_b$. The excellent agreement between the BASP solutions and Eq. (2.7) limited by buckling between braces indicates that discrete braces can be represented by equivalent continuous bracing.

By adjusting Eq. (2.7) for top flange loading and other loading conditions, the following general formula can be used for the buckling strength of all torsionally braced stringers and girders:

$$M_{cr} = \sqrt{C_{bu}^2 M_o^2 + \frac{C_{bb}^2 \bar{\beta}_T EI_y}{C_T}} \leq M_y \text{ or } M_s \quad (2.10)$$

where $C_T$ = 1.2 and $C_{bu}$ and $C_{bb}$ are the two limiting $C_b$ factors corresponding to an unbraced beam (very weak braces) and an effectively braced beam (buckling between the braces). $C_T$ is a top flange loading modification factor; $C_T$ = 1.0 for centroid loading. $\bar{\beta}_T$ is the equivalent continuous torsional brace (in-k/radian/in. length) from Eqs. (2.8) and (2.9).

Figure 2.22 shows the correlation between the approximate buckling strength, Eq. (2.10) and the exact BASP solution for the case of a concentrated midspan load at the centroid with three equally spaced braces along the span. Stiffeners at the three brace points prevent cross section distortion. If a K factor of 1 is used in the buckling strength formula, the comparison between Eq. (2.10) and the BASP solution is good. Equation (2.10) should not be used with K factors less than 1.0; the results will be unconservative at high loads as shown by the dashed line in Figure 2.22. Since the load is at the centroid, $C_T$ = 1.0 and both $C_{bb}$ and $C_{bu}$ were taken as 1.3

The case of a single torsional brace at midspan shown in Figure 2.23 shows good agreement with Eq. (2.10). For the combination of one torsional brace plus top flange loading, it was found that $\bar{\beta}_T = \beta_T / L$, not 0.75L. For centroid loading, 0.75L can be used. With no stiffener, $\beta_{sec}$ from Eq. (2.9) is 114 in-k/radian. This means that the effective brace stiffness $\beta_T$ cannot be greater than 114 regardless of the magnitude of the brace stiffness at midspan. Equations (2.8), (2.9), and (2.10) predicted the buckling very accurately for all values of attached bracing, even at very low values of bracing stiffness. A 4 X 1/4 stiffener increased $\beta_{sec}$ from 114 to 11038 in-k/radian. This makes the effective brace stiffness very close to the applied stiffness, $\beta_b$. For example, with a 4 X 1/4 stiffener, the effective stiffness is 138 in-k/radian if the attached brace stiffness is 140 in-k/radian. The bracing equations can be used to determine the stiffener size necessary to reduce the effect of distortion to some tolerance level, say 5%. This
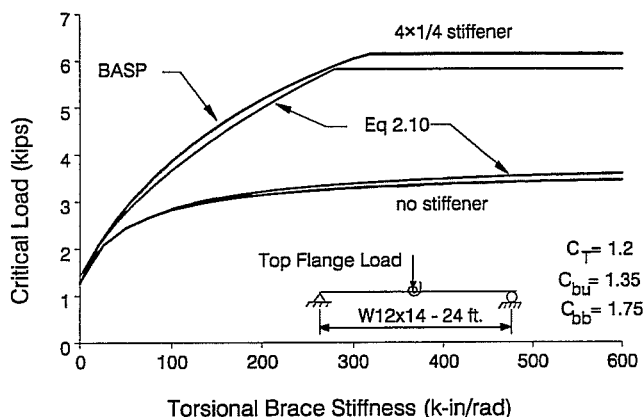
Figure 2.23  Effect of stiffener.

may be especially useful in the design of through girders where the floor beams act as torsional braces.

Equations (2.7) and (2.10) were developed for doubly symmetric cross sections. The torsional bracing effect for singly symmetric sections can be approximated by replacing $I_y$ in Eqs. (2.7) and (2.10) with $I_{eff}$ defined as follows:

$$I_{eff} = I_{yc} + \frac{h_t}{h_c} I_{yt} \qquad (2.11)$$

where $I_{yc}$ and $I_{yt}$ are the lateral moment of inertia of the compression flange and tension flange respectively,

and $h_c$ and $h_t$ are the distances from the neutral bending axis to the centroid of the compression and tension flanges respectively, as shown in Figure 2.24(a). For a doubly symmetric section $h_c = h_t$ and Eq. (2.11) reduces to $I_y$. Therefore, for doubly and singly symmetric sections

$$M_{cr} = \sqrt{C_{bu}^2 M_o^2 + \frac{C_{bb}^2 \bar{\beta}_T E I_{eff}}{C_T}} \leq M_y \text{ or } M_s \qquad (2.12)$$

A comparison between BASP solutions (solid line) and Eq. (2.12) (dashed line) for three different 40-ft. girders with seven torsional braces spaced 5 ft. apart is shown in Figure 2.24(b). The lowest curves for a W16 x 26 show very good agreement. In the other two cases, one of the flanges of the W16 x 26 section was increased to 10 x 1/2. In one case the small flange is in tension and in the other case, the compression flange is the smallest. In all cases Eq. (2.12) is in good agreement with the theoretical buckling load given by BASP.
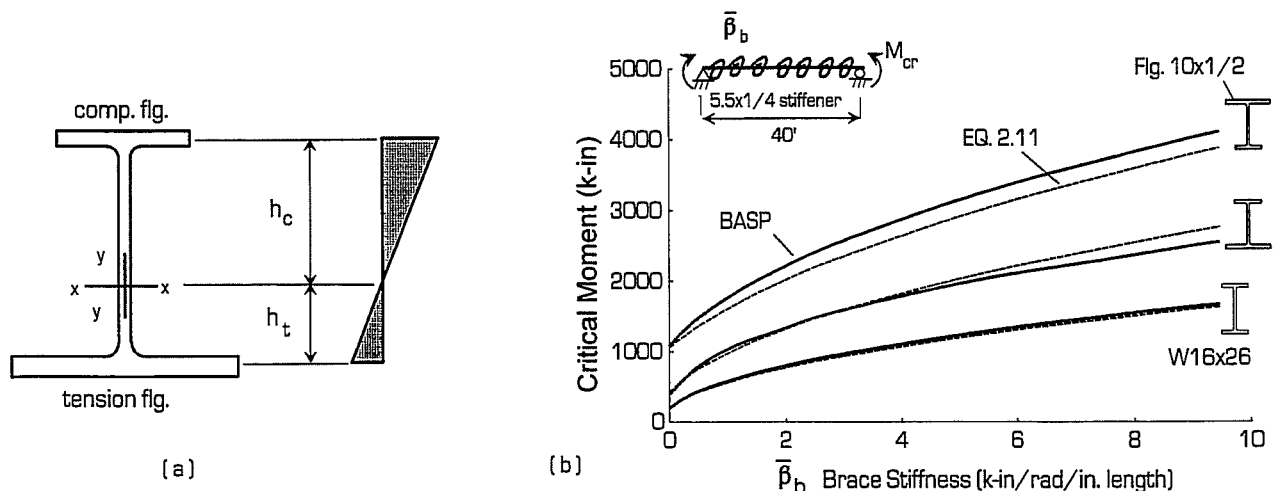


Figure 2.24  Singly symmetric girders.
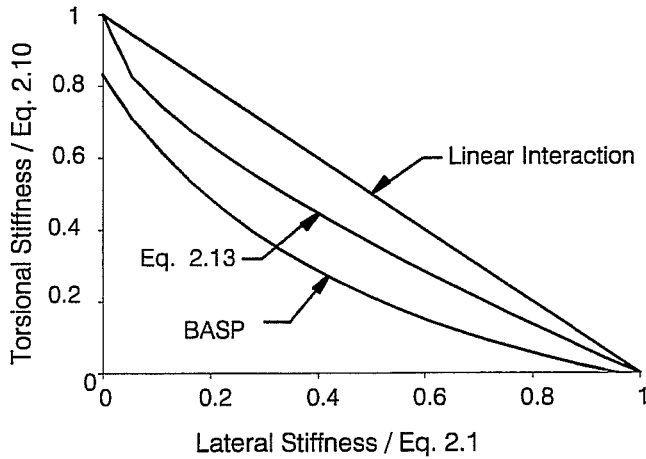
Figure 2.25      Interaction of lateral end torsional bracing.

### 2.4    Combined Lateral and Torsional Bracing

A typical interaction solution is shown in Figure 2.25 for a 24-ft W12 X 14 section braced at midspan. The theoretical bracing required to enable the section to support a moment of 212 k-ft is given by the BASP solution. This exact relationship is non-linear indicating that combined lateral and torsional bracing is more effective than torsion or lateral bracing alone. If a lateral brace stiffness of one-half the ideal stiffness is used, the BASP solution indicates that an additional torsional brace with a stiffness one-quarter of the ideal value will force the beam to buckle between braces. The BASP solution shown in Figure 2.25 agrees with the solution of combined bracing given by Tong and Chen (1988).

The Tong solution is only valid for uniform moment loading and no cross section distortion. A conservative approach for general loading and bracing conditions can be obtained by combining the equation for lateral bracing, Eq. (2.1), with Eq. (2.10) for torsional bracing

$$M_{cr} = \sqrt{ \left[ C_{bu}^2 M_o^2 + \frac{C_{bb}^2 P_y^2 h^2 A}{4} \right] \left[ 1 + a \right] + \frac{C_{bb}^2 \bar{\beta}_T E I_y}{C_T} } \leq M_y \text{ or } M_s \qquad (2.13)$$

Equation (2.11) is a conservative approximation of the interaction between lateral and torsional bracing. The line labeled "Linear Interaction" corresponds to the levels of bracing that would be required if Eq. (2.1) and Eq. (2.10 were applied independently.

The ideal torsional bracing stiffness given by Eq. (2.5) varies between ($\pi$ and $2\pi$)$h^2$ times the ideal lateral bracing for the uniform moment case when $\alpha_c$ given by Eq. (2.6) varies between 0 and 2, the practical range. This fact can be used to approximately convert torsional bracing into equivalent lateral bracing and vice versa.

### 2.5    Summary

Equations (2.1) and (2.12) will form the basis for the development of practical bracing design formulas in Chapter Five. Factors of safety must be incorporated and adjustments made for initial beam out-of-straightness. These formulas only address the <u>stiffness</u> of bracing. Strength must also be considered. At this stage, the bracing equations illustrate the significance of the moment diagram, load position, cross section distortion, and that a single formulation can handle both discrete and continuous bracing. In the following two chapters an experimental program is described which was used to check the validity of the theoretical results.

# CHAPTER 3
# TWIN BEAM BUCKLING TESTS

## 3.1    General

An experimental program, consisting of 76 tests, was designed to evaluate the effects of lateral and torsional brace stiffness, brace location, stiffener size, and initial imperfections on the lateral torsional buckling of steel beams. Two identical simply-supported beams with a 24-ft span were loaded at midspan, as shown in Figure 3.1, until buckling occurred. A twin-beam arrangement was used because the loading system and torsional bracing systems were simpler than designs with a single test beam. The buckling load determined from this beam arrangement was an average buckling load for the two beams. Figure 3.2 shows the overall test setup. Both W12X14 test beams were taken from the same mill batch of high-strength steel so that all buckling would occur in the elastic range and the same beams could be used for all bracing experiments. The measured yield strengths of the flange and web were 65 ksi and 69 ksi, respectively. Figure 3.3 shows the average measured cross section properties of the two beams. Details of the test fixtures are presented elsewhere (Yura and Phillips, 1992).
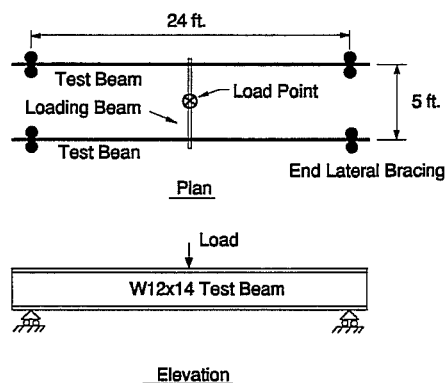
Figure 3.1    Schematic of test setup.
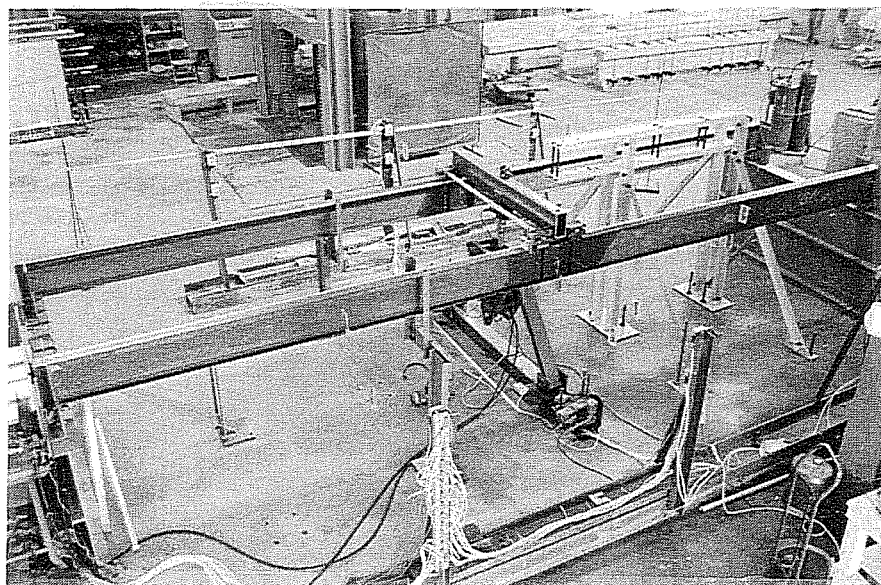


Figure 3.2    Test setup.

23

Calculated Properties

$A = 4.19\ \text{in}^2$

$I_x = 86.7\ \text{in}^4$

$S_x = 14.6\ \text{in}^3$

$I_y = 2.32\ \text{in}^4$

$S_y = 1.16\ \text{in}^3$

$J = 0.065\ \text{in}^4$

$h = 11.71\ \text{in}$

3.94"

0.220"

0.212"

0.223"

Overall Depth =11.91"

4.00"
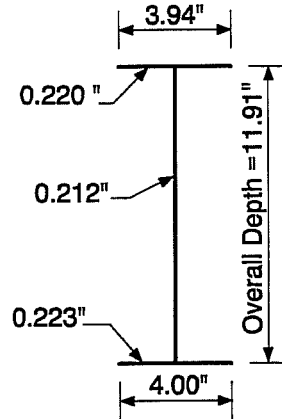
Figure 3.3   Measured properties.
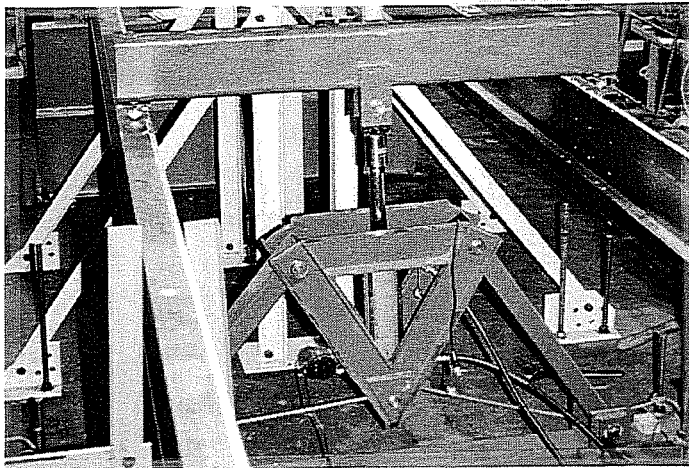


Figure 3.4   Gravity load simulator.

## 3.2   Test Setup

The test setup was designed to apply equal loads at the midspans of the two twin test beams. Bracing was also applied at or near the midspan load location. The loading system was designed to permit lateral movement and twist at the midspan and to minimize restraint to these displacements. A hydraulic jack attached to a Gravity Load Simulator mechanism (Yarimci, Yura and Lu, 1966) at the center of the loading beam, shown in Figure 3.4, permitted load to move laterally at midspan when weak bracing systems were used. Calibration tests (Yura and Phillips, 1992) showed that the GLS provided a small lateral restraint due to friction in the bearings so a small vibrating motor was attached to the GLS to further reduce the restraint. Usually knife edges at the ends of the loading beam and centered on the test beams, as shown in Figure 3.5, were used to minimize torsional restraint by the loading system. Disk bearings at the knife edges reduced out-of-plane bending restraint. For tests considering the tipping effect, the knife edges were removed and the loading beam rested directly on the full width of the flange. The knife edge system simulates the more critical top flange loading arrangement for beam buckling.

Load, lateral deflections, midspan vertical deflections, and flange rotation were recorded during testing. Load was measured using a load cell with a precision of 50 pounds located between the ram and loading tube. Lateral deflection measurements were recorded on both the top and bottom flange at the midspan and quarter points of each beam. By placing gauges at both the top and bottom flanges, the average twist of the cross section could be calculated at each gauge location. Additional measurements of twist were recorded using two electronic tilt meters. These meters were located at the midspan of one beam, one on the top flange and one on the bottom flange. Since these meters recorded the tilt of each flange near the brace point, an estimate of the cross section distortion was obtained for each test. All displacement and load readings were recorded using a computer-controlled data acquisition unit in which all data during a load cycle could be recorded within a few seconds.
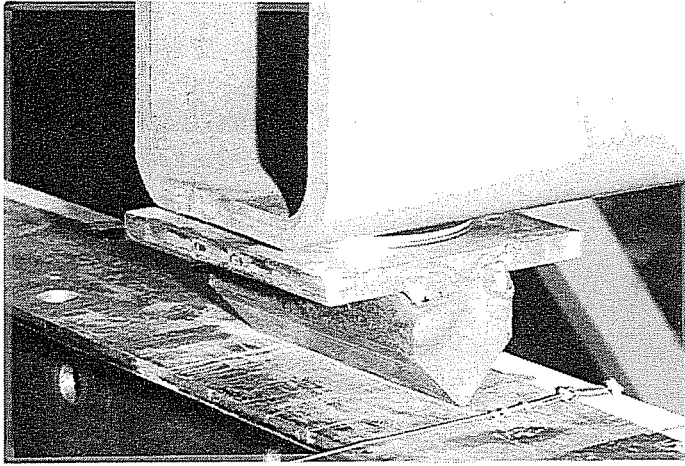
Figure 3.5  Knife edges.
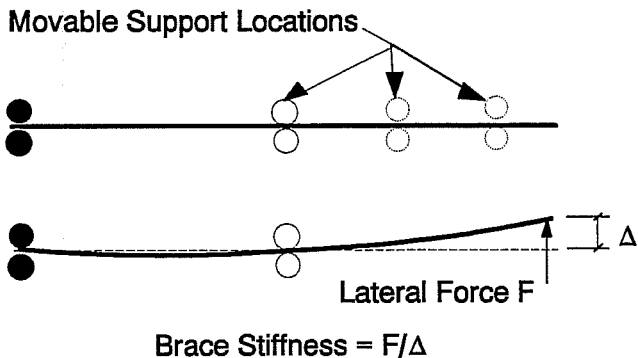


Brace Stiffness = F/Δ

Figure 3.6  Schematic of lateral brace.
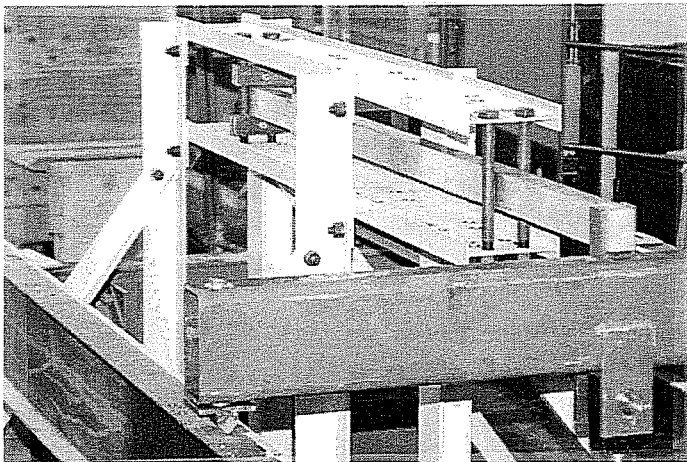


Figure 3.7  Lateral bracing system.

## 3.3    Bracing Systems

The lateral bracing was provided by a simply supported aluminum bar with an adjustable overhang (Figure 3.6). Six different levels of stiffness were provided in this fashion by simply changing the size of the aluminum bar or the location of the adjustable support. Figure 3.7 shows the lateral bracing system used in the test setup. The stiffness of the lateral bracing system was significantly affected by the stiffness of the accompanying supports, so it was necessary to obtain the effective stiffness of the bar-support system experimentally.

Torsional bracing was provided by connecting a flexible aluminum bar to each test beam spanning between the two beams. During testing the lateral deflection of the test beams forced the aluminum brace into double curvature, as shown in Figure 1.6. Since the brace is bent in double curvature, the bar stiffness is equal to $6EI/L$ of the aluminum brace. The torsional braces were attached six inches on each side of the midspan of the test beam to avoid interfering with the loading beam and to provide symmetry, as shown in Figure 3.8. The torsional brace attachment fixtures were designed to prevent the addition of any significant warping restraint to the test beams, especially for buckling in the second mode shape. This required the brace and fixtures to provide a high stiffness in the vertical plane while simultaneously providing little or no restraint in the horizontal plane. The stiffness of each torsional brace attachment fixture was determined experimentally. The calibrations showed that the fixture stiffness was sensitive to the preload in the attachment bolts to the test beams. Details of the calibration are given elsewhere (Yura and Phillips, 1992). Based on the possible variation in fixture stiffness, the torsional bracing stiffness of the system reported herein might vary between 3% for the lowest level of bar stiffness to 17% for the highest level.

26
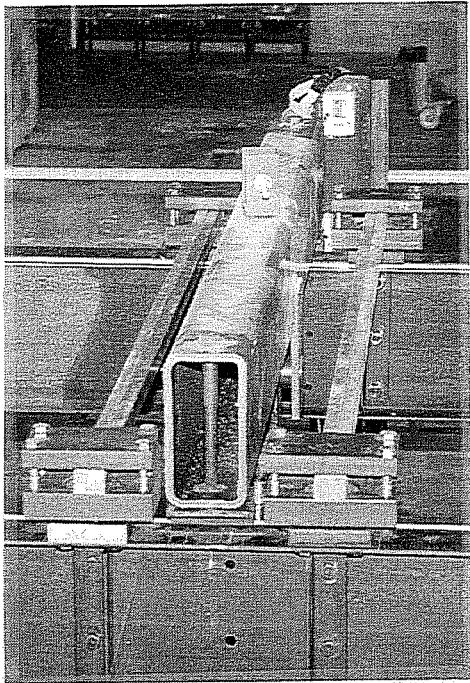


Figure 3.8   Torsional bracing.
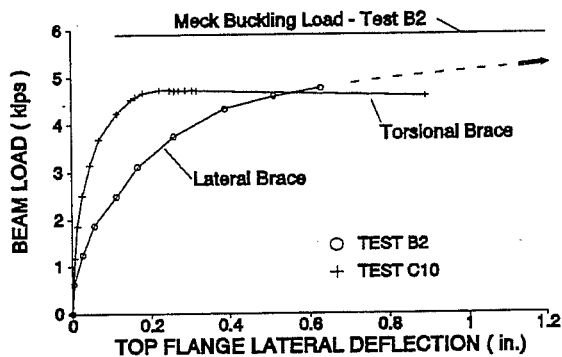


Figure 3.9   Typical test results.

Many beam buckling tests were performed with stiffeners placed directly beneath the brace attachment points. The stiffeners were 11-inch-long steel angles with slotted holes bolted on each side of the web. This permitted both the stiffener size and vertical location of the stiffener to be easily adjusted.

## 3.4    Test Procedure

A load of approximately one kip was applied to the beams before the vibration equipment was activated so that the knife edges would seat in the grooves on the top flanges of the test beams. Data were recorded at an increment of about 500 pounds until the load on the beams was near the buckling load; the frequency of the readings were then increased. During each test, the twist of the compression and tension flanges were measured near the brace point.

The critical buckling load was determined from plots of the load-lateral deflection-twist data. Typical load vs. top flange deflection response are shown in Figure 3.9. In Test C10 a peak load is reached which defines the buckling load. On the other hand Test B2 was terminated before the buckling load was reached to prevent yielding as lateral displacements became large. The same two beams were to be used in all of the twin beam buckling tests so yielding was undesirable.

Methods have been developed to determine the experimental buckling strength of structures that cannot be loaded to the actual buckling load because of initial out-of-straightness. Some of the better known procedures for this type of analysis include techniques presented by Southwell (1932) and Meck (1977). The Meck plotting technique, which is used herein, was developed specifically for beams. The applied load is plotted against the experimental twist and lateral deflection as shown in Figure 3.10. For beams loaded on the top flange, the inverse slopes of the lines of best fit through the data points for these plots are defined as $\alpha$ and $\beta$ and the critical load is given by

$$P_{cr}^2 + \beta \frac{d}{2} P_{cr} - \alpha\beta = 0 \qquad (3.1)$$

The initial lateral twist, $\theta_o$, and deflection $\Delta_o$, are found from negative horizontal intercepts of the plots and can be compared to measured values. The Meck buckling load determined from this procedure for Test B2 is shown in Figure 3.9.



Figure 3.10   Meck plots.
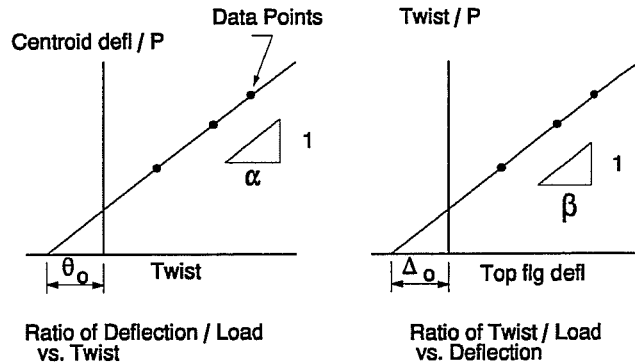
## 3.5    Test Results

The experimental program of 76 tests was divided into six groups. Group A tests had no bracing. Group B tests had lateral bracing located at midspan attached to the compression flange. Group C tests had compression flange torsional bracing located at midspan as discussed in Section 3.3. Group D contains results from tests with forced imperfections. Group E tests had tension flange torsional bracing and Group F had a combination of tension flange and compression flange torsional bracing.

Two types of initial imperfections were studied during the testing program. The first type of imperfection will be referred to as natural imperfections. All tests, except Group D, were performed with permanent out-of-straightness. Tests A1, A5, and A6 in Table 3.1 give values of initial top flange displacement and initial twist at midspan for the three levels of imperfections used during testing. The second type of imperfection will be referred to as forced imperfection. These were applied at the quarter point of the beam by displacing the compression flange of the test beam laterally with a rigid stop and then securing the stop in the displaced position. Tests D1 through D4 give measured values of initial deflection and initial twist at the midspan of the test beams for tests with forced imperfections. All forced imperfections listed are in addition to the 0.04-inch natural out-of-plane sweep of test beam A1.

### Table 3.1   Measured Imperfections

| Test Number | Initial Top Flange Deflection (in.) | Initial Twist (degrees) |
| --- | --- | --- |
| A1 | 0.04 | 0.26 |
| A2 | 0.45 | 0.95 |
| A5 | 0.16 | 0.01 |
| A6 | 0.22 | 0.13 |
| D1 | 0.26 | 0.17 |
| D2 | 0.15 | 0.07 |
| D3 | 0.12 | 0.05 |
| D4 | 0.31 | 0.12 |

***3.5.1    Test Series A - No Bracing.*** The first test series consisted of six tests with different loading beams. Test A1 was loaded with knife edges between the loading member and the test beam, and can be considered a basically straight beam with no bracing other than the friction in the gravity load simulator. Test A2 had the same configuration as A1 with a forced imperfection imposed at the quarter point of one beam.

Table 3.2   Test Series A, No Bracing

| Test No. | Description | Stiffener Size | Initial Imperfection (inches) | Critical Load (kips) | "S" Shape |
|---|---|---|---|---|---|
| +A1 | Knife edge loading | None | 0.04 | 1.55 | No |
| A2 | Knife edge loading | None | 0.45 | 1.59 | No |
| +A3 | Tipping effects | None | 0.04 | 3.91 | No |
| A4 | Tipping effects | 2-in.X1/4-in. | 0.04 | 6.2 | Yes |
| +A5 | Knife edge loading | None | 0.16 | 1.56 | No |
| +A6 | Knife edge loading | None | 0.22 | 1.67 | No |

+   Test was repeated

Table 3.3   Test Series B, Lateral Bracing

| Test Number | Brace Stiffness (kips/in.) | Stiffener Size | Initial Imperfection (inches) | Critical Load (kips) | "S" Shape |
|---|---|---|---|---|---|
| B1 | 0.22 | 4-in.X1/4-in. | .19 | 3.17 | No |
| B2 | 0.75 | 4-in.X1/4-in. | .24 | 6.02 | No |
| B3 | 0.36 | 4-in.X1/4-in. | .36 | 4.11 | No |
| B4 | 1.20 | 4-in.X1/4-in. | .35 | 6.54 | No |
| B5 | 0.36 | 4-in.X1/4-in. | .15 | 3.97 | No |
| B6 | 1.20 | 4-in.X1/4-in. | .16 | 6.73 | Yes |
| B7 | 1.90 | 4-in.X1/4-in. | .15 | 6.62 | Yes |
| B8 | 0.65 | 4-in.X1/4-in. | .15 | 5.39 | No |
| B9 | 0.65 | None | .15 | 5.47 | No |
| B10 | 1.90 | None | .16 | 6.75 | Yes |

29

The term "tipping effects" describes tests in which the loading beam was placed directly on the compression flanges of the test beams without the use of the knife edges. Tests A3 and A4 were performed to study the effects of the externally applied flange rotation which occurs when the loading member is placed directly on the compression flanges of the test beams. Tests A5 and A6 were loaded with the original knife edge loading and are similar to test A1 except for the level of initial imperfection present. Table 3.2 gives a summary of these tests and the corresponding experimental buckling loads. The reported buckling load is an average of the two test beams. Tests marked with a plus sign were reproduced to check for repeatability. With the exception of tests C4 and C29 presented in Section 4.6, all duplicate tests gave a critical load within six percent of the original test. Test C4 had a variation of 20 percent and test C29 had a variation of 8 percent.

*3.5.2 Test Series B - Lateral Bracing.* The second series of tests, as well as subsequent tests, were loaded using the steel loading beam and knife edges as shown in Figure 3.5. All boundary conditions were the same as Test Series A except that a lateral brace was added as shown in Figures 3.6 and 3.7. Six levels of lateral bracing and two levels of initial imperfections were tested. Table 3.3 shows the amount of lateral bracing attached to the test beams through the bracing device and the corresponding critical load per beam. The brace stiffness given in this table and subsequent tables is the stiffness per beam (the measured lateral brace system stiffness divided by two).

*3.5.3 Test Series C - Compression Flange Torsional Bracing.* Test Series C, with results summarized in Table 3.4, consisted of 40 tests with varying levels of torsional brace stiffness, initial imperfection and stiffener size. A total of eight levels of brace stiffness, three levels of initial imperfection, and two stiffener sizes were tested. Tests were also performed with no stiffener and with the 4X1/4-in. stiffener touching the compression flange at both brace locations. Tests performed with the stiffeners touching the compression flange are marked with an asterisk in the table. The torsional bracing was attached to the compression flange of each test beam with half the indicated amount being placed six inches on either side of the midspan.

*3.5.4 Test Series D, E, and F.* Test Series D consists of six tests where the initial imperfection was applied to the beam by a forced displacement at the quarter span of one beam. The forced displacement was transferred to the other beam through the loading tube. As mentioned in the previous sections, the initial imperfection reported for all other test series was the natural state of test beams due to a previous yielding or manufacturing process. Test Series E consisted of ten tests similar to those in Series C except the torsional bracing was attached to the tension flange instead of the compression flange. Test Series F consisted of six tests similar to those in Series C except half the indicated value of torsional bracing was attached to the compression flange and half was attached to the tension flange. Table 3.5 contain a summary of these tests and the corresponding experimental buckling loads.

## 3.6    Discussion of Twin-Beam Test Results

*3.6.1 Unbraced Beams.* Series A had no apparent lateral or torsional bracing other than the lateral restraint provided by the friction in the loading device (gravity load simulator). The seven tests with knife-edge loading on the top flange varied between 1.53 and 1.69 kips, with an average of 1.60 kips. All test loads reported herein include the weight of the loading beam. With no bracing, BASP gives a predicted buckling load of 1.29 kips which indicates that some lateral restraint is present. At a ram load of 3.2 kips corresponding to the average

Table 3.4   Test Series C, Compression Flange Torsional Bracing.

| | Test Number | Brace Stiffness (k-in/rad) | Stiffener Size | | Initial Imperfection (inches) | Critical Load (kips) | "S" Shape |
|---|---|---|---|---|---|---|---|
| | C1 | 55 | NONE | | 0.22 | 2.87 | NO |
| | C2 | 55 | 2"X1/4" | | 0.22 | 3.13 | NO |
| | C3 | 55 | 4"X1/4" | | 0.22 | 3.17 | NO |
| + | C4 | 89 | NON | | 0.22 | 3.44 | NO |
| + | C5 | 89 | 2"X1/4" | | 0.22 | 3.49 | NO |
| + | C6 | 89 | 4"X1/4" | | 0.22 | 3.55 | NO |
| | C7 | 175 | NONE | | 0.22 | 4.37 | NO |
| + | C8 | 175 | 2"X1/4" | | 0.22 | 4.40 | NO |
| | C9 | 175 | 4"X1/4" | | 0.22 | 4.54 | NO |
| | C10 | 462 | NONE | | 0.22 | 4.83 | NO |
| | C11 | 462 | 2"X1/4" | | 0.22 | 5.17 | NO |
| | C12 | 462 | 4"X1/4" | | 0.22 | 5.31 | NO |
| | C13 | 666 | NONE | | 0.22 | 5.05 | NO |
| | C14 | 666 | 2"X1/4" | | 0.22 | 5.45 | NO |
| | C15 | 666 | 4"X1/4" | | 0.22 | 5.73 | NO |
| | C16 | 855 | 4"X1/4" | | 0.22 | 5.80 | NO |
| + | C17 | 1030 | 4"X1/4" | | 0.22 | 5.72 | NO |
| | C18 | 1190 | 4"X1/4" | | 0.22 | 5.98 | NO |
| | C19 | 1190 | * | 4"X1/4" | 0.22 | 6.83 | YES |
| | C20 | 1030 | * | 4"X1/4" | 0.22 | 6.82 | YES |
| | C21 | 666 | * | 4"X1/4" | 0.22 | 6.81 | YES |
| | C22 | 462 | * | 4"X1/4" | 0.22 | 6.87 | YES |
| | C23 | 175 | * | 4"X1/4" | 0.22 | 5.45 | NO |
| | C24 | 89 | * | 4"X1/4" | 0.22 | 3.38 | NO |
| | C25 | 55 | NONE | | 0.16 | 2.89 | NO |
| | C26 | 55 | 2"X1/4" | | 0.16 | 3.03 | NO |
| | C27 | 55 | 4"X1/4" | | 0.16 | 2.96 | NO |
| | C28 | 89 | NONE | | 0.04 | 4.48 | NO |
| + | C29 | 89 | 2"X1/4" | | 0.04 | 4.33 | NO |
| | C30 | 89 | 4"X1/4" | | 0.04 | 5.14 | NO |
| | C31 | 175 | NONE | | 0.04 | 5.55 | NO |
| + | C32 | 175 | 2"X1/4" | | 0.04 | 6.38 | YES |
| + | C33 | 175 | 4"X1/4" | | 0.04 | 6.54 | YES |
| | C34 | 175 | * | 4"X1/4" | 0.16 | 4.83 | NO |
| | C35 | 462 | * | 4"X1/4" | 0.16 | 6.58 | YES |
| + | C36 | 462 | 4"X1/4" | | 0.16 | 5.71 | NO |
| + | C37 | 666 | 4"X1/4" | | 0.16 | 5.92 | NO |
| | C38 | 855 | 4"X1/4" | | 0.16 | 6.33 | NO |
| | C39 | 1030 | 4"X1/4" | | 0.16 | 6.50 | YES |
| | C40 | 1190 | 4"X1/4" | | 0.16 | 6.41 | YES |

* Stiffener touching tension flange        +Test was repeated

Table 3.5   Test Series D, E, and F

| Test Number | Brace Stiffness (k-in/rad) | Stiffener Size | Initial Imperfec-tion (inches) | Critical Load (kips) | "S" Shape |
|---|---|---|---|---|---|
| Forced Imperfections | | | | | |
| D1 | 89 | NONE | 0.26 | 3.59 | NO |
| D2 | 175 | NONE | 0.15 | 4.13 | NO |
| D3 | 175 | 4"X1/4" | 0.12 | 5.8 | NO |
| D4 | 175 | 4"X1/4" | 0.31 | 5.27 | NO |
| Tension Flange Torsional Bracing | | | | | |
| E1 | 175 | NONE | 0.22 | 4.25 | NO |
| E2 | 175 | * 4"X1/4" | 0.22 | 6.53 | YES |
| E3 | 666 | * 4"X1/4" | 0.22 | 6.69 | YES |
| E4 | 666 | 4"X1/4" | 0.22 | 6.79 | YES |
| E5 | 666 | NONE | 0.22 | 4.72 | NO |
| E6 | 175 | NONE | 0.16 | 3.83 | NO |
| + E7 | 175 | * 4"X1/4" | 0.16 | 5.15 | NO |
| E8 | 666 | * 4"X1/4" | 0.16 | 6.99 | YES |
| E9 | 666 | 4"X1/4" | 0.16 | 7.03 | YES |
| E10 | 666 | NONE | 0.16 | 4.78 | NO |
| Combined Compression and Tension Flange Torsional Bracing | | | | | |
| F1 | 462 | NONE | 0.22 | 6.53 | YES |
| F2 | 175 | NONE | 0.22 | 4.89 | NO |
| F3 | 175 | 4"X1/4" | 0.22 | 4.99 | NO |
| F4 | 462 | NONE | 0.16 | 6.94 | YES |
| F5 | 175 | NONE | 0.16 | 4.87 | NO |
| F6 | 175 | 4"X1/4" | 0.16 | 4.86 | NO |

* Stiffener Touching Tension Flange
+ Test was repeated

32
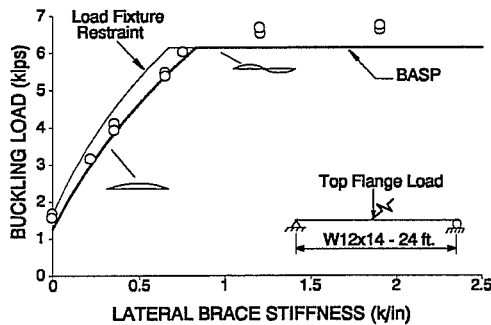


Figure 3.11   Lateral bracing tests.
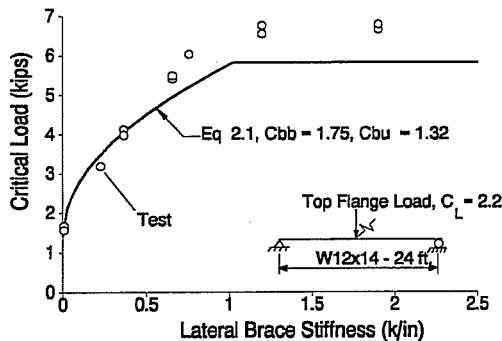


Figure 3.12    Comparison of tests and Eq. 2.1.

unbraced beam test load, the measured lateral stiffness of the gravity load simulator is 0.083 k/in. (Yura and Phillips, 1992). For one beam with a lateral restraint of 0.042 k/in., the BASP buckling load is 1.65 kips which is within three percent of the average test load. The small vibration motor probably reduced the restraint below the measured stiffness. The magnitude of the initial out-of-straightness did not affect the buckling load.

When the loading beam without knife edges was placed directly on the top flange of the twin test beams, the buckling load increased from 1.60 kips to 3.91 kips when no web stiffener was used. The 244 percent increase was due to the tipping effect. When the beam tried to twist at 1.6 kips, the top flange load was then applied at the flange tip and a restoring torque (shown in Figure 1.2(a)) kept the beam in the straight position. The test beam A3, however, did twist at the load point at 3.91 kips because of cross section distortion, as illustrated in Figure 1.2(b). When a 2X1/4-in. web stiffener was attached at the load point to control distortion, the beam load (Test A4) reached 6.2 kips corresponding to buckling between the midspan and the end support (S shape).

*3.6.2    Beams with Lateral Bracing.*    A summary of the Series B lateral bracing tests is given in Figure 3.11. The test results show good agreement with the BASP theory. At brace stiffness below 0.8 k/in., the beams buckled in a single half sine curve as predicted. For brace stiffnesses greater than 0.8 k/in., full bracing is achieved and the test beams buckled into an S shape between brace points. The dashed line is the theoretical solution assuming that the gravity load simulator provides additional lateral restraint. The test results are closer to the theory neglecting this fixture restraint which indicates that the vibration motor was effective in reducing the friction at the higher loads.

The tests had initial top flange out-of-straightness between 0.15 in. and 0.36 in. but there was no apparent effect on the buckling loads. The experimental buckling loads obtained from Meck plots of the load-twist-lateral deflection data give the expected buckling load if the beams would have been deformed beyond the 1 in. displacement limited in the experiments to control yielding of beams.

A comparison of the test results with the continuous lateral bracing formulation, Equation 2.1, is shown in Figure 3.12 by the solid line. The figure shows that Equation 2.1 gives conservative results at brace stiffness near the ideal value, but in general the results are similar. As discussed in Chapter 2, the use of an equivalent continuous

bracing formula for discrete braces produces the most error for the single brace at midspan. The Series B tests with no stiffener, B9 and B10, gave approximately the same results when a 4X1/4 in. web stiffener was used in B8 and B7, respectively. The test results and theoretical studies indicate that web distortion is not an important factor when lateral bracing is attached to the top compression flange of a beam.

### 3.6.3 Beam with Torsional Bracing.

The Series C torsional bracing tests were designed to study the influence of brace stiffness and the effect of cross section distortion. A typical load-lateral displacement response (Test C10) is shown in Figure 3.9. A peak load was reached at a displacement of approximately 0.2 in. which is taken as the buckling load. This behavior is very different from the typical response for the lateral bracing tests represented by Test B2 in Figure 3.9. For lateral bracing, no peak was reached in the experiment and the buckling load had to be determined by the Meck plotting technique. The Meck buckling load is the load that would be reached at large lateral displacement represented by the dashed line. The difference between the two responses is caused by local distortion of the cross section at the points at which the torsional bracings are attached. Without distortion, the two flanges and the web should have the same angle of twist. The twist of the top flange and the bottom flange were measured near the brace at midspan in all experiments. The twist data show that at the brace there is no difference in the measured twist of each flange for lateral bracing but there was a significant difference for torsional bracing as the peak load was reached. In Test C10 at the peak load, the bottom flange twist of 1.23° was 2.3 times the top flange twist.

Cross-section distortion can be controlled by properly attached stiffeners. In Series C there were three general stiffener arrangements; namely, no stiffener, a stiffener in contact with the flange where the brace is attached which controls cross-section distortion, and a web stiffener which does not touch either flange. This latter type of stiffener arrangement controls bending of the web but each flange is permit-



Figure 3.13    Torsional brace - no stiffener.

ted to twist relative to the web. Figure 3.13 shows a comparison of the Series C tests with no stiffener and the buckling load predicted by BASP. In all of these tests, the beam buckled in a single half wave. No brace was sufficient to force the beam to buckle into an S-shape because of local distortion at the brace point. The test loads are significantly greater than the BASP solution assuming no lateral restraint by the loading fixture (heavy solid line). Two additional BASP solutions are shown which indicate that the effect of lateral restraint is very significant. The 0.026 k/in. restraint level is approximately 1/4 of the measured fixture restraint with no vibration motor (Yura and Brett, 1992). The highest BASP solution corresponds to the full calibrated lateral restraint by the gravity-load simulator. The test results fall within the bounds of the BASP solutions. In the lateral bracing tests, Series B, the effect of the fixture restraint was relatively minor, but this is not the case for torsional bracing. As indicated in Figure 2.24, the interaction of lateral and torsional bracing is very effective. For example, a lateral brace of 10 percent of the required lateral bracing reduces the torsional bracing requirement by 40 percent.

The data in Figure 3.13 indicates that the beams with the smallest initial sweep had the largest buckling loads. This was probably due to smaller lateral displacements and the likelihood that friction in the test fixture was

not broken. The test results for initial sweep equal to 0.04 in. are very close to the BASP solution with full fixture restraint.

The Series C results for a stiffener in contact with the torsionally braced flange compare very well with the BASP results, as shown in Figure 3.14. These tests simulate the typical design situation of a stiffener welded to the compression flange and cut short of the tension flange. The effect of possible fixture restraint is not as important for this case where cross section distortion is prevented by the 4X1/4-in. stiffener at each brace location. The ideal brace stiffness is approximately 320 kip-in/radian. At the ideal stiffness, the buckled shape changes from a single half wave to the S-shape corresponding to full bracing at midspan. All the tests with bracing greater than 320 kip-in/radian buckled into an S shape.

The torsional bracing formula, Equation 2.10, is compared to the test results for the stiffened and unstiffened cases in Figures 3.15 and 3.16, respectively. The difference between these two cases is caused by cross section distortion. In the torsional bracing formula, $\beta_{sec}$ = 114 kip-in/radian for the unstiffened web and 11030 for a beam with a 4X1/4-in. stiffener at the brace points. As $\beta_{sec}$ gets smaller, the attached braces becomes less effective. An attached brace with a stiffness of 250 kip-in/radian is almost fully effective (247 kip-in/radian from Eqs. 2.8 and 2.9) but the same brace is effectively reduced to 119 kip-in/radian, about a fifty percent reduction, if the web is unstiffened. The design equations follow the trend of the data very well.

When the stiffener is not welded or in contact with the braced flange, then the web can twist relative to the flange as illustrated in Figure 1.2(b). In such a case, the effectiveness of the stiffener in controlling distortion is reduced and Equation 2.10 is not applicable. Tests in which the 4X1/4-in. web stiffener did not touch the braced flange are summarized in Figure 3.17. The web was stiffened, but the 90° angle between the flange and web was not maintained. The tests are similar for a 2X1/4 in. stiffener. The tests compare
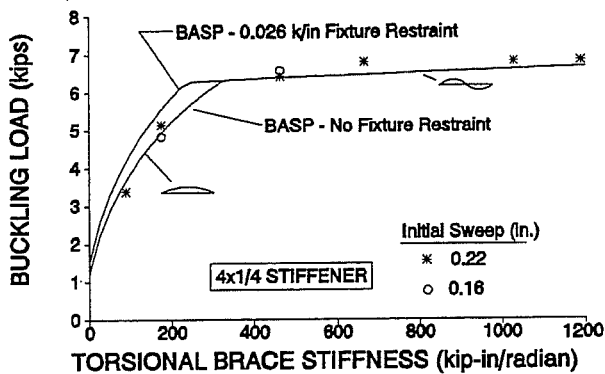


Figure 3.14    Torsional brace - full stiffener.
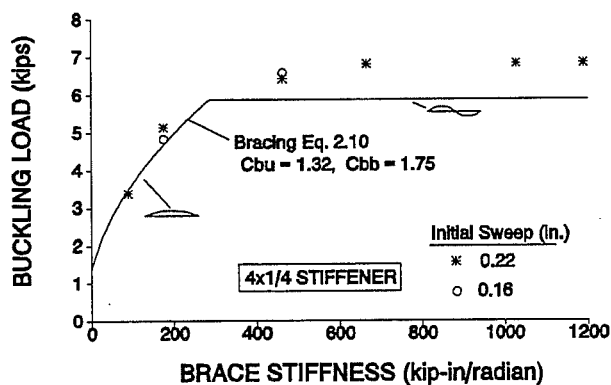


Figure 3.15    Eq. 2.10 - full stiffener.
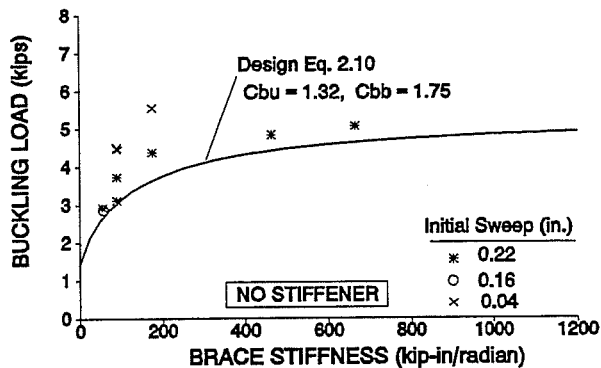


Figure 3.16    Eq. 2.10 - no stiffener.

favorably with BASP solution in which the web stiffener is assumed to be 10 in. long or 11 in. long and not attached to either flange. The actual stiffener was an angle 11 inches long but it was bolted to the web and the distance between connectors was 9 in. Therefore, it is questionable that the total length of the stiffener is effective. Stiffeners that do not contact the braced flange are not recommended and these tests illustrate the reduced strength when compared with the results in Figure 3.15.

### 3.6.4 Effect of Torsional Brace Location.

Theoretically, the attachment height of a torsional brace should have no effect on the buckling load if the bea m web does not distort. Figures 3.18 and 3.19 show values of critical load for tests with torsional bracing placed on the compression flange, tension flange or split evenly between the compression and tension flanges (combined bracing). Figures 3.18 and 3.19 show that the combined bracing produced a slightly higher critical load for beams with no stiffener; however, the beam with a 4X1/4 in. stiffener and a brace stiffness of 175 k-in/radian also showed an increase in critical load. Based on these tests, the brace location did not significantly affect the critical load regardless of the cross-section stiffness of the test beam.

### 3.6.5 Forced Imperfections.

In the experiments, two types of imperfections were tested; natural imperfections and forced imperfections. Since a natural imperfection requires equilibrium of internal stresses and forced imprefection requires equilibrium with an applied external reaction, there is no theoretical basis for assuming that both types of imperfection would have the same impact on the effective brace stiffness. Based on Figure 3.20, a forced imperfection has an



Figure 3.17   Web stiffened tests.
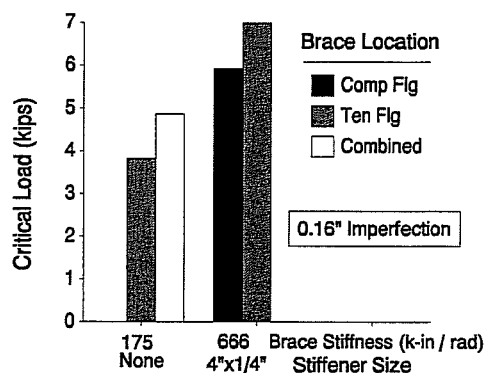


Figure 3.18   Effect of brace location.

effect similar to a natural imperfection.   Since lateral-torsional buckling involves both a twist and a lateral displacement, the magnitude of the initial twist may also have an effect on the brace stiffness.

## 3.7    Summary of Twin-Beam Tests

The BASP program and bracing Eqs. 2.1 and 2.10 showed good correlation with the test results. The tests verified that cross section distortion is very important for torsional bracing. The W12X14 test beams could not reach the load level corresponding to buckling between braces unless web stiffeners in contact with the braced flange were

used. Torsional bracing at the bottom tension flange was just as effective as bracing on the compression. Lateral bracing at the top flange of simply supported beams was very effective and was not affected by cross section distortion (stiffeners are not necessary).

The Meck technique for obtaining experimental buckling loads worked very well for lateral bracing, but was not useful for torsional bracing because of the effect of local cross section distortion. In the torsional bracing experiments, the results were sensitive to the slight lateral restraint provided by the test fixture, especially for very straight beams. Combined lateral and torsional bracing is very effective in controlling lateral buckling of slender beams.

The initial sweep of the beam did not affect the buckling load of laterally braced beams, but did influence the results in the torsional buckling experiments. The experimental buckling were all larger than the BASP prediction regardless of the level of initial imperfection, so the apparent out-of-straightness effect was related to lateral fixture restraint.
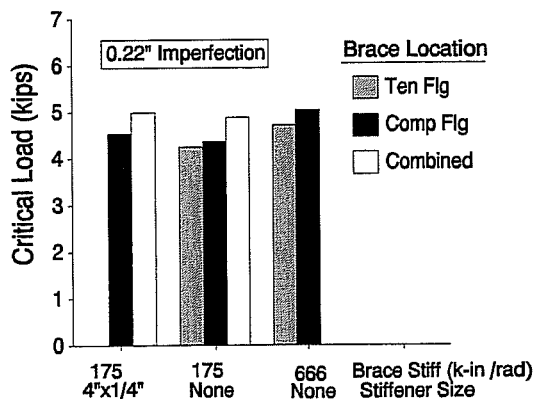


Figure 3.19    Brace location effects.
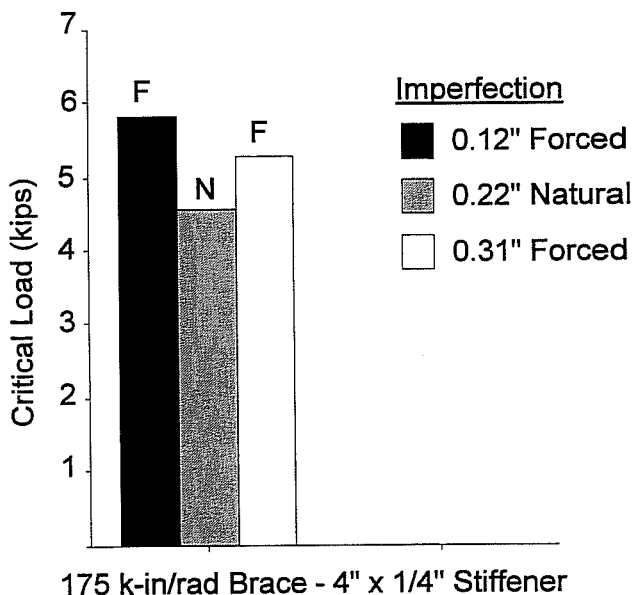


Figure 3.20    Forced initial imperfections.

# CHAPTER 4
# FULL-SIZE BRIDGE TEST

## 4.1    Experimental Program

The experimental program involved the design, construction and testing of a full scale 24 ft span multi-girder bridge with a wood deck, shown schematically in Figure 4.1. The bridge was load tested with a moving wheel load until failure as shown in Figure 4.2. The bridge was comprised of five S6×12.5 steel stringers and a wood deck. The steel stringers, spaced at 3 ft, were bolted to W12×30 steel supporting beams at the two ends with two 3/8-in. dia. bolts at each end. The treated No. 2 southern pine (wolmanized) wood deck was made of thirty-five 4×8 planks 16 ft long and was nailed to four 2×6 nailers. The middle two nailers also served as a guide for the loading cart. The deck rested on the beams directly and there was no positive connection between the deck and the beams. In order to test the worst possible case, the loading was through a standard tandem (two tires on each side of axle) truck axle and only one axle of the truck was on the bridge. Preliminary tests were conducted to study the lateral buckling behavior and plastic bending strength of an individual beam. Lateral



Figure 4.1    Sketch of the Test Bridge.
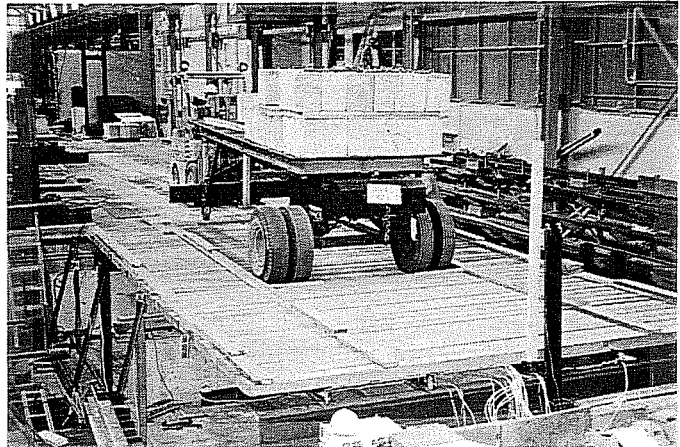


Figure 4.2    Bridge and Loading Cast.

stiffness tests were conducted to evaluate the strength and stiffness of the deck and beams (Webb and Yura, 1991). The average measured static yield strength of the S6×12.5 section was 42.1 ksi (flange = 41.8 ksi, web = 42.4 ksi) and measured cross-section properties were almost identical to the handbook values. All stringers were from the same heat of steel.

*4.1.1    Design and Construction of the Bridge.*    The sections and span were chosen so that there was a significant difference between the single mode (unbraced) buckling capacity and the yield capacity of the stringers. This way, the bracing effect of the deck if any, could be clearly demonstrated. The size of the beams was also limited by the magnitude of dead weight that could be safely used to load the bridge. A maximum load of 30,000 lbs on the cart to produce an axle load of 22,000 lbs was practically feasible in the laboratory. The end supports, beam spacing and other details were based on conditions found on typical bridges in Texas. The size of the wood planks was controlled by the bending moment in the planks as the wheel loads are distributed to the five stringers.

37

38

Figure 4.3 and were nailed to each plank with two 3-in. long steel screw nails spaced at 5.5 in. The wood deck was connected to an external support at the south end, through connecting beams, to prevent it from moving off the steel beams longitudinally due to the braking action of the loading cart. The connection was designed to minimize any in-plane restraint to the steel stringers. At the north abutment, lateral movement was prevented by nailing wood boards between the beams. Additional details are given elsewhere (Vegnesa and Yura, 1991).
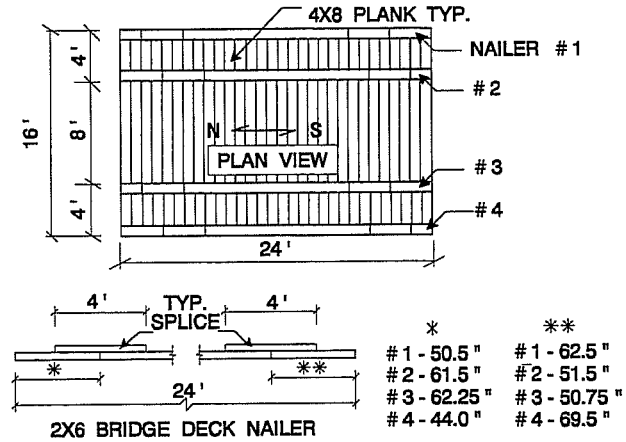


Figure 4.3   Bridge Deck Details.

### 4.1.2 Loading System and Instrumentation.

A steel cart loaded with concrete blocks was used to load the bridge. The cart was fitted with a truck axle (tandem) on one end and rested on castors at the other. The center to center distance between the tires was 6 ft. The cart was positioned along the bridge centerline so the center of each set of tires was directly over steel stringers #2 and #4. The exterior stringers were #1 and #5 and the centerline stringer was #3. This load location was chosen to prevent the wood deck from controlling the failure of the bridge. Only the axle load was applied to the bridge, the castors remained on an elevated slab adjacent to the test bridge. A forklift was used to push the cart on and off the bridge. At each load stage the wheel load on each side of the axle was weighed . The cart was used as a loading system instead of a hydraulic ram since it closely simulated a real vehicle in terms of tire contact area and load distribution. The slow movement of the cart required by laboratory testing did not represent vibrations associated with actual truck loading. Vibrations may affect the frictional restraint provided by the deck. To overcome this deficiency, a concrete vibrator was attached to the deck.

The bridge was instrumented extensively with displacement transducers, twist gauges, and strain gauges (Vegnesa and Yura, 1991). The instrumentation was used to determine the load that each stringer supported as the truck moved over the bridge. A 400-in. stroke displacement transducer kept track of the position of the cart on the bridge. Lateral displacements of each stringer and the deck were monitored. At each stage of loading, the axle load of the cart was measured using two 20000 lb weighing scales which were accurate to 100 lbs.. The central 8 ft portion of each beam was whitewashed as an aid to detect yielding.

### 4.1.3 Preliminary Tests.
Various preliminary tests gave information on the components of the bridge system as shown schematically in Figure 4.4. To get an estimate of the single mode lateral torsional buckling capacity of the bridge, twin S6×12.5 beams on a 24 ft span were tested with a concentrated load on the top flange at midspan. The twin beam test setup is described in Chapter 3. The load was applied through knife edges. The buckling
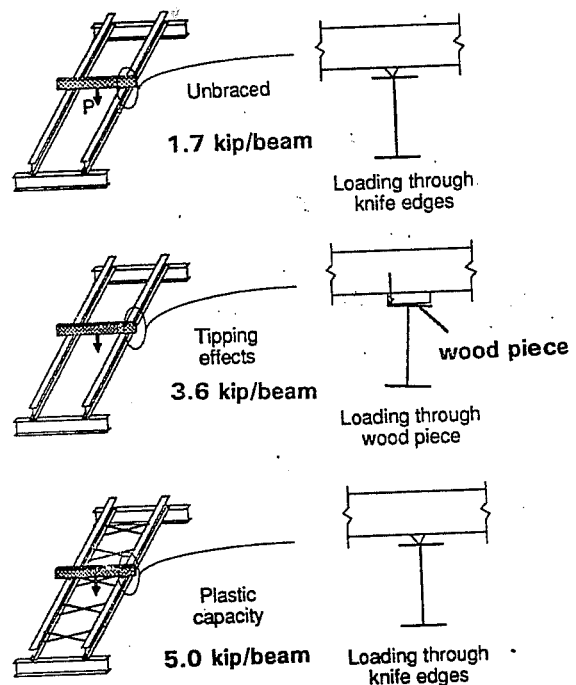


Figure 4.4   Preliminary Tests

capacity was 1.7 kips. A second test, with the midspan load applied through a steel tube directly supported by wood pieces on the top flange of the beams with no positive attachment, studied the "tipping effect" and is similar to the load transfer from the deck to the bridge beams. The capacity was found to be 3.6 kips. However, the wood pieces were in full contact with the top flange, which was not true in the case of the test bridge. Placing a single plank at midspan with no positive attachment increased the buckling load from 1.7 kips to 3.6 kips. In both cases, the buckled shape was a single mode shape, so the plank did not act as an ideal brace. If the beam was fully braced at midspan, the expected capacity would be 4.3 kips the measured yield capacity of the stringer. The measured plastic capacity of a single stringer was 5.0 kips.

## 4.2 Test Results

### 4.2.1 Test Procedure.
The bridge was loaded with a cart filled with increasing weights of concrete blocks in 0.6 - 1.4 kip increments until failure. Failure was defined as significant lateral movement of beams and deck or yielding of beams. At the beginning of every run, the cart was positioned so that the tires rested on the weighing scales. The cart was then slowly pushed on to the bridge until the wheels reached midspan and then the cart was pulled off the bridge. Readings were taken every few seconds. The cart was stopped at the quarter point and midspan so that the bridge could be examined, photographs taken, and static data recorded. There were three runs at each load increment. The first and third runs were done without the vibrator, while the second run was done with the vibrator.

There was no significant difference in the gauge readings for the three runs except in the final load stage then the bridge failed. Hence, only the data from the third run at each load level was used for the analysis. For the last load level, only two runs were completed before the bridge failed and both were used for data analysis. The load carried by each beam in the bridge system was calculated from two sources, the strain gauge data and the vertical gauge data and they were within 4% of each other. From data recorded when the deck was placed, the strain gauge data gave the closest correlation to the measured weight of the planks, so the beam loads given in the subsequent sections are based on the strain gauge data .

### 4.2.2 General Behavior.
The axle load - midspan vertical deflection response of three of the stringers is given in Figure 4.5. Only three stringers are shown for clarity. The interior stringers deflected more than the exterior stringers because of the load location. The response was elastic until an axle load of 12.8 kips was reached. At this point stringer #3 laterally buckled about one inch but the overall inplane behavior of the bridge was not significantly affected. When the load was removed from the bridge, stringer #3 returned to an almost straight position. The behavior remained linearly elastic up to 14.1 kips. At the next load level of 15.4 kips, buckling started in stringers #2, #4 and #5 and the inplane
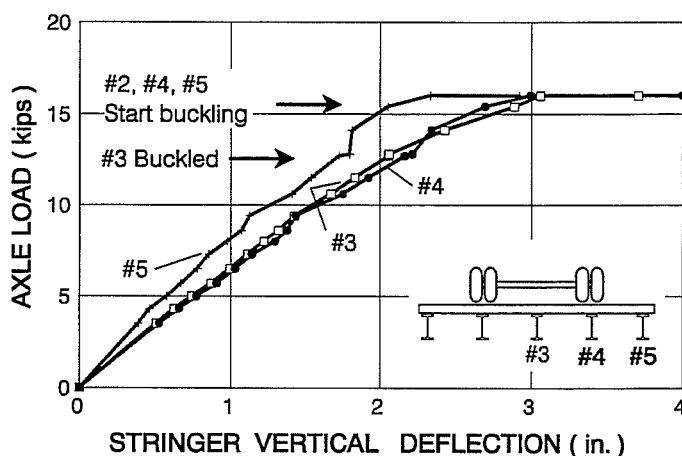
Figure 4.5     Midspan vertical deflection of the stringers

stiffness began to deteriorate. The bridge failed at 16.0 kips when the deck along with all five stringers deflected laterally more than two inches at midspan when the axle reached midspan during the second load pass with the bridge vibrator active. The stringers hit the safety stops which prevented complete failure. Upon unloading, the deck returned to its original position and all the stringers were permanently deformed.

The midspan lateral deflection of three stringers is given in Figure 4.6 which shows that stringer #3 started to buckle first. The lateral movement of stringers #1 and #2 at loads below 15 kips is not lateral buckling but merely deformation consistent with the deformed shape of the plank under the live load at midspan. Stringers #1 and #2 are pushed towards the east while #4 and #5 (not shown in Figure 4.6) are pushed towards the west. This also explains to some extent the fact that stringer #5 buckled earlier than #1 since # 5 was bent in the direction of overall system lateral buckling whereas #1 was bent in the opposite direction.

Figure 4.7 shows the lateral displacement curve for the deck and stringer #2 for comparison. The deck did not show any lateral displacement until a load of 16.0 kips when it moved laterally instantaneously. The deck and stringer #2 moved laterally almost the same amount which indicates that friction was sufficient to transmit the lateral brace forces. When the bridge was unloaded, the deck exhibited elastic behavior and returned to its original straight position. Table 4.1 summarizes the behavior during the test.

When the truck was on the bridge, only the single plank supporting the tires was in contact with the steel stringers as shown in Figure 4.8. The other wood planks were supported only by the exterior stringers which deflected less than the more highly loaded interior stringers. Stringer #3
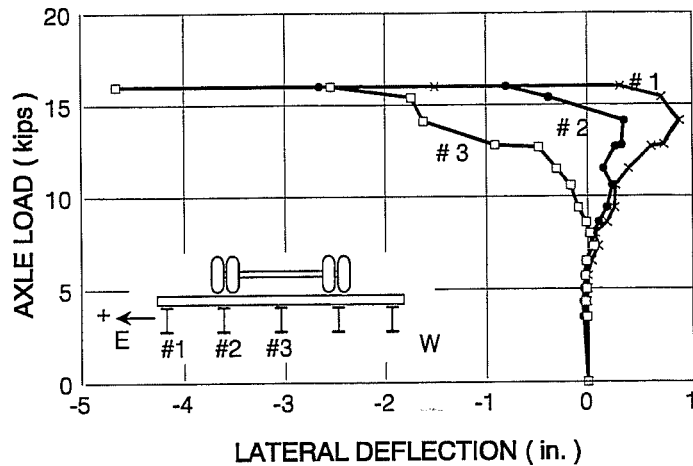


Figure 4.6     Stringer Lateral Displacement at Midspan.
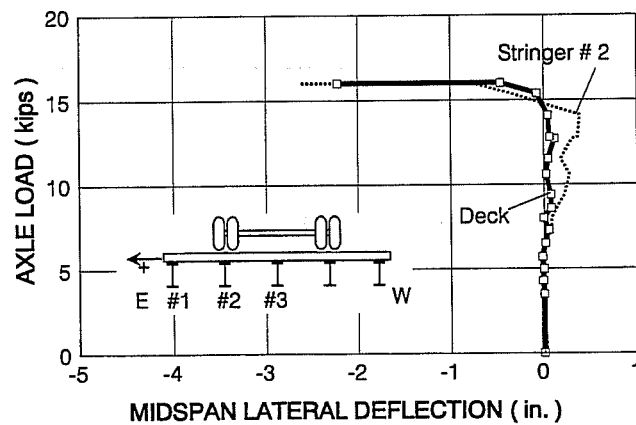


Figure 4.7     Deck Lateral Displacement at Midspan
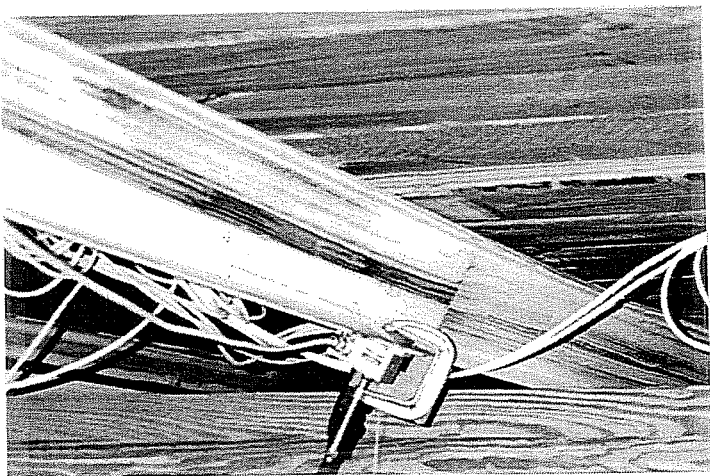


Figure 4.8    Buckled Position - Stringer #3

Table 4.1    Observed Behavior During Test

| Load Level | Axle Load (kips) | Observed Behavior During Test |
|---|---|---|
| 1 | 3.5 | Vertical displacement of the beams increased linearly with load.    No lateral movement was observed on the beams or the deck. |
| 2 | 4.3 | - Do -    Nailers started lifting off the deck |
| 3 | 5.0 | - Do - |
| 4 | 5.7 | - Do - |
| 5 | 6.5 | - Do - |
| 6 | 7.3 | Beam #3 shows some lateral movement |
| 7 | 8.0 | - Do - |
| 8 | 8.6 | - Do - |
| 9 | 9.4 | - Do - |
| 10 | 10.6 | - Do - |
| 11 | 11.5 | - Do - |
| 12 | 12.8 | Beam #3 buckled |
| 13 | 14.1 | - Do - |
| 14 | 15.4 | Beams #2, #4, and #5 start buckling.  Yield lines were observed in the midspan region on the top right and bottom left flanges of beams #2, #3, #4 and #5. |
| 15 | 16.0 | Beam #1, #2, #3, #4, #5 experience lateral torsional buckling.  Beams #2-5 touched safety supports below.  Deck showed 2 in. lateral movement at midspan. |
| 16 | After the Test | Deck came back to initial straight position.  The five beams showed a residual lateral displacement of 0, 1.44, 3.25, 1.25, 1.5 inches, respectively, at top flange midspan.  Yield lines were observed in the midspan region of all the beam. |

started to buckle when the  load was only 4 ft from the end support (the unbraced length was 20 ft) as shown in Figure 4.9.  As the load moved towards midspan the lateral displacements increased and the deck held the beams in the new deflected position. From visual observation, the plank directly below the truck axle was not in full contact with the top flange of the beams as they buckled. The plank was bearing on the flange tip which provided a restoring torque to the beams.



MIDSPAN LATERAL DEFLECTION ( in. )
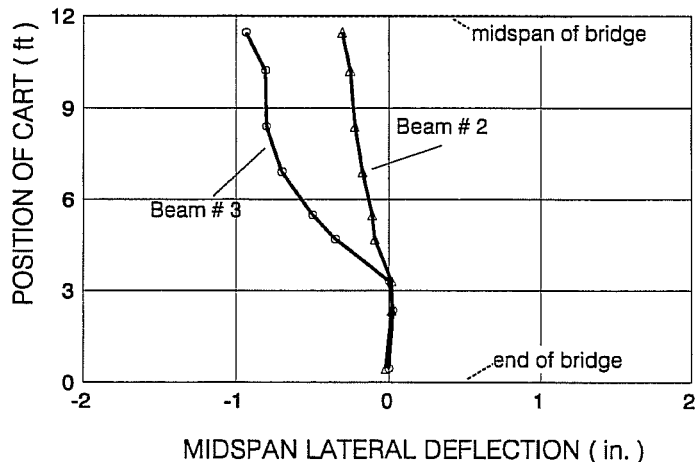
Figure 4.9    Cart position of start of buckling.

### 4.3    Load Distribution

The weight of the deck was determined by measuring the strains before and after the deck was constructed. The distribution of the deck load is shown in Figure 4.10.

From visual observation it was noted that, as the wheel load moved on to the bridge, the three central beams picked up more truck load than the exterior beams and hence they deflected more

42
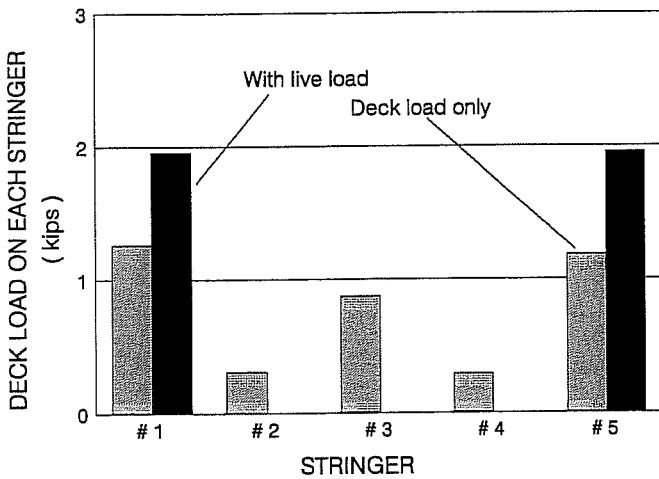


Figure 4.10    Distribution of deck load.



Figure 4.11    Total load distribution at different loads



Figure 4.12    Live load distribution at different loads.

than the exterior beams thereby causing the deck itself to rest on the exterior beams. This caused the entire deck load to be transferred to beam #1 and beam #5, the exterior beams, except for the particular plank supporting the axle load. The planks did not touch the three interior beams at all, except for the one which was loaded. This plank was in contact with all five beams. Figure 4.10 shows the distribution of the deck load among the five beams before (deck load only) and after the cart comes on to the bridge (with live load). Initially, before the cart came on to the bridge, the two exterior and the center stringers picked up most of the deck load. After the cart came on to the bridge, the deck load was carried mainly by the exterior stringers.

The transverse distribution of wheel loads among the stringers of a bridge is a function of the deck stiffness, beam stiffness, stringer spacing etc. The wheel load distribution controls the member size and consequently the strength and serviceability. Empirical wheel load distribution factors for stringers and longitudinal beams are given in Table 3.23.1 of AASHTO (AASHTO, 1990). For a timber deck, made of 4×8 planks, resting on steel stringers, the fraction of total wheel load a beam has to be designed for is S/4.5, where S is the stringer spacing. For the test bridge, which has five stringers at a spacing of 3 feet, the distribution factor is 0.67, i.e., each stringer has to be designed for a load of 0.67 times the total wheel load or 0.33 times the axle load.

Based on the principle of virtual work, the distribution of the wheel loads among the five beams was determined. The analysis indicated that 75% of the axle load is supported equally by the three interior stringers, while 25% is carried by the two exterior stringers.

The measured total load (live plus deck load) distribution and the live load distribution in each stringer for different load levels are shown in Figures 4.11 and 4.12, respectively. The fraction of the total load or live load carried by each beam is plotted on

the y-axis. The central three beams pick up most of the live load. The deck load is redistributed to the outer beams as described earlier, so the total load distribution is nearly uniform among the five beams. The data are shown at three different load levels to check if the magnitude of the load affects the load distribution. The total load distribution and the live load distribution remained nearly constant at loads less than 8 kips. At the ultimate load of 16 kips, stringer #3 shed load to the other beams as it lost in-plane stiffness due to its earlier lateral buckling. The AASHTO load distribution is conservative compared to the experimental values.
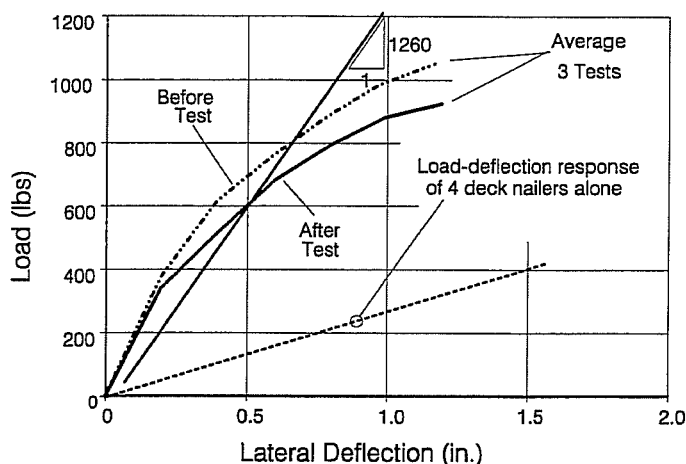


Figure 4.13    Measured deck stiffness

## 4.4    Lateral Deck Stiffness Test Result

The lateral stiffness of the deck was measured before any truck loading and after failure of the bridge. As shown in Figure 4.13 the deck stiffness after failure was slightly less than the original stiffness because a significant number of nails attaching the nailers to the planks worked out of the wood during the many loading cycles as shown in Figure 4.14. The representative deck stiffness is 1260 lb/in which is 4.6 times the stiffness of the nailers alone as shown in Figure 4.13. This indicates that the two nail connection to each plank adds significant stiffness to the system.
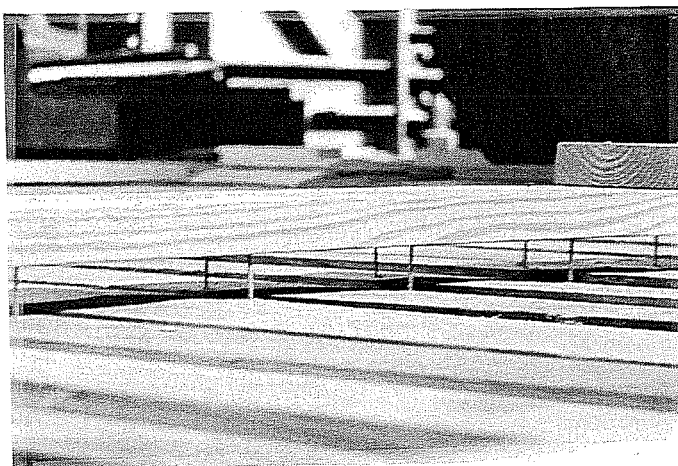


Figure 4.14    Deck damage by truck loading.

## 4.5    Capacity of the Test Bridge

The measured axle load at failure was 16.0 kips. The uniformly distributed dead weight of the deck and steel beams was equivalent to a concentrated load at midspan of 2.0 kips. Therefore, the ultimate capacity is 18.0 kips. From the test, it is clear that the bridge beams were braced. The lateral stiffness of the deck was established at 1.26/5 = 0.252 k/in. per beam from the deck stiffness tests, If the lateral deck stiffness is assumed as a lateral brace at midspan, the bridge capacity is 5×3.3 = 16.5 kips from Figure 4.15. In this case, the deck stiffness is about 1/4 of the ideal stiffness. Assuming that the deck provided torsional restraint through "tipping effects" gives a bridge capacity of 18 kips (5 times the capacity established from the tipping effects test on a single stringer in the preliminary tests). Assuming that the deck provided torsional restraint of 6EI/S at midspan gave a single beam capacity of 4.3 kips. The yield capacity of the bridge is 21.5 kips. These results are presented in  Figure 4.16.

44

Figure 4.16 shows that assuming the deck as a lateral brace at midspan gives a capacity within 10% of what was observed during the test. Some relative movement between the deck and the stringers did occur but it is not clear that this movement can be classified as slip. The midspan lateral movement of the interior stringers occurred before the midspan plank made contact with the steel stringers. It is unconservative to assume that the deck can provide a torsional stiffness of 6EI/S because the planks were only bearing on the flange tips. The maximum bridge load compares closely to the tipping effect load determined by the preliminary tests in which the tipping effects raised the beam capacity by a factor of 2. The same increase was noted from the bridge test. The relative contributions of lateral bracing and tipping effects cannot be established from the experiment. It was clear that the deck provided restraint (combination of lateral and torsional restraint) and increased the bridge capacity from 8.5 kips (assuming no bracing from deck) to 18.0 kips which is within 15% of the yield capacity of 21.5 kips. The test bridge was designed to have a deck of minimum lateral stiffness so as to test the worst case. In reality, bridges have decks of reasonable lateral stiffness and usually provide enough bracing to cause the stringers to fail by yielding. The bracing design equations can be used to calculate the braced capacity of the bridge. This requires a quantification of the amount of bracing as discussed in Chapter 5.
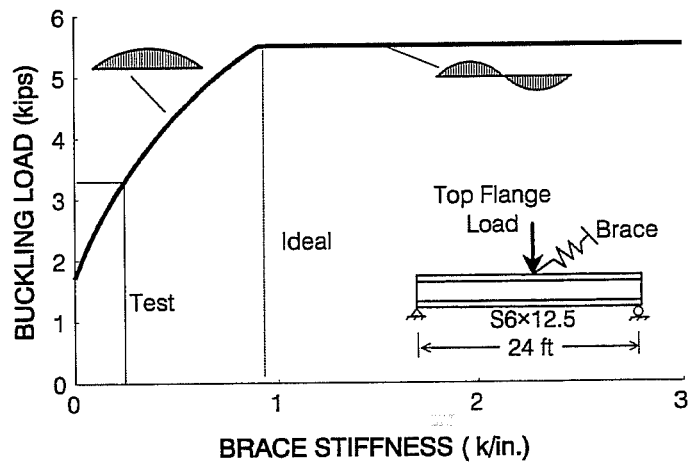


Figure 4.15    Top flange brace at midspan
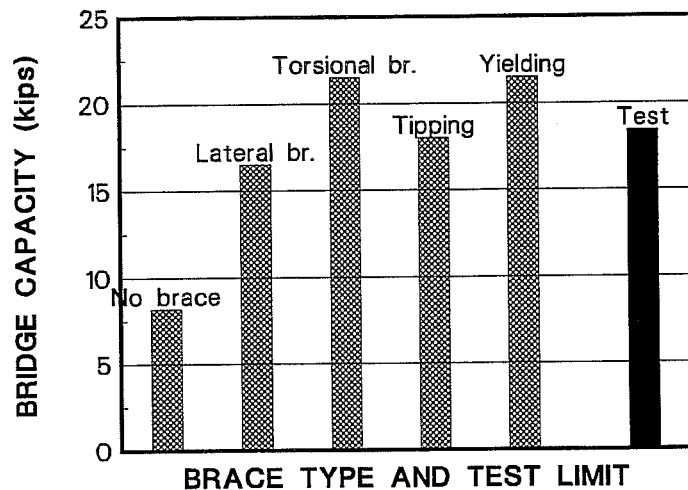


Figure 4.16    Theoretical bridge capacity

## 4.6    Summary

The ultimate load carried by the bridge indicated that the beams were partially braced by the deck. The bracing was mainly due to the lateral restraint provided by the friction mobilized at the deck beam interface and torsional restraint due to tipping effects. It was observed from the test that the deck was in full contact with the beam only at the location of the wheel load. Hence, there can be restraint only at the wheel location. As the beams tried to buckle there was contact between the top flange of the beams and deck only at the flange tips. Hence, the torsional restraint of 6EI/S cannot be assumed though there is help from tipping effects. At the midspan, the interior beams move relative to the decks but this lateral movement occurred before the load reached midspan.

The design equations can be used to calculate the improved capacity of the beams due to the effects of bracing. This requires the quantification of a brace stiffness. Based on the lateral stiffness tests of the deck, A conservative estimate of the lateral stiffness of a wood deck can be obtained by considering only the bending stiffness of the nailers.

The load distribution factors given by the AASHTO Bridge specifications are conservative; more realistic factors would result in better utilization of bridges. For example, when assessing lateral buckling, all five girders must buckle before collapse. So, the load rating controlled by lateral buckling could be calculated using the five girders rather than the 3.3 girders as per the AASHTO load distribution factors. The bracing provided by the bridge deck is a significant contribution to the overall capacity of the bridge. The bridge test showed that the capacity was twice the unbraced capacity. In order to evaluate the bracing effect, the lateral and torsional restraint provided by the deck must be assessed based on the deck to beam connection details.

# CHAPTER 5
## BRACE DESIGN AND BRIDGE DECK EVALUATION


### 5.1    Design Requirements for Lateral Braces

In the previous chapters it was shown theoretically and experimentally that the bracing equations, Eq. 2.1 and 2.10, could be used to predict the buckling strength of beams with discrete or continuous bracing. These two equations rely on the stiffness of the lateral or torsional braces, respectively. Winter (1960) showed that effective braces require not only adequate stiffness, but also sufficient strength. The strength requirements are related to the initial out-of-straightness of the member to be braced. Winter's approach will be illustrated for column bracing because the derivation of strength requirements is relatively simple for this case.

*5.1.1    Brace Strength.*    In the column braced at midspan, shown in Figure 5.1, the ideal brace stiffness corresponding to buckling between the brace points is $\beta_i = 2P_e / L_b$ as given in Table 2.1. This stiffness requirement is applicable to columns which are straight. For a column with an initial out-of-straightness, $\Delta_o$, and a brace stiffness, $\beta_L$, there will be an additional deflection $\Delta$ as load P is applied which can be determined by taking moments about point n

$$P \left( \Delta_o + \Delta \right) = \beta_L \Delta L_b / 2 \qquad (5.1)$$

Substituting the total column deflection $\Delta_T = \Delta_o + \Delta$ into Eq. (5.1) gives

$$\Delta_T = \frac{\Delta_o}{1 - \dfrac{2P}{\beta_L L_b}} = \frac{\Delta_o}{1 - \dfrac{P}{P_{cr}}} \qquad (5.2)$$
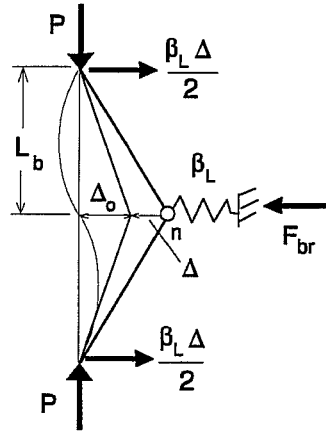


Figure 5.1    Imperfect column.

If $\Delta_o = 0$ and $P = P_e$, Eq. (5.1) gives $\beta_L = \beta_i$ the ideal stiffness. If $\beta_L = \beta_i = 2P_e / L_b$ and $\Delta_o$ is not zero, the heavy solid line in Figure 5.2(a) shows the relationship between $\Delta_T$ and P given by Eq. (5.2). For $P = 0$, $\Delta_T = \Delta_o$. When P increases and approaches the buckling load, $\pi^2 EI/L_b^2$, the total deflection $\Delta_T$ becomes very large. For example, when the applied load is within 5% of the buckling load, $\Delta_T = 20\Delta_o$. If a brace stiffness twice the value of the ideal stiffness is used, Eq. (5.2) gives much smaller deflections, as shown in Figure 5.2(a). When the load just reaches the buckling load, the $\Delta_T = 2\Delta_o$. For $\beta_L = 3\beta_i$ and $P = P_e$, $\Delta_T = 1.5\Delta_o$.

From Figure 5.1 and Eq. (5.1) the force in the brace, $F_{br}$, is

$$F_{br} = \beta_L \Delta = \frac{2P}{L_b} \left[ \Delta_o + \Delta \right] \qquad (5.3)$$

47
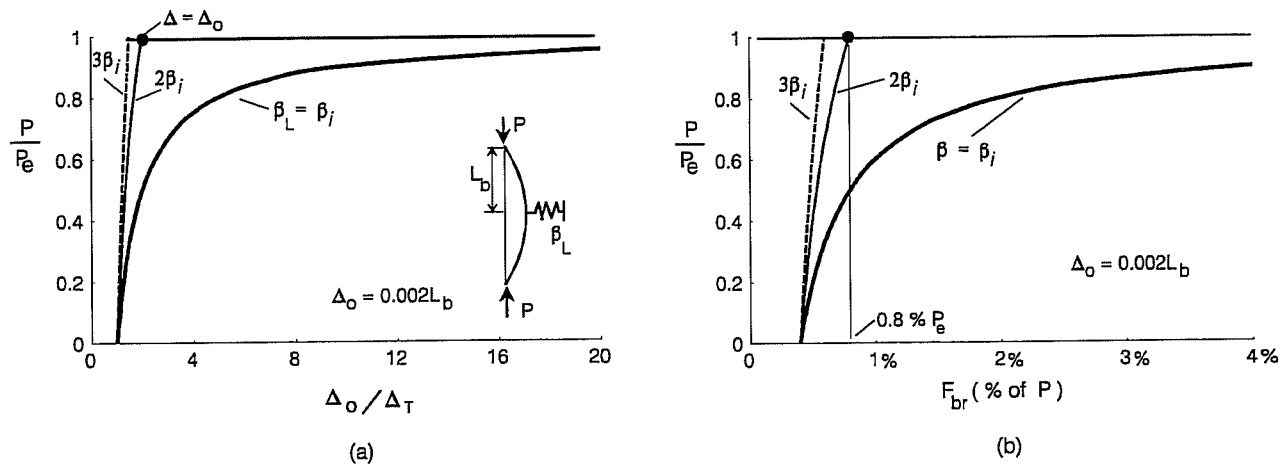
Figure 5.2   Braced column with out-of-straightness.

Substituting Eq. (5.2) into Eq. 5.3 gives

$$F_{br} = \frac{2P}{L_b} \frac{\Delta_o}{1 - \dfrac{2P}{\beta_L L_b}} \tag{5.4}$$

which shows that the brace force is directly related to the magnitude of the initial imperfection. If a member is fairly straight, the brace forces will be small. Conversely, members with large initial out-of-straightness will require larger braces. A plot of Eq. (5.4) for an initial imperfection $\Delta_o = L_b / 500$ is shown in Figure 5.2(b). If the brace stiffness is equal to the ideal stiffness, then the brace force gets very large as the buckling load is approached because $\Delta_T$ gets very large, as shown in Figure 5.2(a). For example, at $P = 0.95P_e$, Eq. (5.4) gives a brace force of 7.6% of $P_e$. Theoretically the brace force will be infinity when the buckling load is reached if the ideal brace stiffness is used. Thus, a brace system will not be satisfactory if the theoretical ideal required stiffness is provided because the brace forces get too large. If the brace stiffness is over designed, as represented by the $\beta_L = 2\beta_i$ and $3\beta_i$ curves in Figure 5.2(b), then the brace forces will be more reasonable. For a brace stiffness twice the ideal value and a $\Delta_o = L_b / 500$, Eq. (5.4) gives a brace force of only 0.8% $P_e$ at $P = P_e$, not infinity as in the ideal brace stiffness case. For a brace stiffness ten times the ideal value, the brace force will reduce even further to 0.44%. The brace force cannot be less than that 0.004P corresponding to $\Delta = 0$ (an infinity stiff brace) in Eq. (5.3) for $\Delta_o = L_b / 500$. For columns Yura (1971) showed that the brace force could conservatively be taken as 0.008 of the column load. This force is based on a brace stiffness at least twice the ideal value and an initial out-of-straightness of $L_b / 500$.

The effect of initial out-of-straightness on bracing requirements for beams follows a similar trend. Figure 5.3 shows the theoretical response of twin girder Test B9; 24-ft. span, W12X14 section midspan load at the top flange, lateral brace stiffness = 0.65 k/in. which is less than ideal, and top and bottom flange out-of-straightness = 0.16 in. and 0.13 in., respectively. The finite element computer program, ABAQUS, was used to develop the load-deflection response and $P_{cr} = 5.18$ kips at very large deflections. The BASP buckling program gave $P_{cr} = 5.34$ kips. These two $P_{cr}$ estimates are within three percent of each other. The experimental $P_{cr}$ from a Meck plot of test data
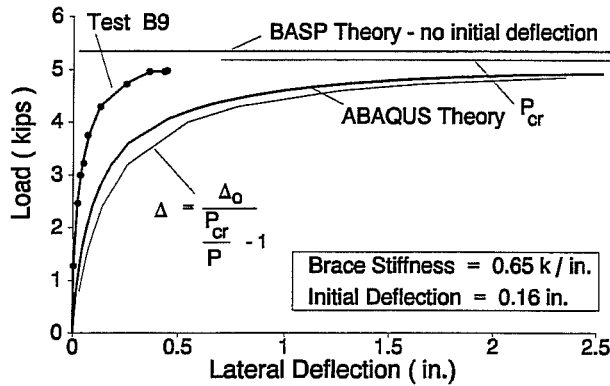
Figure 5.3        Beam with initial out-of-straightness.

gave $P_{cr}$ = 5.47 kips, as listed in Table 3.3.   The experimental lateral deflections are much less than the theoretical values.  This is probably due to the fact that the experimental midspan lateral deflection is for two beams with some difference in out-of-straightness. The test result is an average of two beams.  Even though the measured lateral displacements are one-third of the expected, the buckling loads are very similar.  Equation 5.2 developed for columns gives results very close to the ABAQUS solution when $A_0$ is taken as the initial out-of straightness of the compression flange.

Since the behavior of beams and columns with initial out-of-straightness is similar, the brace strength requirement for column, 0.008P, can be converted to beams by replacing P with M/h,

$$F_{br} = 0.008\,M\Big/h \qquad\qquad (5.5)$$

where M is the maximum beam moment and h is the distance between the centroids of the top and bottom flanges. M/h is an equivalent compressive force acting at the compression flange.  In Load Factor design M is based on factored loads, 1.3 dead + 2.2 live, and in Allowable Stress design, M is based on the service loads.  Impact should also be considered in determining M.  Nethercot (1989) has also verified that the brace force is less than 1% of the flange force when brace stiffness is at least twice the ideal stiffness.  The brace force recommendation given by Eq. 5.5 is based on an initial out-of-straightness of adjacent brace points of $L_b/500$.  For example, if lateral braces are spaced at 15 ft, the initial relative lateral displacement between adjacent brace points could be 3/8 in.

**5.1.2 Brace Stiffness.**   The lateral brace stiffness in Eq. (2.2) must be divided by two to limit the lateral deflection as the critical buckling load is reached as described above.  Therefore, for design, the brace stiffness effect

$$A_d = \frac{L^2}{\pi}\sqrt{\frac{.67\,\overline{\beta}_L}{2EI_y}} = L\sqrt{\frac{.33\overline{\beta}_L}{C_L\,P_y}} \qquad\qquad (5.6)$$

should be used with Eq. (2.1).   The general design recommendations for lateral bracing stiffness and strength are summarized in Appendix A.  The buckling moment can be calculated for any magnitude of lateral bracing stiffness from Eq. (A1).  In addition, Equation (A1) can be used to determine the brace stiffness required to force buckling between the braces (full or complete bracing) by setting $M_{cr} = M_s$ and solving for $A_d$.  This will be illustrated later.

In most practical situations, the bracing provided or available will be much greater than that required to force buckling between braces (full or complete bracing).  In such situation, Eq. (A1) may be unduly burdensome to check for all problems.  For discrete braces, Winter (1960) derived the ideal stiffness for full bracing.  For beams under uniform moment the Winter brace lateral stiffness required to force buckling between the braces is

$\beta_i$ = #$P_f$ / $L_b$ where $P_f = \pi^2 EI_{yc} / L^2_b$, $I_{yc}$ is the out-of-plane moment of inertia of the compression flange, $I_y/2$ for doubly symmetric cross sections, and # is a coefficient depending on the number of braces within the span, as given in Table 2.1. For other moment diagrams and top flange load, Winters ideal bracing stiffness can be modified as follows,

$$\beta_i^* = \frac{\# \, P_f}{L_b} C_{bb} \, C_L \qquad (5.7)$$

where $C_{bb}$ is the moment diagram modification factor given by Eq. 1.2 for braced beams, $C_L$ is the top flange factor defined by Equation 2.3, and # = 4 - (2/n) or the coefficient in Table 2.1. The modifications were developed from the analytical studies presented in Chapter 2. For the twin girder test beams, laterally braced at midspan, # = 2, $C_{bb}$ = 1.75, $C_L$ = 1 + 1.2/1 = 2.2, $L_b$ = 144 in. and $P_f = \pi^2$ (29000) (232/2)/(144)$^2$ = 16.01 kips, $\beta_i^*$ = 0.856 k/in. which is shown by the * in Figure 5.4. A linear response between zero bracing and ideal bracing is assumed and shown by the dashed line. Equation 5.7 compares very favorably with the test results and is a simpler alternative to the use of Eq. (2.1). For design Eq. (5.7) must be doubled for beams with initial out-of-straightness as given by $\beta_L^*$ in Eq. (A6) in Appendix A. It is recommended that Eq. (A6) be checked first for full bracing. If Eq. (A6) is not satisfied, then Eq. (A1) can be used to get $M_{cr}$.

**5.1.3  Relative Braces.** In the previous sections discrete or continuous braces were considered that can be represented by springs attached to the braced beams. The solution assumes that all braces have the same stiffness. In addition, each brace laterally supports a single point along the span. For example, a wheel load can transmit the lateral bracing stiffness of a deck slab only at the wheel location. Another example is a girder temporarily braced during construction by several guy cables attached between the top flange and the ground, each attached at a different discrete location along the span. A more common top flange lateral bracing system that is not a discrete system is shown in Figure 5.5. In this case the lateral brace prevents the relative lateral movement of the two points a and b along the span of the girder. The system relies on the fact that if the girders buckle laterally, points a and b would move different amounts. Since the diagonal brace prevents points a and b from moving different amounts, laterally buckling cannot occur except between the brace points.
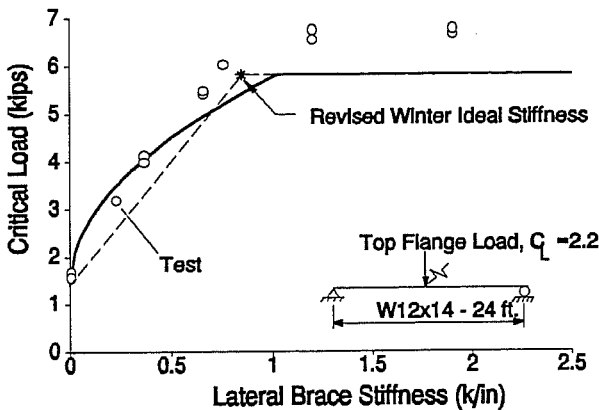


Figure 5.4   Revised Winter stiffness.
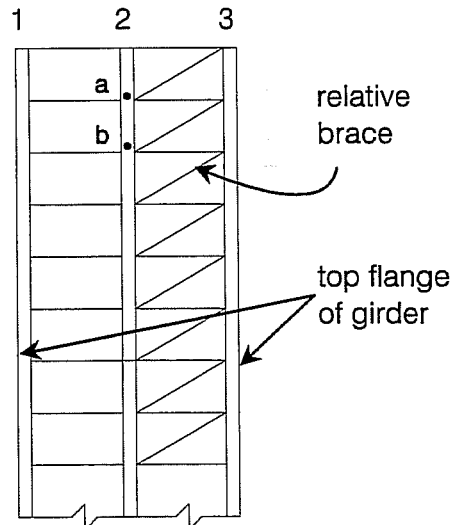


Figure 5.5      Relative lateral bracing.
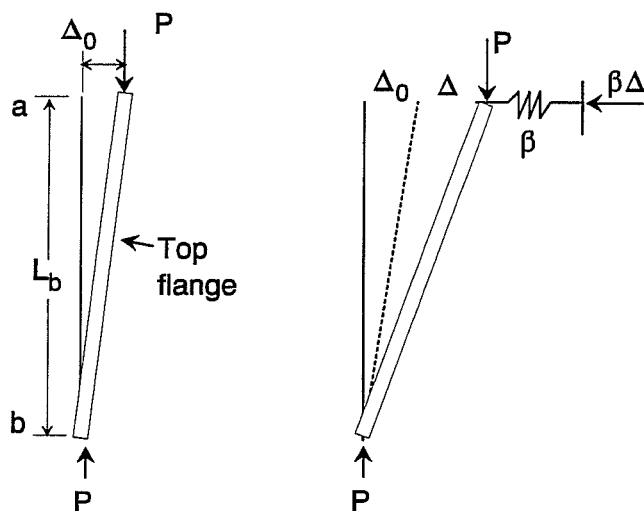
Figure 5.6 Relative brace requirements.

The strength and stiffness requirements for relative bracing can be derived by referring to Figure 5.6. The brace force $\beta\Delta$ must resist the overturning moment $P(\Delta_o + \Delta)$; $\beta\Delta L_b = P(\Delta_o + \Delta)$. If $\Delta = 0$, the ideal stiffness is $P/L_b$. Solving for the brace stiffness,

$$\beta = \frac{P}{L_b}\left[1 + \frac{\Delta_o}{\Delta}\right] \tag{5.8}$$

Choosing $\Delta_o = \Delta$ as for the discrete braces, the required stiffness is $\beta_L = 2P/L_b$. The brace force is

$$F_{br} = \frac{P}{L_b}\left(\Delta + \Delta_o\right) \tag{5.9}$$

Using $\Delta_o/L_b = 0.002$ and twice the ideal stiffness as presented previously for discrete braces, the brace force requirement becomes $F_{br} = 0.004\ M_f/h$, or one-half the value for discrete braces. The full bracing stiffness requirement becomes

$$\beta_L^* = 2\ P_f\ C_{bb}\ C_L\big/L_b \tag{5.10}$$

after making modifications for top flange loading and non-uniform flange force due to variation in moment along the span. The relative brace requirements for stiffness and strength are also summarized in Appendix A. The use of the discrete and relative bracing formulations will be illustrated in the following two example problems.

*5.1.4 Example Problems.* Two different lateral bracing systems are used to stabilize five composite steel plate girders during construction; a discrete system in Example 1 and relative bracing in Example 2. Each brace in Example 1 controls the lateral movement of one point along the span, whereas the diagonals in the top flange truss system shown in Example 2 controls the relative lateral displacement of two adjacent points. Relative systems require 1/2 the brace force and from 1/2 to 1/4 of the stiffness for discrete systems. In both examples, a tension type structural system was used but the bracing formulas are also applicable to compression systems such as K-braces. In Example 1 the full bracing requirements for strength and stiffness given by Equations (A6) and (A7) in Appendix A are used because they are simple and conservative compared to the general solution given by Equation (A1). The results should be fairly accurate, however, since the required moment (1211 k-ft) is close to the full bracing moment (1251 k-ft).

In both examples, stiffness controls the brace area, not the strength requirement. Note that in Example 1 that the stiffness criterion required a brace area 3.7 times greater than the strength formula. Even if the brace was designed for 2% of the compression flange force (a commonly used bracing rule), the brace system would be inadequate. It is important to recognize that <u>both</u> stiffness and strength must be adequate for a satisfactory bracing system.

# LATERAL BRACING - DESIGN EXAMPLE 1

Span = 80 ft. ; 10 in. concrete slab

5 girders @ 8 ft spacing, A36 steel

Design a lateral bracing system to stabilize the girders during the deck pour. Use the external tension system shown. The form supports transmit some load to the bottom flange so assume centroid loading.

Use Load Factor Design for the construction condition - L.F. = 1.3

**Girder Properties**

$S_x = 561$ in$^3$
$I_{yc} = 32.0$ in$^4$
$J = 12.9$ in$^4$

3/4 x 8
1/2 x 48
1-1/4 x 15

335 in

Loads:    Steel girder:   A = 48.75 in.$^2$,   wt = 165 lb/ft

Conc. slab:   $8' \times \dfrac{10}{12} \times 150$ lb/ft$^3$ = 1000 lb/ft

w = 1165 lb/ft = 1.165 k/ft

$$M = \frac{1}{8} w L^2 \times L.F. = \frac{1}{8}(1.165)(80)^2 1.3 = 1211 \text{ k-ft}$$

$$M_y = 36(561)/12 = 1682 \text{ k-ft} > 1211 \text{ k-ft}$$

$C_b = 1.0$

**Try 4 lateral braces @ 16-ft spacing**

Check lateral buckling - center 16-ft is most critical (AASHTO 10-102c)

$$M = 91 \times 10^6 (1.0) \frac{32.0}{16 \times 12} \sqrt{0.772 \frac{12.9}{32.0} + 9.87 \left(\frac{50}{16 \times 12}\right)^2}$$

= 15020000 lb-in = 1251 k-ft > 1211 k-ft      **4 braces required**

**Brace Design:** Use the full bracing formula - discrete system -
See Appendix A, Eq A6 & A7

$$P_f = \frac{\pi^2 (29000)(32.0)}{(16 \times 12)^2} = 248 \text{ kips}; \quad \# = 4 - \frac{2}{4} = 3.5 ; \quad C_{bb} = 1.0 ; \quad C_L = 1.0$$

$$\beta_L^* = 2 \frac{3.5(248)(1.0)(1.0)}{16 \times 12} = 9.04 \text{ k/in. for ea. girder} = 45.2 \text{ k/in. for 5 girders} = F/\Delta$$

Brace stiffness = $\cos^2 \theta \left(\dfrac{AE}{L}\right)_b = \dfrac{A_b (29000)}{(\sqrt{5})^2 335} = 45.2$ k/in.

| $A_b = 2.61$ in.$^2$ |   ⟵ **CONTROLS**

**Brace Strength:**   $F_{br} = 0.008(5)(1211 \times 12 / 49.0) = 11.86$ k
(A36 steel)         ⟍ five girders

$$A_b F_y = 11.37 / \cos\theta; \quad A_b = \frac{11.86\sqrt{5}}{36} = 0.74 \text{ in.}^2$$

## LATERAL BRACING  -  DESIGN EXAMPLE 2



PLAN VIEW

Top flg of girder

Same as Example 1 except the bracing system is a relative system - a top flange horizontal truss. Each truss stabilizes 2 1/2 girders. The unbraced length of the girder flange is 16 ft which was checked in Example 1.

Brace stiffness:

$$\beta_L^* = \frac{2 P_f \, C_{bb} \, C_L}{L_b}$$

$$= \frac{2(248)\,1.0\,(1.0)}{16 \times 12}$$

$P_f = 248$ kips

$C_{bb} = 1.0$

$C_L = 1.0$

$= 2.58$ k/in for ea. girder

$= 6.45$ k/in for 2 1/2 girders

$$\cos^2\theta \left(\frac{AE}{L}\right)_b = \left(\frac{1}{\sqrt{5}}\right)^2 \frac{A_b\,(29000)}{(8 \times 12 \times\sqrt{5})} = 6.45 \text{ k/in}; \quad A_b = 0.239 \text{ in}^2 \quad \longleftarrow$$

Brace strength: $\quad F_{br} = 0.004\,(2\,1/2)\,\dfrac{(1211 \times 12)}{49} = 2.97$ kips

$$A_b\,F_y = 2.97\,\sqrt{5} \quad ; \quad A_b = \frac{2.97\sqrt{5}}{36} = 0.184 \text{ in}^2$$

Stiffness controls the brace size; $9/16\phi$ $\qquad$ OK $\qquad A = 0.248 \text{ in}^2$

---

The simpler modified Winter full bracing requirements (Eqs. A6, A7) were used to design the braces in Example 1 because the buckling moment between brace points (1251 k-ft) was close to the maximum applied moment (1211 k-ft). Eq. (A1) could have also been used for the discrete braces in Example 1 as follows (see Appendix A for the equations):

Set $\quad M_{req'd} = \quad M_{cr} = \quad 1211 \times 12 \quad = \quad 14530$ in-k

(Eq. A5) $\quad M_o = \quad 91 \times 10^3 \left(\dfrac{32.0}{80(12)}\right) \sqrt{0.772\,\dfrac{12.9}{32.0} + 9.87\left(\dfrac{50}{12 \times 80}\right)^2} = 1763$ in-k

(Fig. A1) $\quad \overline{\beta}_L = \quad \dfrac{\beta_L \times 4}{80(12)} = \dfrac{\beta_L}{240} \; ; \quad P_{yc} = \dfrac{\pi^2\,(29000)\,(32.0)}{(80 \times 12)^2} = 9.94$ k

(Eq. A3) $\quad A_d = \quad 80(12) \sqrt{\dfrac{.17\,\overline{\beta}_L}{(1.0)9.94}} = 125\,\sqrt{\overline{\beta}_L} = 8.10\,\sqrt{\overline{\beta}_L}$

(Eq. A1) $\quad 14530 = \quad \sqrt{\left[\,(1763\,)^2 + (9.94 \times 49.0\,)^2\left(8.1\,\sqrt{\overline{\beta}_L}\right)\right]\left(1 + 8.1\,\sqrt{\overline{\beta}_L}\right)}$

54
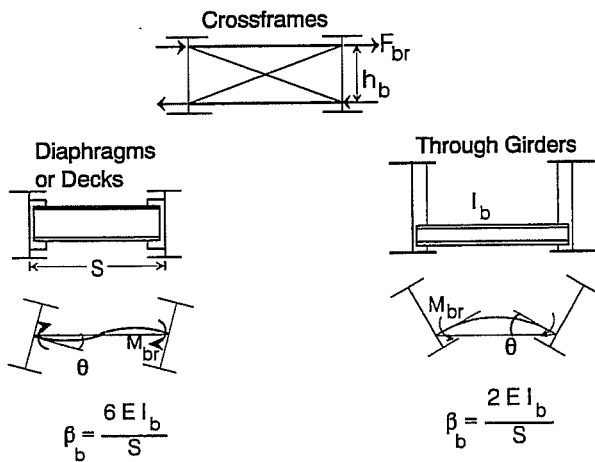
Crossframes



Figure 5.7   Torsional bracing systems.

Solving for $\beta_L$ gives 8.34 k/in./girder and the required area reduces to 2.41 in.$^2$ The required brace area is less than required for full bracing because the required moment of 1211 k-ft. is less than critical buckling moment between braces (1251 k-ft). If the critical moment for buckling between braces (1251 k-ft) was used in Eq. (A1) instead of the required moment (1211 k-ft), then $\beta_L = 9.04$ k/in., the same as given by Eq. (A6) for full bracing.

## 5.2    Design Requirements for Torsional Braces

In Chapter 2 the effect of the torsional brace stiffness on the lateral buckling strength of a single straight beam was given by Eq. (2.10). Most torsional brace systems are diaphragms, decks, cross frames or floor beams spanning between adjacent girders at points along the span, as shown in Figure 5.7. There are two basic structural systems in this figure: bending members represented by diaphragms, decks or floor beams; and trusses for the cross frames. The two systems can be correlated by noting that $M_{br} = F_{br} h_b$, where $h_b$ is the depth of the cross frame. The term "brace forces" used hereinafter refers to both $M_{br}$ and $F_{br}$.

*5.2.1   Brace Strength.* Equation (2.12) gives the relationship between continuous torsional brace stiffness and the buckling load for singly and doubly symmetric sections. That equation can be rearranged to give the ideal continuous brace stiffness

$$\bar{\beta}_T = \left(M_{cr}^2 - C_{bu}^2 M_o^2\right) \frac{C_T}{C_{bb}^2 E I_{eff}} \tag{5.11}$$

Equation (5.11) can be simplified by conservatively neglecting the $C_{bu}M_o$ term which will be small compared to $M_{cr}$ at full bracing. Taking the maximum $C_T$, which is 1.2 for top flange loading, the ideal continuous torsional stiffness becomes

$$\bar{\beta}_{Ti} = \frac{1.2 M_{cr}^2}{E I_{eff} C_{bb}^2} \tag{5.12}$$

where $M_{cr}$ is the maximum moment in the beam. The most common type of torsional bracing system is a cross frame or diaphragm between adjacent stringers or girders at a number of points, n, along the span. The ideal discrete stiffness, $\beta_{Ti}$, is

$$\beta_{Ti} = \frac{\bar{\beta}_{Ti} L}{n} = \frac{1.2 L M_{cr}^2}{n E I_{eff} C_{bb}^2} \tag{5.13}$$

For beams with an initial twist, $\theta_o$, it is assumed that the brace requirements are affected in a similar manner as that developed for lateral bracing of beams with initial out-of-straightness in Eq. (5.8). The required brace stiffness, $\beta_T$, is

$$\beta_T = \frac{1.2 \, L \, M_{cr}^2}{n \, E \, I_{eff} C_{bb}^2} \left[ 1 + \frac{\theta_o}{\theta} \right] \qquad (5.14)$$

and the brace strength requirement for diaphragms is

$$M_{br} = \beta_T \theta = \frac{1.2 \, L \, M_{cr}^2}{n \, E \, I_{eff} C_{bb}^2} \left( \theta_o + \theta \right) \qquad (5.15)$$

As described in detail for lateral bracing, a brace stiffness of at least twice the ideal stiffness is recommended to control $\theta$ and keep brace forces small. For $\beta_T = 2 \, \beta_{Ti}$, $\theta = \theta_o$ and assuming that $\theta_o = 1°(0.0175$ radians$)$ gives

$$M_{br} = F_{br} \, h_b = \frac{0.04 \, L \, M_{cr}^2}{n \, E \, I_{eff} C_{bb}^2} \qquad (5.16)$$

and

$$\beta_T = \frac{2.4 \, L \, M_{cr}^2}{n \, E \, I_{eff} C_{bb}^2} \qquad (5.17)$$

for strength and stiffness, respectively. For a 14-in. deep section, the 1° assumed initial twist corresponds to a 0.25-in. relative displacement between the top and bottom flanges.

The brace force given by Eq. (5.16) is based on a brace stiffness twice the ideal value. In most situations, the torsional strength requirement controls the size of the brace so the actual stiffness will be much greater than required. In such cases, the brace force from Eq. (5.16) can be modified by the factor,

$$\frac{.5}{1 - \left( \beta_{Ti} / \beta_{actual} \right)} \qquad (5.18)$$

which takes the same form as that developed by Winter (1960) for columns. For $\beta_{actual}$ twice the ideal values, the factor is 1.0. For $\beta_{actual} = 10\beta_{Ti}$, the factor becomes 0.55. For large $\beta_{actual}$, the brace force is reduced to one-half the value given by Eq. (5.16). For simple design applications, the conservative Eq. (5.16) is recommended.

The torsional brace requirements Eq. (5.16) through (5.18) were checked using the computer program, ANSYS. Two W16×26 sections with a 20-ft span were connected by a cross frame at midspan. A concentrated load at midspan was applied to each beam. The beams were spaced 42 in. apart. An initial twist of 1° was specified at
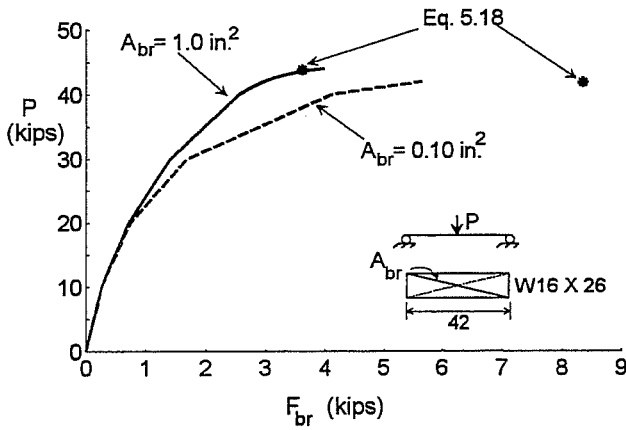
midspan. The imperfection along the length of the beam followed an S-shape pattern (Helwig 1993). A tension system for the cross frame was assumed; only one of the diagonals was assumed to be effective.

The analysis was performed for two different brace areas; 0.10 in.$^2$, which is less than the minimum recommended value of 0.19 in.$^2$ as derived in Appendix B, and 1.0 in.$^2$, about fourteen times the ideal value. The results shown in Figure 5.8 indicate that the brace force is reduced if the brace area (stiffness) is increased. For example, at P = 42 kips the brace force is 5.66 kips for $A_{br}$ = 0.10 in.$^2$ and 2.97 kips for $A_{br}$ = 1.0 in.$^2$. At $A_{br}$ = 0.10 the maximum brace force from the ANSYS analysis was 5.66 kips when one girder bucked between brace points at P = 42 kips. For $A_{br}$ = 1.0 in.$^2$, P increased to 44 kips when one girder buckled between brace points. In this case the maximum diaphragm brace force was 3.99 kips, a 30% reduction from the $A_{br}$ = 0.1 in.$^2$ solution.



Figure 5.8   Brace forces from ANSYS.

The ANSYS results also showed that maximum buckling load of the twin stringer system was different for the two cases in Figure 5.8 even though buckling occurred between the braces in both instances which should correspond to a buckling load of 47.2 kips as shown in Appendix B. The results for $A_{br}$ = 0.1 in.$^2$ and 1.0 in.$^2$ are $P_{cr}$ = 42 kips and 44 kips, respectively. The difference is caused by the torsional brace forces. When lateral buckling occurs, the forces or moments in the bracing system cause a vertical force couple $2M_{br}/S$, as shown in Figure 5.9, which increases the load on one beam and decreases the load on the adjacent girder. Thus, in calculating the load on the beam, the torsional brace forces should be considered. For the $A_{br}$ = 0.10 in.$^2$ case in Figure 5.8 the brace force per beam of 5.66 kips causes a vertical beam force of 2(5.66)(15.34)/(42) = 4.13 kips. Since $P_{cr}$ = 47.2 kips, the factored beam load which can be supported by the W16×26 beams is 47.2 - 4.1 = 43.1 kips, a ten percent reduction (The stiffer brace system had smaller brace forces so the applied force was larger at buckling when $A_{br}$ = 1.0 in.$^2$). The vertical force from the bracing system can be reduced by bracing each panel in a multi-girder system (a), shown in Figure 5.9. In this case the vertical force will be 2/3 that in system (b). In addition, the extra force in system (a) is applied to the exterior stringers which are usually more lightly loaded.
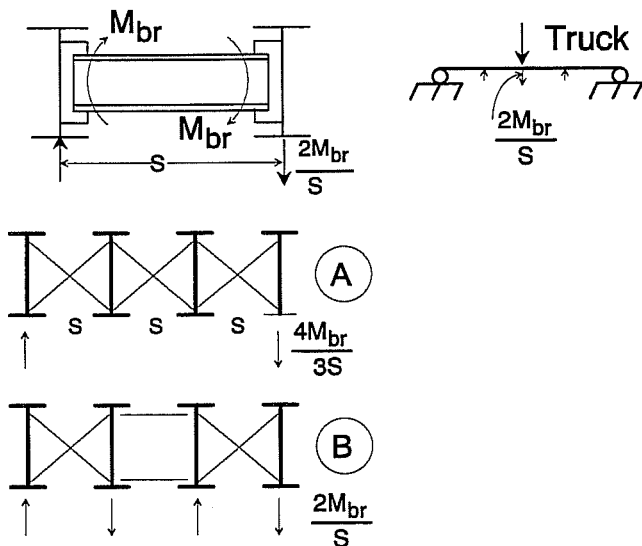


Figure 5.9   Beam load from braces.

The brace force given by Eq. (5.16) is 5.9 kips which assumes that the brace stiffness is twice the ideal value. As shown in the detail hand calculations given in Appendix B, the modified brace forces from Eq. (5.18) which accounts for the actual stiffness for the two cases of $A_{br} = 0.1$ and $1.0$ in.$^2$ gives $F_{br} = 8.40$ kips and $3.63$ kips, respectively. These two values are shown in Figure 5.8 by the asterisks, and it appears that Eq. (5.18) gives very conservative results for the $A_{br} = 0.1$ in.$^2$ case, $8.40$ kips versus $5.66$ kips from ANSYS. Helwig (1993) showed that this conservative result is due to the choice of an S-shaped initial-out-of-straightness for the ANSYS analysis. If the initial imperfection pattern is a sine curve, Eq. (5.18) and ANSYS compare very favorably.

**5.2.2    Brace Stiffness.**    The minimum recommended torsional brace stiffness is twice the ideal stiffness; so for design Eq. (2.12) becomes

$$M_{cr} = \sqrt{C_{bu}^2 M_o^2 + \frac{C_{bb}^2 E I_{eff} \overline{\beta}_T}{2C_T}}$$

(5.19)

For double symmetric sections $I_{eff} = I_y$. For any moment requirement, $M_{cr}$, Equation (5.19) can be solved for the required brace stiffness $\overline{\beta}_T$. This expression can be conservatively simplified as illustrated in the previous section by using Equation (5.17) which assumes $C_T = 1.2$ (top flange loading) and neglectes the $M_o$ term in Equation (5.19). The actual brace stiffness must be compared to the required values from either Eq. (5.19), which is the most exact formulation, or Eq. (5.17) which is a conservative approximation. For some common cross frame arrangements, formulas for brace stiffness, $\beta_b$ , are provided in Figure 5.10. In the tension system, diagonals are not designed to support compressive forces so only one diagonal is assumed effective. In the tension system, horizontal members must be provided which support the compressive forces shown. If the diagonals are designed to support compression, then horizontal members are not required. In the K brace system, a top horizontal is required. For the load system shown with equal lateral force on the two beams, there is zero force in the top horizontal; but if there is any different in the forces, the top horizontal will have a force in it. For torsional bracing systems relying on bending members, the stiffness is defined in Figure 5.7.

In crossframes and diaphragms, the torsional bracing forces are resisted by in-plane forces on the main girders as illustrated in Figure 5.9. The vertical girder deflections associated with the bracing forces cause a rotation of the cross frame or diaphragm which reduces the effective stiffness of the cross frame. Helwig (1993) has shown that for twin girders the strong axis stiffness $\beta_g$ is

$$\beta_g = \frac{12 S^2 EI_x}{L^3}$$

(5.20)

58

**TENSION SYSTEM**

$$\theta = \frac{\Delta + \Delta_h}{h_b} \quad ; \quad M = F h_b$$

$$\beta_b = M / \theta$$

$$\beta_b = \frac{ES^2 h_b^2}{\dfrac{2L_c^3}{A_c} + \dfrac{S^3}{A_h}}$$

Tension System - horizontals are required

**COMPRESSION SYSTEM**

$$\beta_b = \frac{A_c ES^2 h_b^2}{L_c^3}$$

and

Tension - Compression System horizontals not required

**K BRACE**

$$\beta_b = \frac{2ES^2 h_b^2}{\dfrac{8L_c^3}{A_c} + \dfrac{S^3}{A_h}}$$

K Brace System - diagonals designed for tension and compression

$A_h$ = area of horizontal members   $L_c$ = length of diagonal members
$A_c$ = area of diagonal members   $S$ = spacing of girders
$E$ = modulus of elasticity   $h_b$ = height of the cross frame

Figure 5.10   Stiffness formulas for cross frames.

where $I_x$ is the strong axis moment of inertia of one girder. As the number of girders increase, the effect of girder stiffness will be less significant. In mult-girder systems, the factor 12 in Eq. 5.20 can be changed to 24 $(\# - 1)^2/\#$ where # is the number of girders. For example, in a six-girder system, the factor becomes 100 or more than eight times the twin girders value of 12.

As discussed in Chapter 2, cross section web distortion must be considered when evaluating the stiffness of torsional brace systems. The recommendations for stiffeners, including distortion effects, are summarized in Appendix A. In general, stiffeners or connection details, such as clip angles, can be used to control distortion. For decks and through girders, the stiffener must be attached to the flange that is braced. Diaphragms are usually W shapes or channel sections connected to the web of the stringer or girders through clip angles, shear tabs or stiffeners. When full depth stiffeners or

Figure 5.11   Partially stiffened webs.

connection details are used to control distortion, then the stiffener size can be determined from Eq. (A9). For partial depth stiffening illustrated in Figure 5.11, the stiffness of the various sections of the web can be evaluated separately, then combined as follows:

$$\beta_i = \frac{3.3E}{h_i} \left( \frac{h}{h_i} \right)^2 \left( \frac{1.5\,h_i\,t_w^3}{12} + \frac{t_s\,b_s^3}{12} \right) \tag{5.21}$$

where $h_i = h_c$, $h_s$. or $h_t$ and

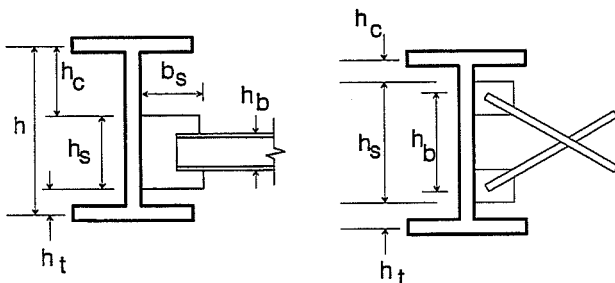$$\frac{1}{\beta_T} = \frac{1}{\beta_c} + \frac{1}{\beta_s} + \frac{1}{\beta_t} + \frac{1}{\beta_b} + \frac{1}{\beta_g} \tag{5.22}$$
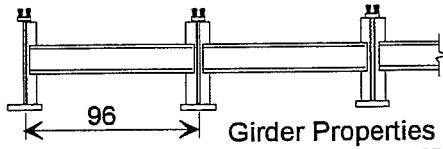
Even further refinement could be made by considering the portion of the web within $h_b$ to be infinitely stiff. For rolled sections, if the connection extends over at least one-half the beam depth, then cross section distortion will not be important as demonstrated in Figure 2.18 and $\beta_b \approx \beta_T$. The location of the diaphragm or cross frame is not very important; it does not have to be located close to the compression flange. The depth of the diaphragm, $h_s$, can be less than one-half the girder depth as long as it provides the necessary stiffness to reach the required moment by Eqs. (5.19) or (5.20). For cross frames, $\beta_s$, should be taken as infinity; only $h_t$ and $h_c$ will affect distortion. The distortion effect will be considered in the design examples.

### 5.2.3 *Example Problem.*
In Example 3, a diaphragm torsional bracing system is designed to stabilize the five steel girders during construction as described in Examples 1 and 2 for lateral bracing. The strength criterion, Eq. A11, is initially assumed to control the size of the diaphragm. A C10 × 15.3 is sufficient to brace the girders. Both yielding and buckling of the diaphragm are checked. The stiffness of the C10 × 15.3 section, 195,500 in-k/radian, is much greater than required but the connection to the web of the girder and the in-plane girder flexibility also affect the stiffness. In this example, the in-plane girder stiffness is very large and its affect on the brace system stiffness is only 2%. In most practical designs, except for twin girders, this effect can be ignored. If a full depth connection stiffener is used, a 3/8 × 3-1/2 in. section is required. The weld design, which is not shown, between the channel and the stiffener must transmit the bracing moment of 293 in-k. If the more exact Eq. (5.19) would have been used, the $\beta_T$ required would reduce to 14,300, a 22% reduction. The difference between the simple Eq. (A10a) and Eq. (5.19) is caused mainly by the top flange factor of 1.2 used in Eq. (A10a).

The 40-in. deep cross frame design in Example 4 required a brace force of 7.13 kips from Eq. (A11). The factored girder moment of 1211 k-ft. gives an approximate compression force in the girder of 1211 × 12/49 = 296 kips. Thus, the brace force is 2.5% of the equivalent girder force. Thus, common rule-of-thumb brace forces of 2% of the girder force would be unconservative in this case. The framing details provide sufficient stiffness. The 3-in. unstiffened web at the top and bottom flanges was small enough to keep $\beta_{sec}$ well above the required value.

For illustration purposes, a 30-in. deep cross frame attached near the compression flange is also considered. In this case, the cross frame itself provides a large stiffness, but the 14-in. unstiffened web is too flexible. Cross-section distortion reduces the system stiffness to 16,900 in.-k/radian, which is less than the required value. If this

# TORSIONAL BRACING - DESIGN EXAMPLE 3



$\leftarrow$ 96 $\rightarrow$

**Girder Properties**

$h = 49.0$ , $h_c = 30.85$ , $h_t = 18.15$ in

$I_x = 17500$ , $I_{yc} = 32.0$ , $I_{yt} = 352$ in$^4$

Same as Example 1 except use the diaphragm system shown.  In Ex. 1, four lateral braces were required which gave $M_r$ = 1251 k-ft, just 3% greater than the required mom.  Since torsional braces will impose some additional vertical forces on the girders as shown in Fig. 5.9, probably five braces should be used.  However, for comparison with Examples 1 & 2, a four-brace system will be designed.    $M_{req'd}$ = 1211 k-ft  (see Ex. 1)

Eq. 2.11: $I_{eff} = 32 + \dfrac{18.15}{30.85}\, 352 = 239$ in$^4$

Eq. (A11)  $M_{br} = \dfrac{0.04\,(80 \times 12)\,(1211 \times 12)^2}{4\,(29000)\,239\,(1.0)^2} = 293$ in-k

A36 Steel:

Req'd $S_x = 293/36 = \underline{8.14}$ in$^3$

Try C10 x 15.39 -

$I_x = 67.4$ in$^4$,  $S_x = 13.5$ in$^3$,  $t_f = 0.436$ in ,  b = 2.60 in ,  J = 0.21 in$^4$

Check lateral buckling of the diaphragm

$I_{yc} = (2.60)^3\,(0.436)\,/\,12 = 0.639$ in

$C_b = 2.3$

$M_r = 91 \times 10^6\,(2.3)\,\dfrac{0.639}{96}\,\sqrt{\dfrac{.772\,(0.21)}{0.639} + \left(\dfrac{\pi\,10}{96}\right)^2}$

$= 837000$ lb-in  $= 837$ in-k  $>$  $M_y = 13.5(36)$  $= 486 > 293$ in-k ,  OK

Check stiffness:   Eq. (A10a);   $\beta_{T\,req'd} = \dfrac{2.4(80 \times 12)\,(1211 \times 12)^2}{4(29000)\,239\,(1.0)^2} = 17550$ in-k/radian



$\leftarrow$ $b_s$

15

17
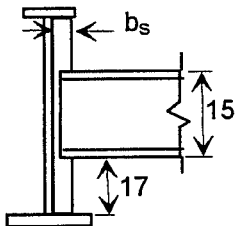
The stiffness of the diaphragms on the exterior girders is $6EI_{br}/S$.  Since there are diaphragms on both sides of each interior girder, the stiffness is $2 \times 6EI_{br}/S$.  The average stiffness available to each girder is $(2 \times 6 + 3 \times 12)/5 = 9.6\,EI_{br}/S$.

$\beta_b = 9.6\,(29000)\,67.4/96 = 195500$ in-k/radian

Girder : Eq. (5.20)    $\beta_g = \dfrac{24\,(5-1)^2\,29000\,(96)\,17500}{5\,(80\times12)^3} = 406000$ in-k/radian

Distortion :  From Fig 5.11 and Eq. (5.21) determine the required stiffener size , t = 3/8 in

$\beta_s = \dfrac{3.3\,(29000)}{19.5}\left(\dfrac{49}{19.5}\right)^2\left(\dfrac{1.5 \times 19.5 \times .5^3}{12} + \dfrac{.375\,b_s^3}{12}\right)$ \qquad (1)

From Eq. (A9)    $\dfrac{1}{17550} = \dfrac{1}{195500} + \dfrac{1}{406000} + \dfrac{2}{\beta_s}$ ;  $\beta_s = 40500$ in-k/radian \qquad (2)

Equating (1) and (2) gives $b_s = 3.17$ in.  -  Use 3/8 x 3-1/2 stiffener

# TORSIONAL BRACING - DESIGN EXAMPLE 4
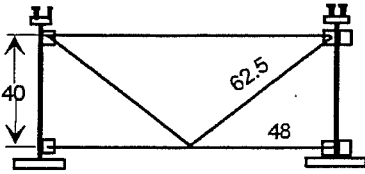
Same as Example 3, but use cross frames. Make all member sizes the same. A K-frame system will be considered using double angle members welded to connection gusset plates. Member lengths are shown in inches. Use four crossframes. See Examples 1 and 3 for section properties. Use A36 steel.

Assume brace strength criterion controls - Eq. (A11)

$$F_{br} \, (40) = \frac{0.04 \, (80 \times 12) \, (1211 \times 12)^2}{4 \, (29000) \, 239 \, (1.0)^2} = 293 \text{ in-k} \qquad ; \quad \underline{F_{br} = 7.31 \text{ kips}}$$

From Fig. 5.10 : Max force = diagonal force = $\dfrac{2F_{br} L_c}{S} = \dfrac{2(7.31) \, 62.5}{96} = 9.52$ kips - comp

The AASHTO Load Factor method does not give a strength formula for compression members so the formulation in Allowable Stress Design will be used. Convert to ASD by dividing the member force by the 1.3 load factor to get an equivalent service load force.

Diagonal Force (ASD) = 9.52/1.3 = 7.3 kips

Try 2L - 2 1/2 x 2 1/2 x 1/4        $r_x$ = .769 in. , A = 2.38 in.$^2$

$\ell / r$ = 62.5 / .769 = 81.2 ; $F_a$ = 16980 - .53 $(81.2)^2$ = 13490 psi = 13.5 ksi

$$P_{allow} = 13.49 \, (2.38) = 32.1 \text{ kips} > 7.3 \text{ kips} \quad OK$$

Check brace stiffness:

Eq. (A10a) ; $\beta_{T \, req'd}$ = 17550 in-k/radian  - see Example 3

Fig. 5.10 :  $\beta_b = \dfrac{2(29000) \, (96)^2 \, (40)^2 \, (2.38)}{8 \, (62.5)^3 + \, (96)^3}$ = 717000 in-k/radian

Girder :  $\beta_g$  = 406000 in-k/radian  - see Example 3

$$\beta_c = \beta_t = \frac{3.3 \, (29000)}{3.0} \left( \frac{49}{3.0} \right)^2 \left( \frac{1.5 \, (3.0) \, (.5)^3}{12} \right) = 399000 \text{ in-k/rad}$$

Eq. (A9) : $\dfrac{1}{\beta_T} = \dfrac{1}{717000} + \dfrac{1}{406000} + \dfrac{2}{399000}$ ; $\beta_T$ = $\underline{113000 > 17550}$ in-k/rad   OK

Evaluate the cross frame shown below
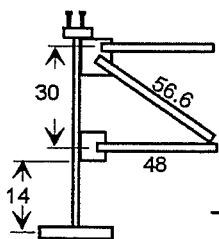
$$\beta_b = \frac{2(29000) \, (96)^2 (30)^2 (2.38)}{8 \, (56.6)^3 + \, (96)^3} = 490000 \text{ in-k/radian}$$

$$\beta_t = \frac{3.3 \, (29000)}{14.0} \left( \frac{49}{14.0} \right)^2 \left( \frac{1.5 \, (14.0) \, (.5)^3}{12} \right) = 18300 \text{ in-k/rad}$$

$\dfrac{1}{\beta_T} = \dfrac{1}{490000} + \dfrac{1}{406000} + \dfrac{1}{18300}$ ; $\beta_T$ = $\underline{16900 < 17550}$ in-k/rad   NG

same cross frame was placed at the girder midheight, the two 7-in. unstiffened web zones top and bottom would be stiff enough to satisfy the brace requirements. For a fixed depth of cross frame, attachment at the mid-depth provides more effective brace stiffness than attachment close to either flange as illustrated in Figure 2.18.

## 5.3 Bridge Deck Evaluation

As discussed in Section 1.5 and Chapter 4, a bridge deck has the potential to act as a lateral and/or torsional brace. Torsional bracing effects should only be considered when there is a positive attachment to the deck which provides a moment connection between the /deck and the supporting stringers. When there is no positive attachment between the deck and the stringers, torsional bracing by the deck is not reliable since the restraint would reduce to zero when flange contact is lost as the beam twists. The tests reported in Chapter 4 show that even when the deck is not attached to the stringers, the deck can still function as a lateral brace at the wheel point due to friction at the contact surface. For these reasons, only lateral bracing by the bridge deck is discussed in this section. The application of the lateral bracing equations for short span bridges must be based on the assumption that sufficient friction or shear connection exists to transfer lateral loads associated with stringer buckling to the bridge deck. The deck can then function as a lateral brace and/or distribute lateral loads among the stringers, such that the most heavily loaded stringers are braced by those with lighter loading as shown in Figure 1.3. The lateral stiffness of a short-span bridge should be based on the stiffness of the total system, to include contributions from the deck and all of the stringers.

For the design or rating of short span bridges with rolled sections, the governing loading condition for flexure is a wheel load near midspan, as shown in Figure 5.12. To determine the lateral bracing effect of the deck at midspan, $\beta_L$, for this loading condition, the general bracing equations can be simplified to the following for the Load Factor Design method in the AASHTO Specification (in-lb units):
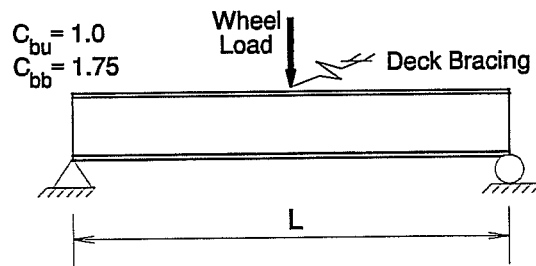


Figure 5.12    Loading condition for short-span bridges.

$$M_{cr} = \sqrt{\left( M_o^2 + 0.766\, P_y^2 h^2 A \right)\left( 1 + A \right)} \leq M_s$$
$$\leq M_y$$

(5.23)

where

$$M_o = \frac{91 \times 10^6}{L} \sqrt{0.772\ I_{yc}J} \qquad (5.24)$$

$$M_s = \frac{91 \times 10^6\ C_b\ I_{yc}}{L_b} \sqrt{0.772\ \frac{J}{I_{yc}} + 9.87 \left( \frac{d}{L_b} \right)^2} \qquad (5.25)$$

with $C_b = 1.75$, $L_b = L/2$

$$M_y = F_y\ S_x \qquad (5.26)$$

$$P_y = \frac{\pi^2\ E\ I_y}{L^2} = \frac{286 \times 10^6\ I_y}{L^2} \qquad (5.27)$$

$$A = 0.45 \sqrt{\frac{\beta_L L}{P_y}} \qquad (5.28)$$

L = span length, $I_y$ = weak axis moment of inertia, $I_{yc}$ = lateral moment of inertia of the compression flange = $I_y/2$, J = St. Venant torsional constant, d = beam depth, h = distance between flange centroids, $C_b$ = factor to account for moment gradient between brace points, $P_y$ = Euler buckling load for columns, A = bracing factor, $M_s$ = buckling capacity between brace points, and $M_y$ = yield moment. $M_o$ is the beam buckling strength assuming no bracing and top flange loading and is approximated by using the AASHTO $C_b = 1.0$ for the case when the moment within the unbraced segment is greater than the end moments and by neglecting the $(d/L_b)$ term in Eq. (5.25). The lateral bracing effect of the bridge deck is represented by $\beta_L$ in Eq. (5.28) which includes a reduction factor of 2 for initial out-of-straightness.

For a known deck stiffness, the buckling strength may be determined directly from Eq. (5.23). If a certain capacity, $M_{req}$, is required for a given bridge system, the bracing factor, $A_{req}$, may be determined by substituting $M_{req}$ for $M_{cr}$ in Eq. (5.23) and solving for $A_{req}$ as follows:

$$A_{req}^2 + \left[ 1 + 1.3 \left( \frac{M_o}{P_y h} \right)^2 \right] A_{req} - \frac{1.3}{P_y^2 h^2} \left( M_{req}^2 - M_o^2 \right) = 0 \qquad (5.29)$$

The required bracing effect may be found by solving for the appropriate root of the quadratic. From the required bracing factor, the corresponding brace stiffness may be determined from Eq. (5.28) as follows:

$$\beta_{Lreq} = A_{req}^2\ \frac{5\ P_y}{L} \qquad (5.30)$$

The equations above can be adapted for Allowable Stress Design by defining $M_{allow} = 0.55\ M_{cr}$ from Eq. (5.23) and using $1.82\ M_{max}$ based on service load in place of $M_{req}$ in Eq. (5.29).

For a single span bridge, the maximum moment in the stringers is related to the axle load; the total bridge lateral brace force $F_{br}$ may be calculated as follows:

$$F_{br} = 0.008 \, \frac{P_{axle}L}{4h} \qquad\qquad (5.31)$$

If there is no positive attachment between the deck and stringers, friction may be adequate to develop the force. The required coefficient of friction can be determined by dividing the total lateral brace force by the corresponding axle load. Stringer depth, d, is usually within 5% of h. It follows from Eq. (5.31) that for a span-to-depth ratio (L/d) of 40, a friction coefficient of 0.08 is required. For a span-to-depth ratio of 20, a friction coefficient of only 0.04 is required. The measured coefficient of friction between wood and steel (Webb and Yura, 1991) is 0.25 which means that friction can be used to mobilize the deck as a lateral brace when there is no mechanical connection between the stringer and the deck.

### 5.3.1  Timber Deck Stiffness.

Timber decks have the potential to increase the capacity of a bridge system by functioning as a lateral brace as well as a connecting link between stringers, so that stringers with lighter loading are able to serve as braces for those supporting heavier loads. Lateral stiffness provided by a timber deck is dependent upon specific construction and details. Except for a laminated deck, which may be treated as a diaphragm for stiffness calculation, the lateral bracing contribution of a timber deck is derived from the stiffness of the deck nailers and the rotational restraint provided by nailer/plank connections. Adequate attachment must be provided between the deck nailers and the planks in order to utilize the lateral stiffness of the nailers. When this attachment is made with two or more spikes, additional lateral stiffness is available through rotational restraint.

Experimental studies on the timber deck of the full-size bridge test presented in Chapter 4 were conducted to determine the deck stiffness. The various tests and procedures for obtaining the deck lateral stiffness are given in the Webb/Yura (1991) report. Experimental studies and structural analysis using the SAP90 program showed that the stiffness of the deck depends on the lateral stiffness of the nailers used to align the deck and the moment-rotation characteristics of the nailed connection between the deck planks and the nailer.

All of the 4×8 planks used to construct the full system bridge deck were significantly warped. Due to this warping, the 2×6 deck nailers were not in full contact with the 4×8 planks. The nailers were fastened to each plank with two 10d screw shank nails. The rotational restraint provided by this connection was determined experimentally for various degrees of contact between the members. The results of the nailer/plank connection rotational restraint test are presented in Figure 5.13. The "No Gap"curve represents full contact between the 2×6 deck nailer and 4×8 plank. the 1/8, 1/4 and 5/16 Gap curves represent tests in which gaps between the members were imposed as illustrated. Two to three specimens were tested for each degree of contact. The rotational stiffness of the full contact curve is due to both friction between the wood members and the lateral capacity of the nails. Figure 5.13 indicates that the rotational stiffness for the members with imposed gaps was fairly uniform, with the stiffness decreasing as the gap increased. As expected, the full contact stiffness was much greater. It can be seen that the loss of friction reduces the rotational stiffness significantly. The stiffness with a 5/16 Gap is only 14% of that with full contact. The

Figure 5.13   Nailer-plank connection.

average rotational stiffness for the nailer/plank connection was postulated as 119 kip-in./rad for SAP90 analysis of the full bridge system because the 5/16 inch gap most closely approximated average actual conditions.

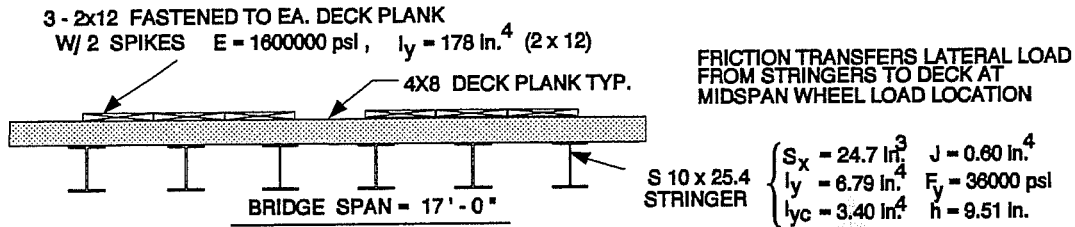The SAP90 evaluation of the timber deck is given in Figure 4.13 as the solid straight line. The SAP 90 calculated stiffness of 1260 lb/in. compares reasonably with the experimental results. The main purpose of the comparison is to show that commercial computer programs are available that can be used to determine deck stiffness. However, this approach is not very practical because the moment-rotation characteristics of the nailer-plank connection must be known. The dashed line in Figure 4.13 gives the stiffness based on the nailers alone, which is about 1/4 of the actual stiffness. Since the brace stiffness requirement for bracing is not very large, this very conservative approach will usually show that the deck provides sufficient bracing to enable the steel stringers to reach their yield strength. An evaluation of a timber deck bridge common to the central Texas area is given in Design Example 5.

**5.3.2    Typical Timber Decks.**    Construction details among off-system short span bridges with timber decks vary considerably. Some bridges still in service were built in the early 1900's. Upgrading and renovation, which has been implemented since the original completion of these bridges, does not follow any uniform set of construction details. Variability in construction often makes evaluation a difficult task. Several short span timber decked bridges located in Bastrop County, Texas, were examined as part of this investigation (Webb and Yura, 1991). A lack of positive attachment between the deck and supporting stringers was common. Two bridges are selected for discussion.

A photograph of the deck for Bastrop County bridge AA-0233-01 is presented in Figure 5.14. Two rows of three 2 × 12's are located in the center of this 34-ft one lane bridge composed of two 17-ft spans. The 2 × 12 overlay detail was found on most of the bridges visited. The 4 × 8 timber deck is supported by six continuous railroad rail stringers. The 2 × 12s serve to tie the deck planks together. Lateral stiffness for this deck is derived from the six 2 × 12's and any rotational restraint provided by their connection to the planks. Typically, the 2 × 12's are fastened to the planks with only one spike and connections have not been provided at every plank. It is recommended that all of the 2 × 12's be fastened to each plank with two spikes. While it may be conservative to ignore the rotational restraint of the nailed connections, the use of two spikes will significantly improve the lateral stiffness of the bridge deck as demonstrated in Figure 4.13. With one connector the lateral stiffness of this deck can be conservatively taken as that provided by the sum of the six 2 × 12's since no splices occur within the middle two-thirds of the span. With friction engaging the deck as a lateral brace at midspan, the discrete brace stiffness, $\beta_L$, based on a midspan loading model is equal to 9.66 kip/in. or 1.61 kip/in. per stringer. The corresponding uniform brace stiffness per stringer is 0.0105 kip/in. per in. of length. The calculations for this deck stiffness are provided in detail as part of Design Example 5 given previously. For simplicity the bridge was conservatively modeled as two simple 17-ft spans.

The deck for Bastrop County bridge AA-0237-01 is shown in Figure 5.15. Two rows of three 2 × 12's are located in the center of this 45-ft. one-lane bridge composed of three 15-ft. spans. This bridge had a posted axle or tandem weight limit of 7500 lb. In addition to the 2 × 12's, 4 × 8 planks are located along the outside edges of the deck. The 4 × 8 deck is supported by ten continuous railroad rail stringers. The 2 × 12's were not uniformly attached, with connections provided at about every other plank. It is recommended that the 4 × 8 side members and the 2 × 12's be fastened with two spikes to each 4 × 8 deck plank. A splice in one of the 2 × 12's and one of the

# DESIGN EXAMPLE 5

3 - 2x12 FASTENED TO EA. DECK PLANK
W/ 2 SPIKES   E = 1600000 psi,   $I_y$ = 178 in.$^4$ (2 x 12)

4X8 DECK PLANK TYP.

FRICTION TRANSFERS LATERAL LOAD
FROM STRINGERS TO DECK AT
MIDSPAN WHEEL LOAD LOCATION

S 10 x 25.4
STRINGER

$\begin{cases} S_x = 24.7 \text{ in.}^3 & J = 0.60 \text{ in.}^4 \\ I_y = 6.79 \text{ in.}^4 & F_y = 36000 \text{ psi} \\ I_{yc} = 3.40 \text{ in.}^4 & h = 9.51 \text{ in.} \end{cases}$
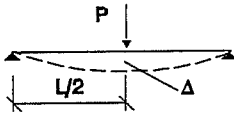
BRIDGE SPAN = 17'-0"

## STIFFNESS OF TIMBER DECK:

With each 2x12 fastened to each 4x8 deck plank with 2 spikes and no splice within the middle two-thirds of the span, the lateral stiffness of the deck can be taken as the sum of the six 2x12.

Discrete Brace Stiffness :   $\beta_L = P / \Delta = 48 E I_d / L^3$   $I_d = 6 (178) = 1068 \text{ in.}^4$

$P \downarrow$

$L/2$   $\Delta$

$= 48 (1.6 \times 10^6)(1068) / (204)^3 = 9660 \text{ lb/in}$

$\beta_L$ per Stringer = 9660 / 6 = 1610 lb/in.

## BUCKLING STRENGTH :

Unbraced Capacity, Eq. (5.24) :   $M_o = \dfrac{91 \times 10^6}{204} \sqrt{0.772 \, (3.40)\, (0.60)} = 559800 \text{ lb - in.}$

Buckling Capacity With Bracing :   Eq. (5.27)   $P_y = 286 \times 10^6 (6.79) / (204)^2 = 46700 \text{ lb}$

Eq. (5.28)   $A = 0.45 \sqrt{\dfrac{1610\,(204)}{46700}} = 1.21$

$M_{cr} = \sqrt{\left[(559800)^2 + 0.766\,(46700)^2\,(9.51)^2\,(1.21)\right](1 + 1.21)} = 1.046 \times 10^6 \text{ lb-in}$

Check Capacity for Buckling Between Braces :

$M_s = \dfrac{91 \times 10^6 (1.75)(3.40)}{102} \sqrt{0.772 \dfrac{0.60}{3.40} + 9.87 \left(\dfrac{10.0}{102}\right)^2} = 2.55 \times 10^6 \text{ lb - in.} > M_{cr}$

Check Material Strength,   $M_y = 36000 (24.7) = 889000 \text{ lb - in.} < M_{cr}$   Yielding Controls

## REQUIRED COEFFICIENT OF FRICTION :

Brace Force per Stringer,   Eq. (5.31)   $F_{br} = 0.008 (889000) / 9.51 = 748 \text{ lb}$

Maximum Wheel Load per Stringer,   $P_{max} = 4 (889000) / 204 = 17400 \text{ lb}$

Required Coefficient of Friction,   $C = 748 / 17400 = 0.043 << 0.25$   Friction *OK*

Figure 5.14   Bastrop County Bridge AA-0233-01.

4 x 8 side members occurs in the middle two-thirds of both exterior spans. Assuming that the recommended connections have been provided, the lateral stiffness for this bridge deck can be conservatively taken as the sum of the individual stiffness for five of the six 2 x 12's and one of the two 4 x8 side members due to the splices. Relying on friction to transfer loads at midspan, the corresponding discrete brace stiffness based on a midspan loading model, is 13.3 kip/in. or 2.67 kip/in. per stringer. The continuous brace stiffness per stringer is 0.0198 kip/in. per in. of length. For an S7 x 15.3, this deck would provide sufficient lateral bracing to force yielding before buckling.

Even though friction requirements are small, there may be some reluctance among engineers to depend upon friction resistance to transfer lateral loads and engage the deck as a lateral brace. Figure 5.16 presents an alternate remedial lateral shear connection detail which can be implemented on any of the bridges that were examined. The 2 x 6 members located adjacent to the stringers have been oriented to provide additional contact with the top flange and minimize end grain splitting which may otherwise result from interaction with the stringer. The connection to the deck for this detail should be designed for brace forces determined as discussed in the previous section on strength requirements for lateral braces.



Figure 5.15    Bastrop County Bridge AA-0237-01.

In the timber decks checked, the deck was found to have sufficient lateral stiffness to brace the stringers at midspan until yielding occurred. While the authors believe that typical bridge decks do provide full bracing at the wheel load, a definite statement to that effect cannot be made since the laboratory test deck did not provide full bracing at midspan due to inadequate deck stiffness. Admittedly, the laboratory test deck had marginal stiffness compared to actual decks.

*5.3.3    Stiffness Evaluation of Concrete Decks.*   A related study of the bracing effects of bridge decks was completed by Kissane (1985) for the New York State Department of Transportation. The objective of that research was to determine the effectiveness of a non-composite concrete bridge deck as a lateral brace for the compression flange of the supporting steel stringers without any positive shear connection between the two. Steps were taken to eliminate any physical or chemical bond between the concrete deck and the supporting S12 x 31.8 steel
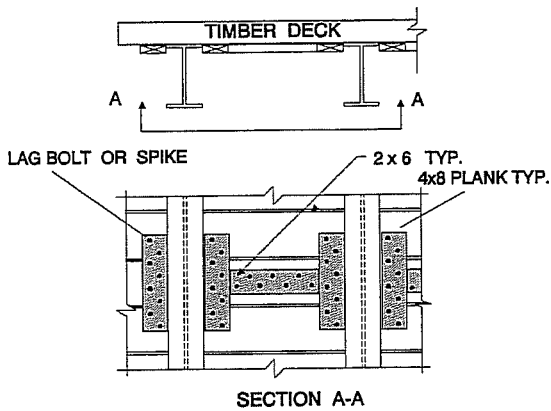
Figure 5.16    Remedial deck/stringer connection

stringers. The steel stringers, which spanned 21 feet, were loaded until flange yield was observed. Kissane concluded that the friction resistance between the concrete deck and stringers was sufficient to mobilize the deck as a brace and allow the stringers to reach their full in-plane bending capacity without buckling laterally. Other factors which may have increased the buckling capacity of the stringers were not discussed. Such factors would include any restraint provided by the connections between the stringers and supporting transverse girders. Also, torsional restraint may have been provided if the deck prevented the top flange of the stringer from twisting. As part of this research (Kissane, 1985) a related field test was conducted on a similarly constructed bridge system. Test results indicated that the steel stringer resisted less than 15% of the applied load. The majority of the load was carried directly by the continuous concrete deck in bending. No conclusions could be drawn from the field test concerning the bracing effects of the bridge deck since the load carried by the stringers was well below that required to cause buckling.

The lateral stiffness provided by concrete decks is significantly greater than that of timber decks. For a five-inch thick normal weight 3000 psi concrete deck supported by six stringers, with a width of 16 ft and a span of 17 ft, the corresponding continuous brace stiffness per stringer, based on a single midspan discrete bracing mode, is 68.0 kip/in. per in. of length. This is 6000 times greater than 0.0105 value for the same bridge with a timber deck (see County bridge AA-0233-01 discussed above). Concrete decks provide much greater lateral stiffness and have better friction resistance than timber decks. For such bridges the axle location can be considered a brace point.

# CHAPTER 6
## CONCLUSIONS AND RECOMMENDATIONS

An effective brace must prevent twist of the cross section. Two types of bracing systems have been considered, top flange lateral bracing systems and torsional bracing systems. These systems must satisfy both stiffness and strength criteria and a summary of the requirements for each system is given in Appendix A. The analytical and experimental studies showed that the bracing requirements for beams are related to the shape of the moment diagrams, the maximum moment, and the location of the load on the cross section (top flange loading is the most critical), and the design methods developed consider all of these factors.

For torsional bracing systems such as cross frames and diaphragms, cross section distortion is a very important parameter that must be considered when evaluating or designing the bracing system (Eqs. 5.21 and 5.22 or Eq. A9). These formulas can be used to design adequate stiffeners and connection details to control distortion. For rolled sections, diaphragm connections should extend at least three-quarters of the depth. For plate girders which have thin webs, the connection of the diaphragm or cross frames should be as close to each flange as practical. Design Examples 3 and 4 illustrate the sensitivity of the brace stiffness to the connection details. For most torsional brace designs, the strength criterion will control the size of the bracing members and the stiffness criterion will control the size of the stiffeners and the connection details.

The test on a full-size short-span bridge with a wooden deck which was not attached to the steel stringers showed the friction at the wheel location was sufficient to mobilize the lateral stiffeners of the deck for bracing the beams. The bridge capacity was doubled by the bracing effect of the deck. Concrete decks are very stiff so the wheel location can be considered a brace point in such bridges. Wooden deck stiffness can vary considerably, depending on the construction details. Wooden decks examined in the central Texas area had sufficient stiffness to prevent beam buckling at the wheel location and the bridges could be rated based on their yield strength. For rating purposes, the lateral stiffness of the deck can be obtained by considering only the lateral stiffness of the deck nailers.

The studies herein have also verified the new lateral buckling equation in the 1990 AASHTO Bridge Specification. Both experiments and theory show that the new formula can be used with confidence. The old formula for lateral buckling gave overly conservative capacities for large unbraced lengths. The new formula should be used in the rating of bridges. A sample rating of an existing bridge (Bridge AA0539-001, Village Creek - Ellis County, Texas) is given in Appendix C. That bridge has a current inventory rating of H3.2; the new rating based on the 1990 AASHTO Specification would be H6.2. Increased rating of short-span bridges should be expected if lateral buckling controlled the current rating. If the bridge is not adequately braced at the wheel location to force either yielding or buckling between existing braces (like the full-size bridge tested), then the buckling capacity should be based on the sum of the lateral buckling capacities of all the girders if positive vertical contact between the deck and the girders can be assumed at the wheel location. In wide bridges it is probably more realistic to sum the buckling capacities of the girders within the lane with plus one or two girders on either side of lane to account for possible uplift of the planks. An example of this lateral buckling concept is given in part 2 of Appendix C. Friction at the wheel location will force all the girders to buckle simultaneously, so the bridge capacity should not be based on just the most highly stressed single girder.

69

# APPENDIX A
## BRACING EQUATIONS FOR DESIGN

## LATERAL BRACING - Load Factor Design

Brace Stiffness - discrete or continuous bracing

$$M_{cr} = \sqrt{\left[ \left( C_{bu} M_o \right)^2 + \left( C_{bb} P_{yc} h \right)^2 A_d \right] \left( 1 + A_d \right)} \quad \le M_y \text{ or } M_s \qquad (A1)$$

where



Figure A1. Equivalent continuous bracing.

$$P_{yc} = \frac{\pi^2 E I_{yc}}{L^2} \qquad (A2)$$

$$A_d = L \sqrt{\frac{.17 \overline{\beta}_L}{C_L P_{yc}}} \qquad (A3)$$

$$C_L = 1 + \frac{1.2}{n} \qquad (A4)$$
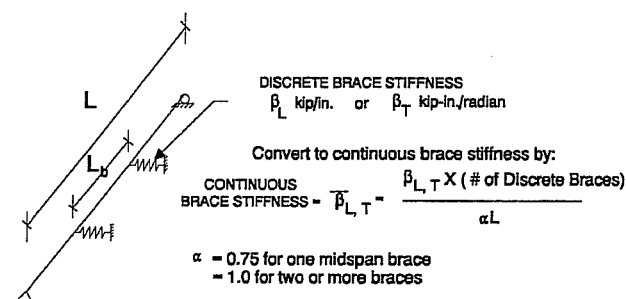(top flange load)

$$= 1.0 \text{ (centroid or moment loading)}$$

$$M_o \text{ (lb-in. units)} = 91 \times 10^6 \frac{I_{yc}}{L} \sqrt{0.772 \frac{J}{I_{yc}} + \left( \frac{\pi d}{L} \right)^2} \qquad (A5)$$

For top flange loading adjust Eq. (A5) as given in the SSRC Guide (Galambos, 1988) or omit the second term under the square root. In the equations above

$M_o$ = buckling strength assuming the beam is laterally unbraced along the span
$M_s$ = buckling strength between braces; Eq. (A5) with $L_b$ instead of L and $C_{bb}$ (same as $M_r$ in AASHTO)
$C_L$ = top flange loading factor
$C_{bu}$ = the $C_b$ factor assuming the beam is unbraced
$C_{bb}$ = the $C_b$ factor assuming the beam braces are fully effective

and

| | | | | | |
|---|---|---|---|---|---|
| n | = | number of discrete braces | G | = | shear modulus (E/2.6 for steel) |
| L | = | span length | J | = | St. Venant torsion constant |
| $L_b$ | = | distance between braces | h | = | distance between flange centroids |
| $I_{yc}$ | = | weak axis moment of inertia of compression flange | $M_y$ | = | yield moment |
| E | = | modulus of elasticity | d | = | beam depth |

71

<u>Full Bracing Stiffness Requirement</u> - Discrete or Relative Bracing

$$\beta_L^* = 2\ \#P_f\ C_{bb}\ C_L/L_b \qquad \text{or} \qquad 2\ \#\ (M_f\ /\ h)\ C_L\ /\ L_b \qquad (A6)$$

where     $\#\ \approx\ 4 - (2/n)$ or the coefficient in Table 2.1 for discrete bracing
          $\#\ =\ 1.0$ for relative bracing
          $P_f\ =\ \pi^2\,E\,I_{yc}/L_b^2$
          $M_f\ =\ $ the maximum beam moment at factored load

<u>Strength Requirement</u>

Discrete bracing:     $F_{br}\ =\ 0.008\ C_L M_f\ /\ h$                     (A7)
Relative bracing:     $F_{br}\ =\ 0.004\ C_L M_f\ /\ h$                     (A8)

---

**LATERAL BRACING**
Allowable Stress Design

<u>Stiffness:</u>    $M_{allow} = 0.55\ M_{cr} \leq 0.55\ M_y$ or $0.55\ M_s$
                    See Eq. (A1-A5)

<u>Full Bracing Stiffness:</u>
    Use Eq. (A6) - no change

Strength:
    Discrete bracing:  $F_{br} = 0.008\ C_L M/h$
    Relative Bracing:  $F_{br} = 0.004\ C_L M/h$

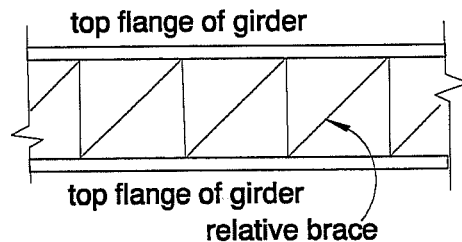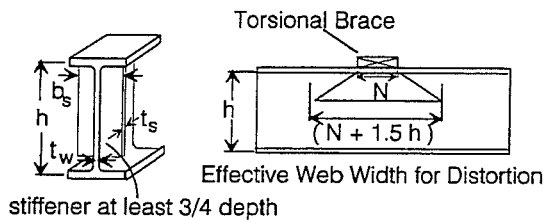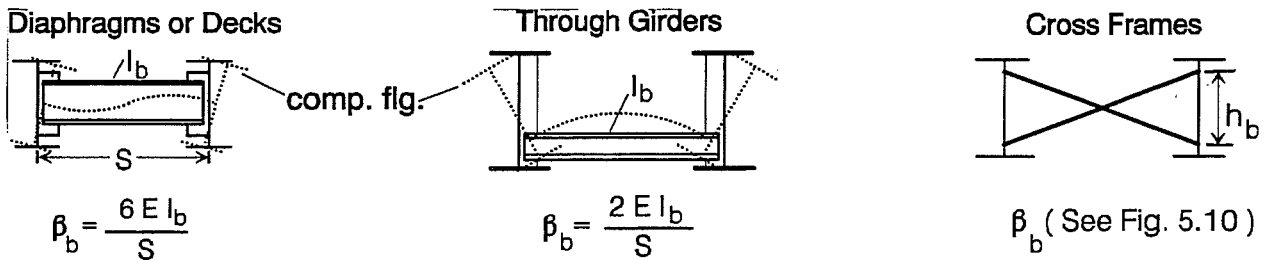    where M is the maximum beam moment at
    service load.

top flange of girder

top flange of girder
relative brace

Figure A.2

## TORSIONAL BRACING - Load Factor Design

**Diaphragms or Decks**

$$\beta_b = \frac{6\,E\,I_b}{S}$$

**Through Girders**

$$\beta_b = \frac{2\,E\,I_b}{S}$$

**Cross Frames**

$$\beta_b \;(\text{See Fig. 5.10})$$

Torsional Brace

Effective Web Width for Distortion

stiffener at least 3/4 depth

$$b_{sec} = \frac{3.3\,E}{h}\left(\frac{t_w^3}{12}(N + 1.5\,h) + \frac{t_s\,b_s^3}{12}\right)$$

use 1 in. for continuous bracing

$\beta_T$ = effective torsional brace

$\beta_b$ = stiffness of attached brace

$\beta_{sec}$ = accounts for cross section distortion, see Eq. (5.21)

$\beta_g$ = girder stiffness = $12\,S^2\,EI_x/L^3$

and

$$\frac{1}{\beta_T} = \frac{1}{\beta_b} + \frac{1}{\beta_{sec}} \tag{A9}$$

<u>Brace Stiffness</u> - discrete or continuous bracing - use Eq. A10 or A10a

$$M_{cr} = \sqrt{C_{bu}^2\,M_o^2 + \frac{C_{bb}^2\,E\,I_{eff}\,\overline{\beta}_T}{2\,C_T}} \;\le\; M_y \text{ or } M_s \tag{A10}$$

where $C_T$ = 1.2 for top flange loading; = 1.0 for other loading

$I_{eff}$ = $I_{yc} + (h_t/h_c)\,I_{yt} = I_y$ for double symmetric sections

Instead of solving Eq. A10 for the required $\overline{\beta}_T$, the following expression can be used for discrete braces

$$\text{Req}'d\ \beta_T = \frac{2.4\,L\,M_f^2}{n\,E\,I_{eff}\,C_{bb}^2} \tag{A10a}$$

where $M_f$ = maximum factored moment

<u>Brace Strength</u>

$$M_{br} = F_{br}\,h_b = \frac{0.04\,L\,M_f^2}{n\,E\,I_{eff}\,C_{bb}^2} \tag{A.11}$$

74

---

**TORSIONAL BRACING** - Allowable Stress Design

Stiffness:   $M_{allow} = 0.55\, M_{cr} \le 0.55\, (M_y \text{ or } M_s)$                    (See Eq. (A.9 - A.10))

or $\beta_{Req'd}$ = Eq. 10a with $M_f = 1.82\, M$

Strength:   Same as A.11 but with M as the maximum moment at service load

# APPENDIX B
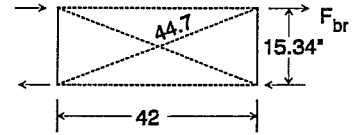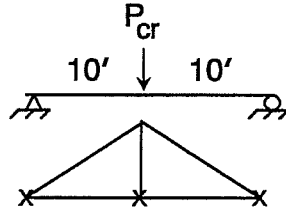## CROSS FRAME BRACE FORCES

**W16 × 26**
$F_y$ = 50 ksi
Top flange loading
$I_y$ = 9.57 in.$^4$, J = .23 in.$^4$,
    d = 15.69 in., h = 15.34 in.,
    G = E/2.6

Find the required size of the cross frame members
for full bracing at midspan.



Lateral buckling capacity, Eq. (1.1):

$$C_b = 2.75 \text{ (Eq.1.2)}, \quad M_{cr} = 1.75 \frac{\pi E}{120} \sqrt{\frac{9.57(.23)}{2.6} \frac{\pi^2 \, 9.57^2 \, (15.34)^2}{4 \, (120)^2}} = 2830 \text{ in-k;}$$

$$P_{cr} = \frac{2830(4)}{240} = 47.2 \text{ kips}$$

Ideal bracing, Eq. (5.13):

$$\beta_{Ti} = \frac{1.2 \, (240) \, (2830)}{(1.75)^2 \, (29000) \, (9.57)} = 2713 \text{ in.-k/radian}$$

Required brace stiffness,          $\beta_T = 2 \times \text{ideal} = 2 \times 2713 = 5430$ in-k/radian

Cross frame stiffness: The diagonals are designed for tension only. Assume that all cross frame members are the same size, $A_c = A_h$ in Figure 5.10.

$$\beta_b = \frac{29000 \, (42)^2 \, (15.34)^2 \, A_c}{2 \, (44.7)^3 + (42)^3} = 47600 \, A_c$$

Girder stiffness, Eq. (5.20):     $\beta_g = 12 \, (42)^2 \, 29000 \, (301) \Big/ (240)^3 = 13370$ in-k/radian

$$\frac{1}{5430} = \frac{1}{47600 \, A_c} + \frac{1}{13370}; \qquad \underline{\text{Req'd } A_c = 0.192 \text{ in.}^2}$$

Required brace force, Eq. (5.16):   $F_{br} = \dfrac{0.04 \, (240) \, (2830)^2}{15.34 \, (29000) \, 9.57 \, (1.75)^2} = \underline{5.90 \text{ kips}}$

76

For comparison with the ANSYS solution in Figure 5.8,

   if $A_c = 0.1$ in.$^2$ and $P = 42$ kips with $P_{cr} = 47.2$ kips

$$\frac{1}{\beta_T} = \frac{1}{4760} + \frac{1}{13370} \; ; \qquad \beta_T = 3510 \text{ in-k/radian}$$

Adjusting Eq. (5.18) for $P < P_{cr}$ gives

$$F_{br} = F_{br} \text{ req'd} \times \frac{.5 \, (P/P_{cr})}{1 - \dfrac{\beta_{Ti}}{\beta_T}\left(\dfrac{P}{P_{cr}}\right)} = 5.90 \; \frac{.5 \, (42/47.2)}{1 - \dfrac{2713}{3510}\left(\dfrac{42}{47.2}\right)} = \underline{8.40 \text{ kips}}$$
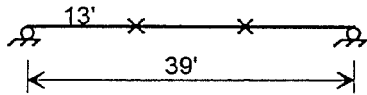
For $A_c = 1.0$ in.$^2$ and $P = 44$ kips

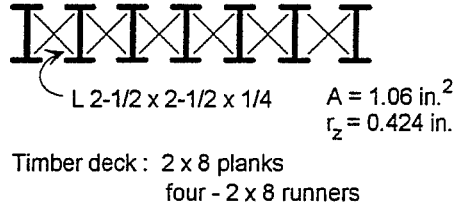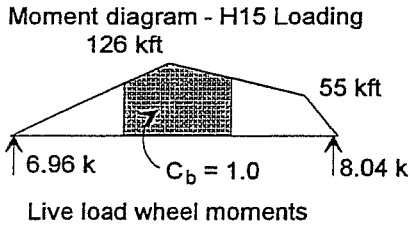$$\frac{1}{\beta_T} = \frac{1}{47600} + \frac{1}{13370} \; ; \qquad \beta_T = 10440 \text{ in.-k/radian}$$

$$F_{br} = 5.90 \; \frac{.5 \, (44/47.2)}{1 - \dfrac{2713}{10440}\left(\dfrac{44}{47.2}\right)} = \underline{3.63 \text{ kips}}$$

# APPENDIX C
## SAMPLE BRIDGE RATING

---

### BRIDGE RATING - Bridge AA0539-001 - Village Creek - Ellis County

Seven stringers @ 2'-3  -  S12 x 31.8
$F_y$ = 33 ksi ;   Corrosion loss = 5%
Cross frames at 1/3 pts.

L 2-1/2 x 2-1/2 x 1/4     A = 1.06 in.$^2$
                         $r_z$ = 0.424 in.

Moment diagram - H15 Loading
126 kft
55 kft
6.96 k    $C_b$ = 1.0    8.04 k
Live load wheel moments

Timber deck :  2 x 8 planks
              four - 2 x 8 runners

<u>S12 x 31.8</u>    $S_x$ = 36.4 in$^3$    $I_y$ = 9.36 in$^4$    J = 0.90 in$^4$
                 d = 12.0 in    $I_{yc}$= 4.68 in$^4$

First consider lateral bracing only at the cross frames.
Unbraced length = 13 ft, $C_b$ = 1.0 near midspan.

$$F_b \text{(ksi)} = \frac{50 \times 10^3}{36.4}(1.0)\frac{4.68}{13 \times 12}\sqrt{\frac{.772(0.9)}{4.68} + 9.87(\frac{12.0}{13 \times 12})^2} = 18.74 \text{ ksi}$$

$F_b$ max = 0.55 F = 0.55 (33) = 18.15 ksi < 18.74    ∴ yielding controls

No need to consider the bracing effect of the timber deck.
Cross frames alone are sufficient to prevent buckling.

corrosion
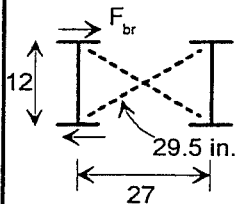$M_{allow}$ = (1 - 0.05) 36.4 (18.15) / 12  = 52.3 k-ft

Dead Load / beam  =  0.075 k/ft;  $M_{DL}$ = 1/8 w L$^2$ = 1/8 (.075) (39)$^2$ = 14.3 k-ft

Distribution Factor = 2.25/4 = .562, Impact factor = 1.3

$H15_{LL}$ = 126 x .562 x 1.3 = 92.1 k-ft

$$\text{Inventory Rating} = H15 \left(\frac{(52.3 - 14.3)}{92.1}\right) = H6.2$$

The current rating  (1988 AASHTO) = H3.2

Check cross bracing:

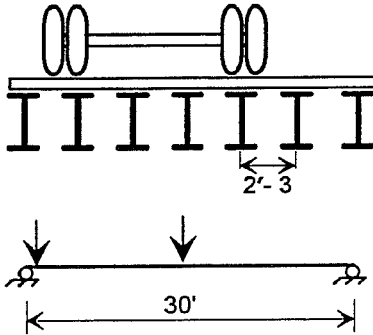$$F_{br} (12) = \frac{0.04 (39 \times 12) (52.3 \times 12)^2}{2 (29000) 9.36} = 13.58 \text{ in-k}$$

$$F_{br} = 1.13 \text{ kips; Diagonal} = 1.13\frac{29.5}{27} = 1.24 \text{ kips}$$

$$\ell / r = 29.5 / .424 = 70; \quad F_a = \frac{33}{2.12}\left[1 - \frac{70^2(33)}{4\pi(29000)}\right]$$

$$P_{allow} = 13.4 (1.06) = 14.2 \text{ k} >> 1.24 \text{ kips} \quad OK$$

Brace stiffness  OK - full depth cross frame - no distortion

## SAMPLE BRIDGE RATING - PART 2

Similar to previous bridge but there are no cross frames.
One lane - bridge width = 13 ft 6 in.  Span = 30 ft
For stringer properties,  see previous example.

The wooden deck runners are badly deteriorated so assume
that the deck can not provide a bracing effect at the wheel
location.  Assume the full span is laterally unsupported.

2'- 3

30'

H15 moment    truck = 185 k-ft
              wheel = 92.5 k-ft

### Recommended Procedure

At least six stringers will be in contact with the wooden cross plank at midspan.
Because of the friction between the plank and the six stringers at the axle location, they
must all move laterally if buckling occurs near midspan.  The lateral buckling strength
of six stringers support the truck load.

Buckling strength :

$$F_b \text{ (ksi)} = \frac{50 \times 10^3}{36.4}(1.0)\frac{4.68}{30 \times 12}\sqrt{\frac{.772\,(0.9)}{4.68} + 9.87\left(\frac{12.0}{30 \times 12}\right)^2} = 7.13 \text{ ksi}$$

$F_b \text{ max} = 0.55\,F = 0.55\,(33) = 18.15 \text{ ksi} > 7.13$    ∴ buckling controls

$M_b = (0.95)\,7.13\,(36.4)\,/\,12 = 20.54 \text{ k-ft}$ (corrosion)    $M_{DL} = 0.075\,(30)^2\,/\,8 = 8.44 \text{ k-ft}$

Truck loading per stringer:  $H15_{LL} = 185.0 \times 1.3 \text{ impact}\,/\,6 = 40.1 \text{ k-ft}$

$$\text{Rating} = H15\left(\frac{20.54 - 8.44}{40.1}\right) = \underline{H4.5} \quad \longleftarrow \text{ CONTROLS}$$

Check stringer yielding at wheel load : $M_b = (0.95)\,18.15\,(36.4)/12 = 52.3 \text{ k-ft}$

Distr. factor = 0.562 , Impact factor = 1.3 :    $H15_{LL} = 92.5\,(1.3)\,(0.562) = 67.6 \text{ k-ft}$

$$\text{Rating} = H15\left(\frac{52.3 - 8.44}{67.6}\right) = H9.7$$

### Current Procdure

$M_b = 20.54 \text{ k-ft}$ ;    Allow wheel $M_{LL} = 20.54 - 8.44 = 12.1 \text{ k-ft}$

Distr. factor = 0.562 , Impact factor = 1.3 :    $H15_{LL} = 92.5\,(1.3)\,(0.562) = 67.6 \text{ k-ft}$

$$\text{Inventory Rating} = H15\left(\frac{12.1}{67.6}\right) = H2.7$$

# BIBLIOGRAPHY

Akay, H.U., Johnson, C.P., and Will, K.M., 1977, "Lateral and Local Buckling of Beams and Frames," *Journal of the Structural Division*, ASCE, ST9, September, pp. 1821-1832.

Choo, K.M., 1987, Thesis presented to The University of Texas at Austin, May, "Buckling Program BASP for Use on a Microcomputer."

Fischer, M., 1970 and 1973, "Das Stabilitätsproblem des in Höhe des oberen Flansches wirklichkeitsnah belasteten I-Trägers. *Der Stahlbau*, 39, H.9, S. 267-275 und 42, H.5, S. 129-138.

Flint, A.R., 1951a, "The Stability of Beams Loaded Through Secondary Members," *Civil Engineering and Public Works Review*, Vol. 46, No. 537-8, pp. 175-177, 259-260.

Galambos, T.V., Ed., 1988, Structural Stability Research Council, *Guide to Stability Design Criteria for Metal Structures*, 4th Edition, New York: John Wiley & Sons, Inc.

Helwig, T.A., Yura, J.A. and Frank K.H., 1993, "Bracing Forces in Diaphragms and Cross Frames," Structural Stability Research Council Conference, April 6-7, Milwaukee, WI..

Kirby, P.A. and Nethercot, D.A., 1979, *Design for Structural Stability*, Wiley.

Kissane, R.J., 1985, "Lateral Restraint of Non-Composite Beams," Research Report 123, New York State Department of Transportation, August.

Linder, J., Schmidt, J.S., 1982, "Biegedrillknicken von I-Trägern unter Berücksichtigung wirklichkeitsnaher Lasteinleitung," *Der Stahlbau*, 51, H.9, S. 257-263.

Meck, H.R., 1977, "Experimental Evaluation of Lateral Buckling Loads," *Journal of the Engineering Mechanics Division*, ASCE, EM2, April, pp. 331-337.

Milner, H.R., and Rao, S.N., 1978, "Strength and Stiffness of Moment Resisting Beam - Purline Connections," *Civil Engineering Transactions, Institute of Engineers, Australia*, CE 20(1), pp. 37-42.

Nethercot, D.A., 1989, "*The Design of Bracing Systems for Plate Girder Bridges,*" Structural Eng. / Earthquake Eng., Vol. 6, No. 1, 10-120, April (Review), Japan Society of Civil Engineers (Proc. of ASCE) No. 404/1-11.

Salmon, C.G., and Johnson, J.E., 1980, Steel Structures, Design and Behavior, Harper & Row, New York.

Southwell, R.V., 1932, "On the analysis of Experimental Observations in the Problems of Elastic Stability," Proceedings of the Royal Philosophical Society of London, Series A, Vol. 135, April, p. 601.

Taylor, A.C., and Ojalvo, M., 1966, "Torsional Restraint of Lateral Buckling," *Journal of the Structural Division*, ASCE, ST2, April, pp. 115-129.

Timoshenko, S., and Gere, J., 1961, *Theory of Elastic Stability*, New York: McGraw-Hill Book Company.

Tong, G.S., and Chen, S.H., 1988, "Buckling of Laterally and Torsionally Braced Beams," *Construction Steel Research.*

Trahair, N.S., and Nethercot, D.A., 1982, "Bracing Requirements in Thin-Walled Structures," Chapter 3, *Developments in Thin-Walled Structures - Vol. 2*, Rhodes and Walker - Ed., Elsevier Applied Science Publishers, pp. 93-129.

Vegnesa, S., and Yura, J.A., "An Ultimate Load Test to Study Bracing Effects of Bridge Decks," Report No. 1239-2, Center for Transportation Research, University of Texas at Austin, August 1991, 59 p.

Webb, S., and Yura, J.A., "Evaluation of Stiffness of Bridge Decks," Report No. 1239-3, Center for Transportation Research, The University of Texas at Austin, September 1991.

Winter, G., 1958, "Lateral Bracing of Columns and Beams," *Journal of the Structural Division*, ASCE, ST2, March, pp. 1561-1565.

Winter, G., 1980, "Lateral Bracing," *ASCE Transactions*, pp. 809-825.

Yarimci, E., Yura, J.A., and Lu, L.W., 1967, "Techniques for Testing Structures Permitted to Sway," *Experimental Mechanics*, Journal of the Society of Experimental Stress Analysis, Vol. 7, No. 8, August.

Yura, J.A., 1971, "Design of Bracing for Columns, Beams and Frames," *AISC National Engineering Conference*, Cleveland.

Yura, J.A., and Phillips, B., "Bracing Requirements for Elastic Steel Beams," Report No. 1239-1, Center for Transportation Research, University of Texas at Austin, May 1992.